

ALMA MATER STUDIORUM  
UNIVERSITY OF BOLOGNA

---

SCHOOL OF ENGINEERING AND ARCHITECTURE  
Department of Electric, Electronic and Information Engineering  
"Guglielmo Marconi"

# Continuous-Flow Magnetic Separation with Permanent Magnets for Water Treatment

Ph.D. Thesis  
by  
Chiara Caterina Borghi

Coordinator: Prof. Domenico Casadei

Supervisor: Prof. Massimo Fabbri

Ph.D. in Electrical Engineering  
Settori concorsuali: 08/A2, 09/E1 (prevalente)  
Settori Scientifico Disciplinari: ICAR/03, ING-IND/31 (prevalente)  
XXVI Cycle

Final Exam Year 2014



# Contents

Forewords and Acknowledgments.....	i
Introduction.....	1
<b>1. Water Treatment and Magnetic Separation.....</b>	<b>3</b>
1.1 Water Treatment.....	3
1.2 Magnetic Separation.....	6
1.3 Initial work at LIMSA – the starting point.....	8
<b>2. Materials and Methods.....</b>	<b>11</b>
2.1 Pollutants.....	11
2.1.1 Surfactants.....	11
2.1.2 Octylphenols and Nonylphenols.....	13
2.1.3 Cations.....	15
2.2 Adsorbents.....	16
2.2.1 Magnetic Activated Carbons (MACs).....	16
2.2.2 Zeolite-Magnetite mixtures.....	19
2.3 Adsorption tests and adsorbents removal tests.....	21
2.4 Filtration experimental setups.....	23
<b>3. Adsorbents Removal.....</b>	<b>27</b>
3.1 Magnetic Activated Carbons (MACs).....	27
3.2 Zeolite-Magnetite mixtures.....	29
<b>4. Numerical Modelling.....</b>	<b>33</b>
4.1 The spheres filter.....	33
4.2 Numerical results.....	42
<b>5. Pollutants adsorption results.....</b>	<b>47</b>
5.1 Adsorption on Magnetic Activated Carbons (MACs).....	47
5.1.1 Surfactants.....	47
5.1.2 Octylphenols and Nonylphenols.....	50
5.1.3 Cations.....	52
5.2 Adsorption on Zeolite-Magnetite mixtures.....	53
5.2.1 Cations.....	53
<b>6. Sustainability and applicability of the process.....</b>	<b>57</b>
6.1 Filter and adsorbents reuse.....	57
6.2 Large scale application.....	58
<b>Conclusions.....</b>	<b>63</b>
<b>Appendix I.....</b>	<b>65</b>

**Appendix II.....77**

**References.....83**

**Acronyms List.....91**

## Forewords and Acknowledgments

I started my experience at DIE (now DEI) department more than three years ago to prepare my master thesis. My interest in Japan and its culture was the unscientific reason I contacted Prof. Negrini; I was hoping on some connections with Japanese Universities to do in Japan my Master thesis. At that time Prof. Negrini had not the possibility to introduce me to a Japanese department but he told me that his research group was looking for an Environmental Engineer to apply a magnetic separation technique to the removal of pollutants from water. Fascinated by the topic, I did my Master thesis at DIE, experience that was very interesting and challenging and that was just the beginning of a research that had many more aspects to study and analyze. To deepen my knowledge on the subject and to continue with experimental campaigns and numerical modelling, I started this PhD; after few months, luckily, I was able to go to Japan for six month at the Graduate School of Engineering of Osaka University, Division of Sustainable Energy and Environmental Engineering. This was an interesting experience both from the scientific and the cultural point of view. Two years after my return to DIE and LIMSA laboratory I realise that I would have many more aspects of this topic to study but also if research never reaches an end, the PhD does.

I want to thank Prof. Fabbri that from the Master thesis until all the PhD was always present for me, both professionally and humanly.

I want to thank Prof. Ribani for his kindness and his help during all my experience at DIE.

I want to thank Prof. Fiorini for his willingness, help and all the advices he gave me every time I needed help and experience from the chemical point of view.

I want to Thank Prof. Akiyama and Prof. Nishijima for the opportunity they gave me at Osaka University (ありがとうございます!).

I want to thank Prof. Maurizio Mancini for his help on water treatment studies.

Finally I want to thank Prof. Passaglia of Modena and Reggio Emilia University for the availability and the precious information on the zeolites.



# Introduction

Within a world, a society, more and more sensitive to the issue of sustainability and sustainable development, management and safeguarding of water resources play a major role. Thus, the water treatment processes turn today towards more and more restrictive quality objectives, not only in relation to the removal of macro/conventional pollutants (solid fraction, BOD, COD, N, P) but also in relation to micro/emerging pollutants (surfactants, endocrine disrupting chemicals, antibiotics, hormones, drugs, heavy metals, chlorinated and aromatic organic compounds. . .). The aims, according with the European Water Framework Directive 2000/60/EC, are the facilitation of water reuse and the maintenance, as unchanged as possible, of the characteristics of the receiving water bodies. To achieve higher levels of depuration new technologies are needed. More efficient water treatment technologies would decrease the water bodies' pollution and the actual intake of water resource (if the concentrations achieved are lower than the values allowed by law for a reuse).

The aim of this thesis is an in-depth analysis of the magnetic separation of pollutants from water by means of a continuous-flow magnetic filter subjected to a field gradient produced by permanent magnets. Different solutions have been studied. This technique has the potential to improve times and efficiencies of both urban wastewater treatment plants and drinking water treatment plants. It might also substitute industrial wastewater treatments. This technique combines a physico-chemical phase of adsorption and a magnetic phase of filtration.

The first chapter briefly describes what are water and wastewater treatments, the magnetic separation and its applications and the previous work I have done at LIMSA (Laboratorio di Ingegneria dei Magneti e Superconduttività Applicata).

The second chapter reports the materials I have used and the methods I have followed in laboratory during the experiments.

The third chapter reports the experimental results obtained during the magnetic phase of filtration. The adsorbents removal results are reported in plots with time as x axis and the removal percentage as y axis.

The fourth chapter describes the numerical model developed to reproduce the magnetic filtration with a steel spheres filter subjected to a field produced by

permanent magnets and the results of the model compared to the experimental ones.

The fifth chapter reports the pollutants adsorption experimental results obtained in laboratory.

The sixth chapter considers the importance of the sustainability of the process discussing about the reusability of the filter and the adsorbents and the possible costs and applications of the magnetic separation in water and wastewater treatment.

## Chapter 1

# Water Treatment and Magnetic Separation

### 1.1 Water Treatment

Water treatment can be divided into three categories: urban wastewater, drinking water and industrial wastewater. The urban plants treat the sewage system effluents before the discharge in the environment and have generally the treatment steps reported in Figure 1.1.a.

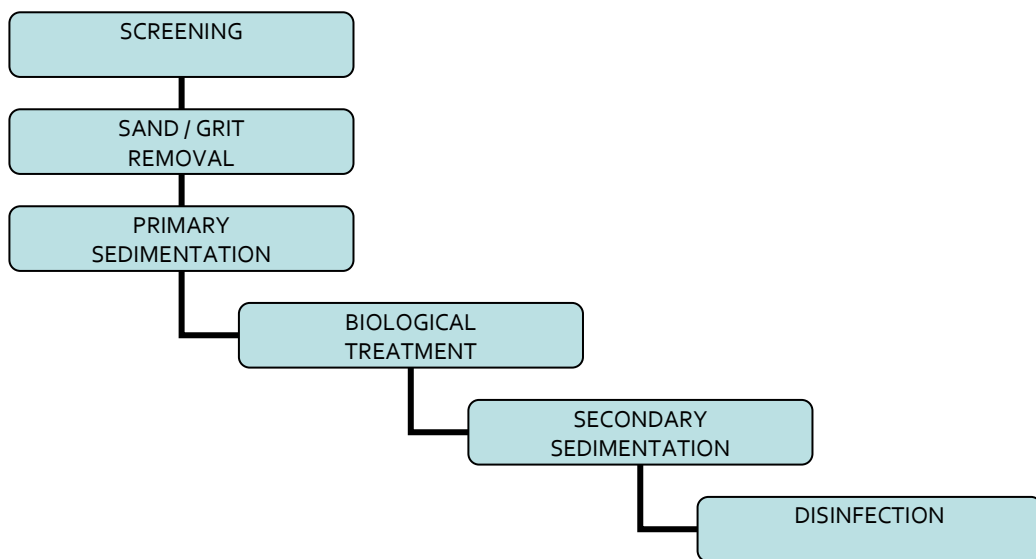


Figure 1.1.a. Wastewater treatment plant conventional steps.

The screening is the first step of the water treatment plants. A grid is a device provided with apertures that presents normally a uniform size and is used to retain the solids contained in the water entering the plant. The sand / grit removal section is designed to achieve the removal of sands, gravels and other heavy solids characterized by sedimentation velocity or specific gravity significantly higher than that of organic solids in wastewater. The primary sedimentation is instead intended for the removal of heavy organic solid particles; the objective is to remove settleable solids and floating material easily, thereby reducing the concentration of suspended solids in the treated wastewater (*Metcalfe&Eddy, 2003*). The biological treatment section involves the use of microorganisms and has the following purposes:

- 1) the transformation (oxidation) of the soluble constituents and biodegradable particulates in final products compatible with the environment;
- 2) the interception of colloidal suspended and not settleable solids and their incorporation within the biological flocs or biofilms;
- 3) the conversion or removal of nutrients such as nitrogen and phosphorus;

4) in some cases, the removal of specific constituents and organic compounds present in traces (*Metcalf&Eddy, 2003*).

The secondary sedimentation section is dedicated to the removal of the flocs of biomass that are created in the biological section. The biomass settles by gravity because it has a specific weight slightly higher than the water one. The term disinfection means the removal of only partial pathogenic organisms. The fact that not all organisms are eliminated differs disinfection from sterilization. The disinfection is commonly achieved through the use of chemical agents, physical agents, mechanical actions and radiation. During the treatment various stages generate different residues due to the removal of solids. These residues are commonly referred as sludge and are treated in a dedicated section of the plant called "sludge line" (the small plants could not have this section and the residues have to be transported to larger plants that have a section dedicated to the sludge treatment). The sludge treatments differ depending on the section that has produced them (*Metcalf&Eddy, 2003*). Recently an increasing number of plants has a tertiary step before the disinfection step (as shown in Figure 1.1.b) to increase the quality of the effluent.

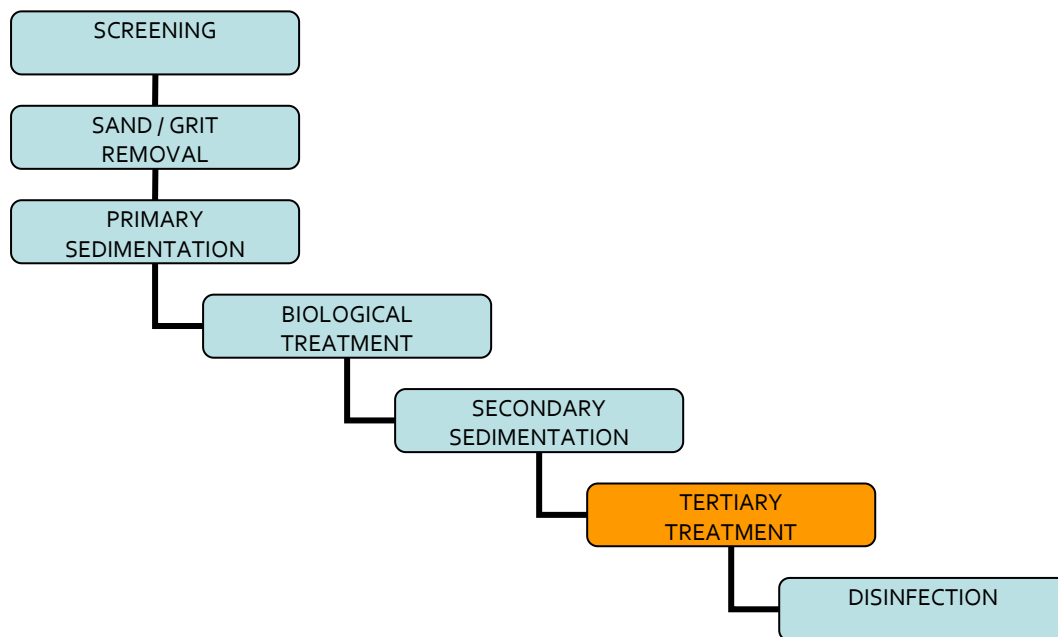


**Figure 1.1.b.** Wastewater treatment plant with a tertiary treatment.

The tertiary treatments of wastewater are all those additional treatments needed for the removal of pollutants in colloidal, suspended or dissolved form still present in the wastewater downstream of the secondary treatment. The requirements imposed on sewage treatment plants are becoming progressively more demanding both in term of maximum concentration limits set for specific pollutants in the effluent, both in terms of limits on the overall toxicity of the effluent. Compliance with these limits in plants often requires modification of the existing secondary treatment units and the introduction of new advanced treatment units. Advanced treatments currently applied are: depth filtration,

surface filtration, ultrafiltration, membrane filtration, adsorption on activated carbons, ions exchange, advanced oxidation processes, reverse osmosis, electrodialysis, chemical precipitation, gas stripping and distillation (Metcalf&Eddy, 2003). Magnetic separation can be another possible tertiary treatment.

Drinking water treatment plants treat water (groundwater, surface water) for human use and combine the processes of coagulation, flocculation, sedimentation, filtration and disinfection. Coagulation is defined as the destabilization of charge on colloids and suspended solids, including bacteria and viruses, by a coagulant. Flash mixing is an integral part of coagulation. Flocculation is the gentle mixing phase that follows the rapid dispersion of coagulant by the flash mixing unit. Its purpose is to accelerate the rate of particle collisions, causing the agglomeration of electrolytically destabilized colloidal particles into settleable and filterable sizes. The terms coagulation and flocculation are sometimes used interchangeably in technical literature. However, the aggregation of particulate material is actually a two-step process. The coagulation is the part where the coagulant reduces or eliminates the interparticulate forces responsible for the stability of the particulate and the subsequent particulate collisions and aggregation into flocks is the flocculation part. In drinking water treatment filtration is the fundamental step that removes particulate matter. The most common filtration process employs a granular medium of a certain size and depth (Kawamura, 2000). Magnetic separation can substitute and/or improve the main steps of water treatment. Water treatment has generally the steps reported in Figure 1.1.c.

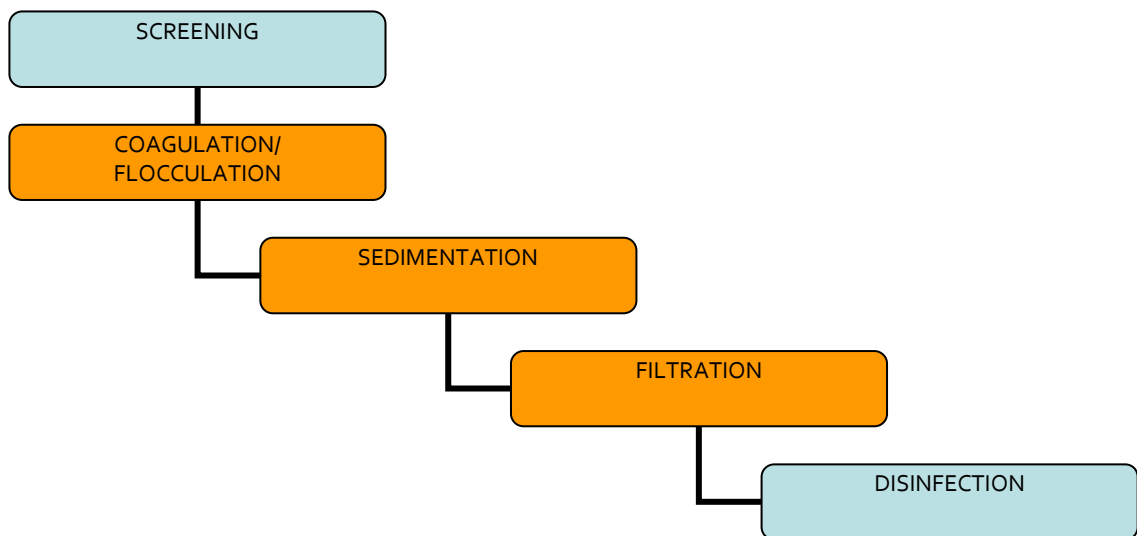


Figure 1.1.c. Water treatment plant conventional steps.

The industrial plants have specific treatments according to the industrial process and the treated water is discharged in the sewage system. Depending on the characteristic of the industrial wastewater, magnetic separation can be a possible treatment technique (Ihara, 2004; Svoboda, 2004; Nishijima, 2006; Mishima, 2010).

Several studies were made on magnetic separation techniques and their applications. During the last forty years of the 20<sup>th</sup> century, magnetic separation evolved from a simple technology for manipulation of strongly magnetic coarse materials into a powerful technique for the treatment of weakly magnetic, finely dispersed particles. Important applications are: the concentration of various ferrous and non-ferrous minerals; the removal of low concentrations of magnetisable impurities; the recycling of metals from industrial wastes; the concentration or removal of biological objects in medicine and bioscience; water treatment (Svoboda, 2004). Considering the field of water treatment, the magnetic technique object of this thesis has the potential to:

- treat part of the wastewater treatment effluent of a big wastewater treatment plant to reuse it in agriculture;
- become a tertiary treatment for average medium urban wastewater treatment plants;
- be applied to any non magnetic adsorbent powder by coagulation using magnetite and a coagulant.
- improve the main treatment steps of a drinking treatment plant (coagulation-flocculation, sedimentation and filtration);
- treat industrial wastewater.

### 1.2 Magnetic Separation

Magnetic phenomena have been known and exploited for many centuries. Practical significance of magnetic attraction as a precursory form of magnetic separation was recognized in an English patent of 1792 on the separation of iron ore by magnetic attraction (Svoboda, 2004). Also the application of magnetic separation of pollutants from water is not a novelty (Oberteuffer, 1976; Anderson, 1982; Anderson, 1983; Svoboda, 1987; Chun, 2001; Anastassakis, 2002; Newns, 2002; Ihara, 2004; Svoboda, 2004; Nishijima, 2006; Hu, 2007; Ihara, 2009; Shen, 2009a; Shen, 2009b; Yavuz, 2006; Yavuz, 2009; Ishiwata, 2010; Mishima, 2010; Nassar, 2010; Rossier, 2012). There are also two patents, CoMag<sup>TM</sup> and BioMag<sup>TM</sup> owned by Siemens Water Technologies S.r.l (<http://www.water.siemens.com>). However, the use of permanent magnets in magnetic separation studies is usually limited to batch tests (Chun, 2001; Nakahira, 2006; Yavuz, 2006; Ihara, 2009; Nassar, 2010) while continuous-flow tests typically employ superconducting magnets (Mitsuhashi, 2003; Ihara, 2004; Svoboda, 2004; Nishijima, 2006; Ishiwata, 2010). A novelty of this work regards the possibility to use a relatively low magnetic field (about 0.5 T) for an effective separation in a continuous-flow filter by using permanent magnets. These magnets do not require an electrical power supply and have smaller footprint with respect to superconductive magnets (Mitsuhashi, 2003; Ihara, 2004; Svoboda, 2004; Nishijima, 2006; Ishiwata, 2010).

A magnetic filter or separator exploits the magnetic force acting on a magnetizable particle (surrounded by non-magnetic fluid) in an externally applied flux density field with a spatial gradient (Svoboda, 2004; Abbasov, 2007; Mariani, 2009; Mariani, 2010; Borghi, 2014a). When the fluid is water at room temperature, the magnetic force  $F_{mag}$  must be able to capture and withhold particles mainly against the drag force of the surrounding fluid and the effects of Brownian motion. Conventional magnetic separators are generally restricted to use ferromagnetic materials. Generally there is a rotating drum separator, feed is introduced at the top of the drum and the magnetic components stick to the rotating drum because of the gradient fields produced by the stationary magnets within it. The nonmagnetic components fall off the drum. These separators are ineffective for very weakly magnetic particles of micron size. High Gradient Magnetic Separation (HGMS) devices utilize a filtering ferromagnetic material such as stainless steel wool which is placed in a magnetic field. This produces a large effective surface area of strong magnetic traps that makes possible the efficient separation of very weakly magnetic particles of micron size (Oberteuffer, 1973). In a HGMS magnetic filtering device (Figure 1.2.a) each particle is magnetized by a field  $\mathbf{B}$  which is made of three terms: a relatively uniform field produced by sources external to the filter, a field produced by the ferromagnetic filtering elements and the field produced by the magnetic moments of the other particles. The external magnetic field can be used to saturate the particle to obtain the maximum possible magnetic force. The same field is used to magnetize the filtering elements which provide the magnetic field gradient.

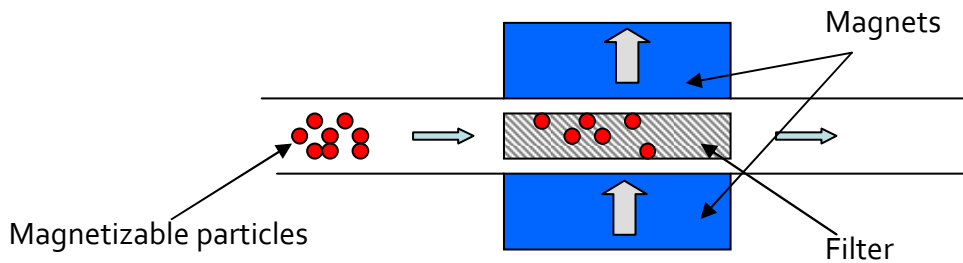


Figure 1.2.a. HGMS magnetic filtering device.

The magnetic force acting on a particle with volume  $V_p$  can be expressed as :

$$\mathbf{F}_{mag} = V_p \mathbf{M}_p \cdot \nabla \mathbf{B} = \frac{V_p \chi_{p,eff}}{\mu_0} \mathbf{B} \cdot \nabla \mathbf{B} \quad (1.2.1)$$

where the magnetization of the particle  $\mathbf{M}_p$  is proportional to the field  $\mathbf{B}/\mu_0$  through an effective susceptibility  $\chi_{p,eff}$  that depends on the material and the shape of the particle (Mariani, 2009).

In order to remove non magnetic pollutants from water with a magnetic separation technique the magnetizable particle must combine adsorption capacity and magnetic properties. Magnetic separation can be extended to materials that are not naturally

magnetic introducing a material (a carrier) which can selectively enhance the magnetic properties of a non magnetic material (a target) that needs to be separated. There are two basic mechanisms for using a magnetic particle so that it renders a non-magnetic particle magnetic, namely as magnetic carrier or as magnetic tag. Magnetic tags are smaller than the targeted magnetic species (usually fine magnetite or ions, e.g.  $Y^{3+}$ ) and are used to coat non-magnetic species in order to allow them to be manipulated by an external magnetic field, i.e. magnetically modified Activated Carbons, zeolites, polymers, etc (*Oliveira, 2004; Svoboda, 2004; Nakahira, 2006; Nah, 2008; Gang, 2010; Lu, 2013; Nethaji, 2013*). Magnetic carriers are usually larger than the target species and used to recover non- magnetic colloidal or macromolecules. Adding a coagulant together with magnetic carriers to treat a polluted water is called magnetic seeding (*Svoboda, 2004*). The addition of a coagulant is not a concern for the application in Water Treatment Plants (WTP) since it is already widely used to clarify suspensions. Usually, the separation of the suspended solid fraction is carried out introducing a coagulant during a rapid mixing to destabilize the suspension and generate aggregates (flocs) removed through a sedimentation followed by a sand or membrane filtration (*Kawamura 2000; Metcalf & Eddy, 2003; Amirtharajah, 2005*). In this thesis is analyzed the coagulation involving a magnetic fraction because this could allows to remove the generated aggregates using a fast magnetic filtration. Beside all the advantages of using an already-known adsorbent powder, avoiding the necessity of a new characterization, this solution can be applied to any non magnetic adsorbent powder and/or any existing coagulation/flocculation treatment in order to reduce the space and times requirements. In all conditions an “adsorption step” to capture the pollutants and an “adsorbent removal step” to remove the adsorbent are needed. Considering the “adsorption step”, several experimental laboratory adsorptions to test the pollutants removal efficiencies were carried out. Considering the “adsorbent removal step”, several experimental tests with two different continuous-flow laboratory setups and a comparison of the results with a numerical model were carried out.

### 1.3 Initial work at LIMSA – the starting point

This work began in LIMSA laboratories as a continuation of my master thesis work (*Borghini, 2010*). The application of the magnetic separation was firstly investigated evaluating the adsorption of detergents and pure surfactants on iron oxides powders (magnetite and hematite) and removing these powders by sedimentation near a magnet or filtration through a HGMS steel wool filter (*Borghini, 2011*). This filter was modeled and manufactured in laboratory by the former PhD student of LIMSA team Giacomo Mariani (*Mariani, 2009; Mariani, 2010*). The removal using only magnetite and hematite technique lead to good results but without the possibility of improvement. Magnetite powder is a ferrimagnetic and non porous iron oxide so only a reduction of the diameter of the

adsorbent could improve the adsorption, due to the increase of the specific area. However, the reduction of the diameter worsens the capture in the magnetic filter reducing the efficiency of the separation. Hematite powder, which is a better adsorbent since it is porous, is paramagnetic and much more difficult to capture. Moreover, the important amounts of sludge generated by the powders and the necessity of disposal of the wool filter after each usage were problems that needed to be solved to have a sustainable process. Thus, this initial work at LIMSA (reported in Appendix I) was the starting point that led me to the research of a solution that employs a powder with both good absorbance and magnetic properties generating a limited amount of sludge and employing a magnetic filter that could be easily assembled, washed and reused.



## Chapter 2

# Materials and methods

## 2.1 Pollutants

### 2.1.1 Surfactants

Surfactants are amphiphilic molecules that have a non-polar tail and a polar head. According to the change of their hydrophilic part they are classified in non ionic, anionic, cationic and amphoteric (*Showell, 2005*). Surfactants are undesirable substances in water bodies and soil and their concentration limits according to Italian legislation, in drinking water, surface water, sewerage and for reuse in agriculture are 0.2 mg/l, 2 mg/l, 4 mg/l, 0.5 mg/l respectively (Decree 31/2001, Legislative Decree 159/2006, Ministerial Decree 185/2003). France has the same limit of 0.2 mg/l only for the anionic ones in drinking water (Decree 1220/2001). The Ministry of Health, Labour and Welfare in Japan gives the same limit DWQS (Drinking Water Quality Standard) of 0.2 mg/l for the anionic surfactants. Since 2003 there is also a DWQS of 0.02 mg/l for non ionic surfactants.

Sources of surfactants in the environment are of different origins: domestic (house cleaning), urban (street cleaning) and industrial (their main application is the industry of detergents but they are used also in textiles, pharmaceuticals, petrochemical products, fertilizer, etc) (*Wang, 2004*). The continuing increase in consumption of detergents and the increase in production of surfactants are the origin of a type of pollution whose most significant impact is the formation of toxic or nuisance foams in rivers, lakes, and treatment plants. Masses of foam floating on river waters represent an aesthetically objectionable nuisance, a problem for the tourism industry and can generate trouble and worries for navigation (mostly in the areas of dams and river locks). In addition, the surfactants reduce the capacity of organic self-purification of natural waters (*Wang, 2004*). The effectiveness of active sludge wastewater treatment plants is reduced by the presence of surfactants as well because the process is based on sedimentation and surfactants are molecules that prevent fine particles from falling (*Wang, 2004*). Furthermore the use of water contaminated with surfactants for irrigation contaminates the groundwater, generates a depletion of soil and adversely affects plant growth (*Bouwer, 2005; Duncan, 2009*). Another impact of these substances is the risks to public health because foams are possible habitat for microorganisms able to resist the disinfecting power of detergents, such as mycobacteria and polio or hepatitis viruses. Human health is also affected when surfactants arrive into drinking water (*Wang, 2004*).

In literature there is no agreement on the degree of ecological danger of synthetic surfactants. Some authors do not include the surfactants between the relevant pollutants and believe that there is virtually no risk to aquatic ecosystems, but there are many

publications on the various biological effects and altered structure and functions of organisms under the influence of synthetic surfactants (Ying, 2004; Ostrumov, 2006). Surfactants with higher volume on the market today, with the exception of soaps, are the linear alkylbenzene sulfonates (LASs), alkylethoxy sulfates (AESs), alkyl sulfates (ASs), alkylphenol ethoxylates (APEs), alkylethoxylates (AEs) and quaternary ammonium-based compounds (QACs). These surfactants are the few for which monitoring and laboratory studies were carried out by following a specific analytical method (Cavalli, 2004; Ying, 2004). Traditionally the examined substances are the ones with significant lethal effects on organisms. The various types of surfactants are considered non-toxic or low toxic and attention to their ecological importance is low. A general rule valid for all surfactants is that toxicity increases with increasing hydrophobicity of the molecule, a characteristic that often coincides with increasing alkyl chain length; on the contrary an increase of the number ethylene oxide (EO) units reduces hydrophobicity and toxicity (Cavalli, 2004). Surfactants are significantly different from the "classical" pollutants (heavy metals, organ metallic compounds and pesticides), because they show a rather broad range of examples of their stimulating action on several enzymatic activities of aquatic organisms (Ostrumov, 2006). The median lethal concentration LC<sub>50</sub> (i.e. the concentration of a pollutant at which 50 % of the test organisms die after some specified exposure time) and the half maximal effective concentration EC<sub>50</sub> (that refers to the concentration of a toxicant which induces a response halfway between the baseline and maximum after some specified exposure time) of many organisms subjected to the most common surfactants, in particular cationic ones, are in many cases lower than the concentration of 2 mg/l, allowed by Italian legislation (Legislative Decree 159/2006) for discharge into surface water bodies (Madsen, 2004; Ying, 2004). However, surfactants degradation products could have a higher toxicity than the former substance. For example, the non ionic APEs nonylphenol ethoxylated and octylphenol ethoxylated are much less toxic to aquatic organisms than their degradation products (nonylphenol and octylphenol) which are endocrine-disrupting chemicals. Thus, the removal of their surfactant precursors, could allow controlling these emerging pollutants (Naylor, 2004; Ying, 2004; EPA, 2005; Jonsson, 2006; Ning, 2007; Soares, 2008; Ifelebuegu, 2011).

Biodegradation is the dominant removal mechanism for surfactants discharged into water bodies. The process can be aerobic or anaerobic depending on the microorganisms present in water. Aerobic biodegradation, however, is of primary importance because the surfactants are discharged into the sewer and eventually into rivers and the sea. Mechanisms of anaerobic biodegradation can take place only in the absence of oxygen and this is possible in sludge and sediments; the end products are CO<sub>2</sub> and CH<sub>4</sub>. The kinetics of biodegradation is influenced by temperature, which is in turn linked to the metabolism of the microorganism (Cavalli, 2004; Ying, 2004). The aerobic and anaerobic biodegradability of surfactants varies greatly depending on the kind of surfactant (Madsen, 2004; Ying, 2004).

The non-ionic and cationic surfactants are significantly slower to decompose in the environment than anionic surfactants (Ying, 2004; Ostrumov, 2006).

For laboratory experiments artificial samples were prepared by mixing distilled water with pure surfactants (all purchased by Sigma-Aldrich S.r.l but Kemfluid EQ18 that was a gift from Biochimica S.p.A). Table 2.1.1.a reports the name, CAS number (Chemical Abstracts Service numerical identifier) and molecular formula of the tested surfactants.

**Table 2.1.1.a.** Tested surfactants.

<b>Surfactant</b>	<b>Name / CAS Number / Molecular Formula</b>
	SDS
Anionic	[Sodium Dodecyl Sulphate] CAS Number 151-21-3 Molecular Formula $\text{NaC}_{12}\text{H}_{25}\text{SO}_4$
	Kemfluid EQ18
Cationic	[Bis-(acyloxyethyl)-hydroxyethyl-methylammonia-methylsulphate] CAS Number 91995-81-2 Molecular Formula $\text{SO}_4\text{CH}_3[(\text{C}_4\text{H}_7\text{O}_3)_2\text{NC}_3\text{H}_8\text{O}]$
	DDAB
Cationic	[Didecyldimethylammonium bromide] CAS Number 2390-68-3 Molecular Formula $[\text{CH}_3(\text{CH}_2)_9]_2\text{N}(\text{CH}_3)_2\text{Br}$
	Triton X-100
Non ionic	[polyethylene glycol p-(1,1,3,3-tetramethylbutyl)-phenyl ether] CAS Number 9002-93-1 Molecular Formula $\text{C}_{14}\text{H}_{22}\text{O}(\text{C}_2\text{H}_4\text{O})_n$ (n=9-10)
	IGEPAL CO-630
Non ionic	[Polyoxyethylene (9) nonylphenylether] CAS Number 68412-54-4 Molecular Formula $\text{C}_{15}\text{H}_{24}\text{O}(\text{C}_2\text{H}_4\text{O})_n$ branched (n=9-10)

### 2.1.2 Octylphenols and Nonylphenols

Octylphenols (OP) and nonylphenols (NP) are endocrine disruptors present in the list of priority substances of the European Directive 2008/105/EC on the environmental quality standards and in the new proposal of the same Directive COM(2011)875. The basic structure of alkylphenols (APs) is a phenol ring with a hydroxyl group, and an alkyl chain. APs have low acute toxicity and OP and NP have low carcinogenic potential. OP and NP have been found to be estrogenic in several *in vitro* and *in vivo* systems (EPA, 2005; Jonsson, 2006; Soares, 2008; Ying, 2012). The general population is mainly exposed to OP and NP from food (especially fish), food packaging, skin care/cleaning products and to some degree drinking

water (Jonsson, 2006; Soares, 2008). OP and NP are reaction intermediates in various industrial formulations but the main source of these substances is the degradation of alkylphenol ethoxylated surfactants (APEs) used in detergents and cleaning products. This degradation often occurs in the wastewater treatment plants (WWTP), mainly in the secondary biological treatment (Frassinetti, 1996; EPA, 2005; Soares, 2008; Ifelebuegu, 2011; Asimakopoulos, 2012). Residues of APEs metabolism in secondary effluents have been shown to be partially halogenated during chlorine disinfection of wastewater and drinking water producing chlorophenols that appear to be more resistant to biodegradation (Bansal, 2005; Ifelebuegu, 2011). Therefore the removal of the APEs surfactants leads to the prevention of APs and chlorophenols productions. The structure of APEs is a fat soluble phenol ring with a varying alkyl chain, and a water soluble chain of 1-100 ethoxylated groups (1EO-100EO). The mostly used APEs, nonylphenols ethoxylated (NPEs) has an alkyl chain ( $C_9H_{19}$ , usually branched) and a chain of 9-10 EO groups. With decreasing length of the EO chain, bioaccumulation and toxicity of APEs increases. The greater the number of EO units, the more water soluble the APE becomes. NPEs comprise about 80% of the total APEs market volume and octylphenols ethoxylated (OPEs) are most of the remaining 20% (Naylor, 2004; Jonsson, 2006).

For laboratory experiments artificial samples were prepared by mixing osmotic water with pure endocrine disruptors or precursors (all purchased by Sigma-Aldrich S.r.l). Table 2.1.2.a. reports the APs and APEs tested: 4-OP, 4-n-NP, TRITON<sup>TM</sup> X-100 and IGEPAL<sup>®</sup> CO-630. TRITON<sup>TM</sup> X-100 is a precursor of 4-*tert*-OP; it is commonly used as detergent in laboratories and it can be found in several types of cleaning compounds. IGEPAL<sup>®</sup> CO-630 is a precursor of branched 4-NP and with 9EO is known as Nonoxynol-9 (used in cleaning, cosmetics and contraceptive products).

Table 2.1.2.a. Tested APs and APEs.

Name	CAS Number Molecular Formula	Molar Weight (g/mol)	Molecular structure
4-n-nonylphenol	CAS 104-40-5 $C_{15}H_{24}O$	220	
4-octylphenol	CAS 1806-26-4 $C_{14}H_{22}O$	206	
IGEPAL CO-630	CAS 68412-54-4 $C_{15}H_{24}O(C_2H_4O)_n$ branched (n=9-10)	617 average	
TRITON X-100	CAS 9002-93-1 $C_{14}H_{22}O(C_2H_4O)_n$ branched (n=9-10)	625 average	

The first precursor was tested instead of 4-*tert*-OP because this OP has a category 2 carcinogenic effect (<http://www.sigmaaldrich.com/>; *Jonsson, 2006*) and the second precursor was tested instead of 4-NP because it has a lower estrogenic potential (*Soares, 2008; Asimakopoulos, 2012; Ying, 2012*). In addition, the removal of the precursors is interesting because it prevents the formation of APs (*Naylor, 2004; Ying, 2004; EPA, 2005; Jonsson, 2006; Ning, 2007; Soares, 2008; Ifelebuegu, 2011*).

### 2.1.3 Cations

Manganese and iron are metallic cations related to the corrosion of iron pipes and are the main source of coloration of drinking water in distribution systems. Corrosion in distribution systems restricts water flow, causing deterioration in terms of quality. The presence of iron and manganese in the systems, which may be soluble in the water, may cause sensory problems such as colored water, stains, dirt in the systems, and complaints by consumers (*Kawamura, 2000; Chaturvedi, 2012; Alvarez-Bastida, 2013*). An iron potential problem is the growth of iron bacteria within the distribution main; these bacteria may become dense enough in population to clog pipes and reduce flow rates (*Kawamura, 2000; Chaturvedi, 2012*). From the toxicological point of view, the adverse effects of manganese on human health depend on the route of exposure, the chemical species, and the age and nutrition status of the consumers. It is known that manganese exposure affects nervous system functions and may even cause an irreversible Parkinson-like syndrome known as manganism, which is characterized by weakness, anorexia, muscle pain, apathy, slow speech, emotionless "mask-like" facial expressions, postural difficulties, rigidity, tremors, decreased mental status, and slow, clumsy movements of the arms and legs. Studies in animals that have been exposed to different concentrations of manganese have revealed neurotoxic effects (*Alvarez-Bastida, 2013*). Iron intake has positive effects on our health in moderate doses and is an essential nutrient. Thus, intake of untreated water would not be harmful to our health (*Chaturvedi, 2012*). The Secondary Drinking Water Standards (EPA) recommends Maximum Contaminants Level (MCL) of 0.3 mg/l for iron and 0.05 mg/l for manganese.

Calcium and magnesium are the major divalent metallic cations that contribute to water hardness. Hard water is not currently known to adversely affect human health in any significant manner. Quite a few studies have demonstrated an inverse correlation between the incidence of cardiovascular disease and the hardness level of drinking water. Yet conflicting studies have also been reported (*Kawamura, 2000*). However many consumers prefer softened water due to convenience issues such as avoidance of removing limescale deposits from household appliances and surfaces, and to reduce consumption of cleaning agents and laundry detergents leading to lower household expenses (*Zappone, 2008; Godskesen, 2012*). Moreover, even though nowadays central softening of drinking water entailed an increased use of energy, sand and chemicals at the waterworks, the distributed

and softened drinking water supported a decrease in consumption of energy and chemical agents in the households along with a prolonged service life of household appliances which heat water (Godskesen, 2012).

For laboratory experiments artificial samples were prepared using a very hard commercial water to test the Ca(II) removal and by mixing osmotic water with  $\text{FeCl}_3 \cdot 6\text{H}_2\text{O}$  or  $\text{MnCl}_2 \cdot 4\text{H}_2\text{O}$  (purchased by Sigma-Aldrich) to test the Fe(III) and the Mn(II) removal respectively. With the purpose to increase the removal of Ca(II) the complexing agent ethylenediaminetetraacetic acid (EDTA purchased by Sigma-Aldrich) was added and the adsorption of the complexed Ca(II) on the powders used was tested.

## 2.2 Adsorbents

### 2.2.1 Magnetic Activated Carbons (MACs)

An adsorbent used to remove the tested pollutants was a Magnetic Activated Carbons (MACs) powder provided by MS-Engineering Ltd. (<http://www.ms-engineering.co.jp/eng/>). This is a synthetic powder obtained by precipitation on activated carbons of nanometric magnetite ( $\text{Fe}_3\text{O}_4$ ) particles. This precipitate reduces the adsorption sites of AC leading to a 20 to 30 % decrease of MACs adsorption ability with respect to ACs (Nakahira, 2006). Figure 2.2.1.a shows Scanning Electron Microscopy (SEM) and Transmission Electron Microscopy (TEM) images of MACs and Energy Dispersive X-ray Spectrometry (EDS) spectra confirming the presence of magnetite on AC surface (Nakahira, 2006).

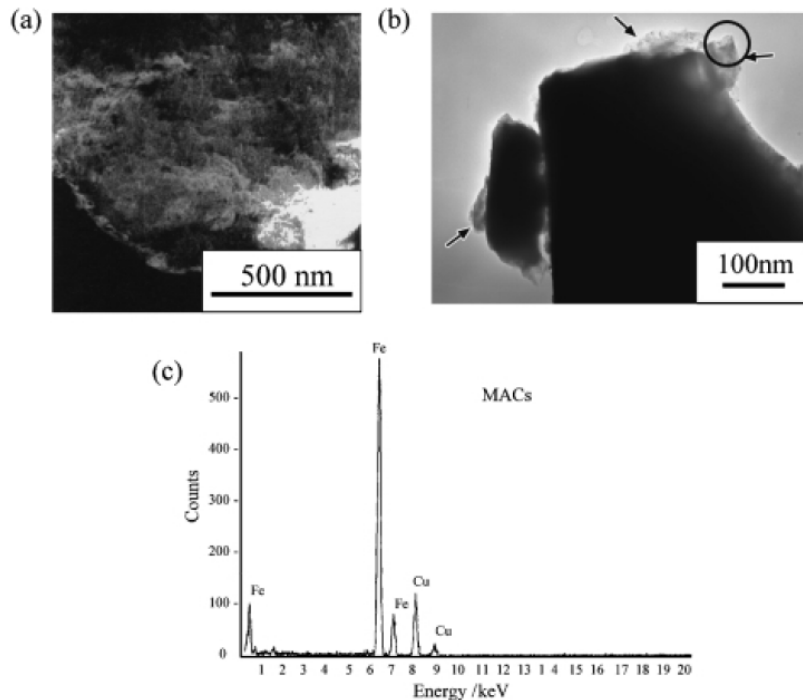


**Figure 2.2.1.a.** Images of (a) Scanning Electron Microscopy (SEM) and (b) Transmission Electron Microscopy (TEM) of MACs and (c) Energy Dispersive X-ray Spectrometry (EDS) spectra results regarding the circular area in the (b) image (Nakahira, 2006).

The particle's diameter is about 40-50 nm, it was measured suspending MACs in ethanol and using a FOQELS particle size analyzer of Brookhaven Instruments Corporation. However, when suspended in water solutions, MACs generate micrometric aggregates due to their hydrophobicity. During this research experiments an ultrasonic washing of 30 seconds was applied after MACs addition to the pollutant-water samples in order to break the particles' aggregates with the purpose of maximizing the MACs surface available for adsorption (Borghi, 2014a). The time necessary for the regeneration of the aggregates is less than 10 minutes; at the end of the adsorption phase the aggregates, which are necessary to allow the capture also with low magnetic fields, were restored. Figure 2.2.1.b shows two distributions of the aggregates' sizes of the MACs suspended in distilled water. They refer to the "as purchased" MACs and to the MACs after the ultrasonic washing. It can be seen that the ultrasonic washing changes the sizes distribution increasing by 2-3% in mass the particles fraction below about 3  $\mu\text{m}$ . The two distributions were obtained taking an image of the suspension with an optical microscope and analysing it with a self-developed Fortran code.

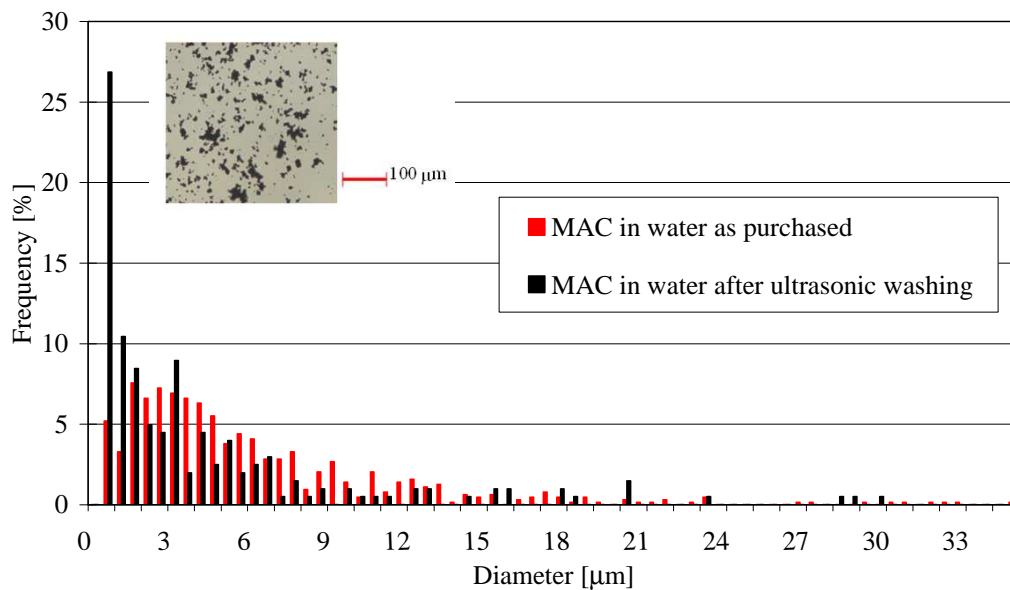


**Figure 2.2.1.b.** Sizes distribution of MACs aggregates in water with and without ultrasonic washing. The insert shows a sample of the optical image obtained with a MO that was numerically processed.

Activated Carbons (ACs) are obtained by the carbonization of carbonaceous raw material followed by an activation phase. They are excellent and versatile adsorbents that are used in many areas to remove organics, inorganics and vapours; the most important application of ACs adsorption is the purification of air and water, where large amounts of ACs are being consumed and where the consumption is ever increasing. ACs are used in powder, granular or fibrous form. In the last two forms they are usually fixed in beds, while ACs powders are suspended in water (Metcalf & Eddy, 2003; Bansal, 2005; Gaspard, 2008). The problem of ACs powder is their lack of magnetic properties that makes them removable

only by filtration or sedimentation with possible time and costs disadvantages. The combination of ACs with magnetite can exploit the advantages of both materials (*Do, 2011; Jia, 2011; Lu, 2013*). Thus this powder has the ACs part in order to adsorb pollutants and the magnetite part to be magnetically filtered. Considering that magnetite in MACs is around 1/3 and the small porosity and specific surface of magnetite compared to the AC it can be assumed that the adsorption on the iron oxide is negligible. The main characteristics of MACs are listed in Table 2.2.1.a. The  $pH_{pzc}$  (point of zero charge pH) was evaluated by measuring the electrophoretic mobility. At the  $pH_{pzc}$  the number of positive groups on the powder surface equals the number of negative ones and, as the pH increases, the number of negative groups increases too (*Bansal, 2005; Borghi, 2011*). The magnetization curve of MACs measured by Quantum Design PPMS is shown in Figure 2.2.1.c ( $\mu_0$  is the magnetic permeability of vacuum). As expected, due to their magnetite content, MACs show a ferromagnetic behaviour.

**Table 2.2.1.a.** Properties of MACs.

<b>Content <math>Fe_3O_4</math></b>	25-35 (% vol)
<b>Average Pore Diameter</b>	2.53 nm
<b>Pore Volume</b>	0.49 ml/g
<b>Specific Gravity (ISO 787/10)</b>	1.7 g/cm <sup>3</sup>
<b>Tamped Density (ISO 787/11)</b>	0.45 g/cm <sup>3</sup>
<b>Specific Surface (<math>\Sigma_A</math>)</b>	773 m <sup>2</sup> /g
<b><math>pH_{pzc}</math></b>	4
<b>Representative particle size</b>	40-50 nm
<b>Representative aggregate size</b>	1-3 $\mu$ m
<b>Magnetism</b>	ferrimagnetic

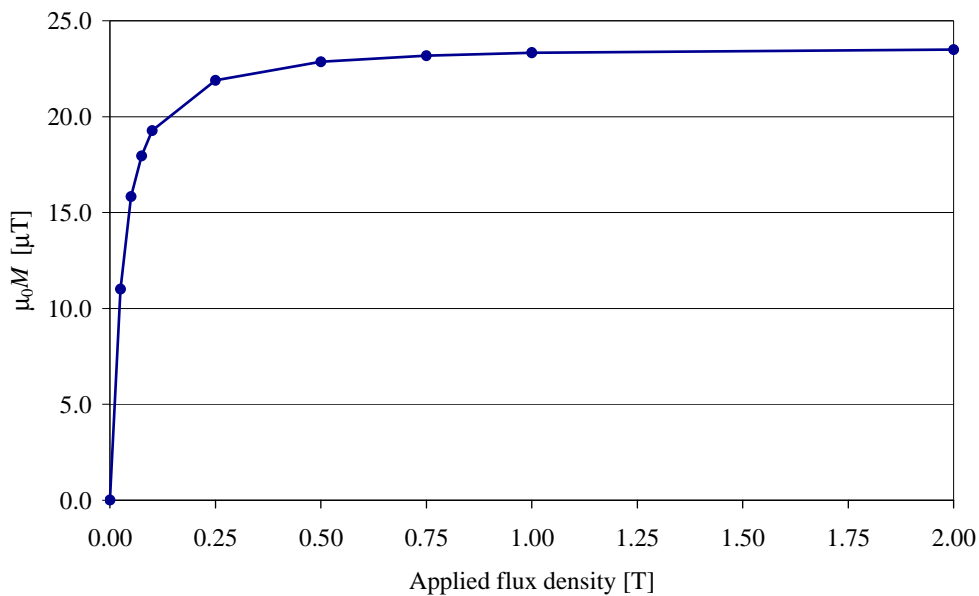


**Figure 2.2.1.c.** Magnetization curve of MACs.

### 2.2.2 Zeolite-Magnetite mixtures

Zeolites are capable of exchanging ions with external medium, which is the significant characteristic of zeolite. Ion exchange proceeds in an isomorphous fashion. The ion-exchange behaviour of natural zeolite depends on several factors, including the framework structure, ion size and shape, charge density of the anionic framework, ionic charge and concentration of the external electrolyte solution. Due to the formation environment, natural zeolite has varying chemical composition and cation-exchange capacity (Wang, 2010). The adsorption characteristics of any zeolite are dependent upon the detailed chemical/structural makeup of the adsorbent; the Si/Al ratio, cation type, number and location are particularly influential in adsorption. These properties can be changed by several chemical treatments to improve separation efficiency of raw natural zeolite (Wang, 2010). Natural zeolites have advantages over other cation exchange materials such as commonly used organic resins, because they are cheap, they exhibit excellent selectivity for different cations at low temperatures, they are compact in size and they allow simple and cheap maintenance in the full-scale applications.

There are many natural zeolites identified in the world. Clinoptilolite, mordenite, phillipsite, chabazite, stilbite, analcime and laumontite are very common forms whereas offretite, paulingite, barrerite and mazzite, are much rarer. The one purchased by Verdi S.p.a. is mainly chabazite thus, as shown in Figure 2.2.2.b (Margeta, 2013), it has a hexagonal structure. The structure of natural zeolite is very interesting and complex. The primary building units (PBU) of zeolites are the  $\text{SiO}_4$  and  $\text{AlO}_4$  tetrahedra. They connect via oxygen ions into secondary building units (SBU), which are then linked into a three-dimensional crystalline structure of zeolite. Substitution of Si by Al defines the negative charge of the zeolite framework, which is compensated by alkaline and earth alkaline metal cations. The higher the aluminium concentration, the higher is the overall lattice charge leading to hydrophilic materials. The adsorption capacity of zeolite decreases with decreasing polarity and polarizability of adsorbates. On the other hand, zeolites with a low aluminium concentration are increasingly more hydrophobic and selectively adsorb hydrocarbons over water (Kogelbauer, 2001). Therefore, natural zeolites appear as cations exchangers because they have negative charge on the surface (Payra, 2003; Wang, 2010; Margeta, 2013). Zeolites are also characterized by the unique property that the internal surface is highly accessible and can compose more than 98% of the total surface area. Surface areas are typically of the order of 300-700  $\text{m}^2/\text{g}$  (Payra, 2003). In the zeolite lattice, substitution is not limited to the Si-Al one. Atoms of iron, boron, chromium, germanium, and titanium may also substitute silicon. The water molecules can be present in voids of large cavities and bonded between framework ions and exchangeable ions via aqueous bridges. The water can also serve as bridges between exchangeable cations (Wang, 2010; Margeta, 2013).

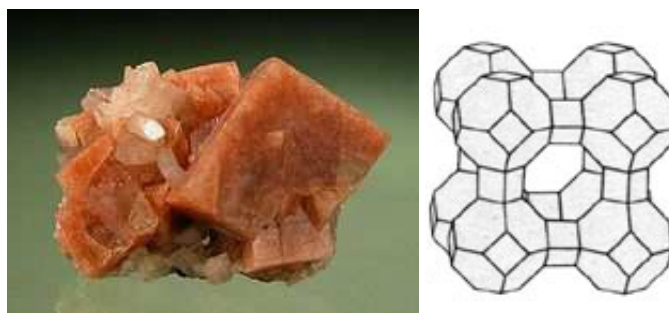
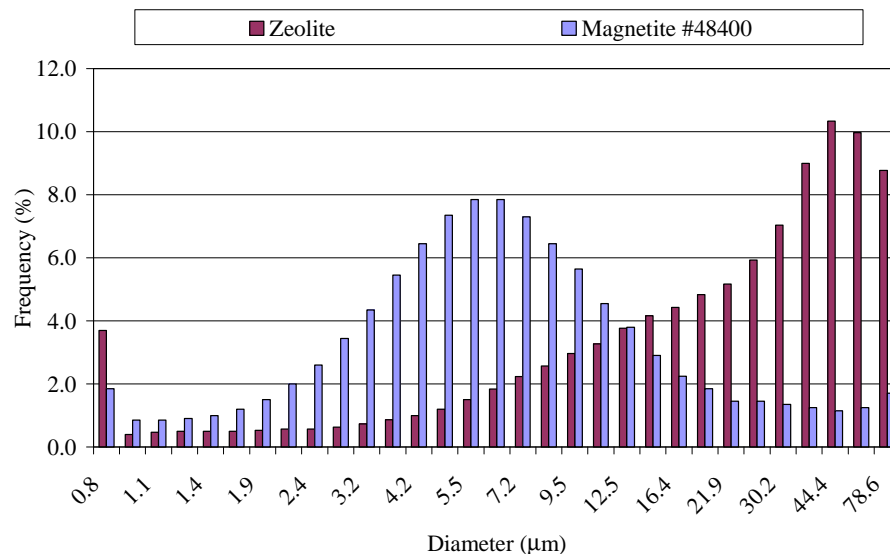


Figure 2.2.2.b. Chabazite hexagonal structure.

As for ACs powder a zeolite powder weakness is the lack of magnetic properties that makes it removable only by filtration or sedimentation with possible time and costs disadvantages. The combination of zeolites with magnetite can exploit the advantages of both materials (*Oliveira, 2004; Nah, 2008*). The synthesis of a modified adsorbent has producing costs. As an alternative to the laboratory-produced MACs powder, two mixtures of zeolite and magnetite bonded through the coagulant ferric chloride ( $\text{FeCl}_3 \cdot 6\text{H}_2\text{O}$  ACS grade) during the experiments, were generated. The properties of the used powders are described in Table 2.2.2.a. Fig. 2.2.2.a shows the frequency of the particle size distribution of each powder measured using Fritsch Laser-Particle-Sizer "Analysette 22". Magnetite #48400 was purchased by Kremer Pigmente GmbH and natural zeolite ZEOVER (Chabazite  $60 \pm 5\%$ , Phillipsite  $5 \pm 3\%$ , K-Feldspar  $4 \pm 2\%$ , Biotite  $2 \pm 1\%$ , Pyroxene  $4 \pm 1\%$ , Volcanic glass  $25 \pm 5\%$  and a Si/Al ratio of 2.5) was purchased by Verdi S.p.a. One mixture was made by the magnetite and the zeolite as purchased, the other was made by the magnetite as purchased and the zeolite after a Na-activation. The Na-activation (*Taffarel, 2009*) of the purchased zeolite ZEOVER was carried out by mixing it with 1 M solution of sodium chloride (NaCl). 50 g of material were mixed to 1 l of solution and left for 24 h at room temperature. The suspension was agitated in a glass flask using a magnetic stirrer and then filtered and washed three times with 1 l deionised water, dried at 120 °C for 24 h before being used in the adsorption studies.

Table 2.2.2.a. Properties of magnetite and zeolite powders.

	Magnetite 48400	Zeolite ZEOVER
Content $\text{Fe}_3\text{O}_4$	90 %	4 %
Average Pore Diameter	none	0.25- 0.7 nm
Pore Volume	none	0.5 ml/g
Tamped Density (ISO 787/11)	0.8-1.2 g/cm <sup>3</sup>	0.7-0.9 g/cm <sup>3</sup>
Specific Surface ( $\Sigma_A$ )	11 m <sup>2</sup> /g	336 m <sup>2</sup> /g
pH <sub>pzc</sub>	7.5	8.4
Representative aggregate size	5-7 μm	50-60 μm
Magnetism	ferrimagnetic	none



**Figure 2.2.2.a.** Experimental size distributions for magnetite powder #48400 and zeolite ZEOVER powder.

## 2.3 Adsorption and adsorbents removal tests

The adsorption of a solute from a solution is influenced by several factors: the porosity and the chemical nature of the solid surface, the nature of the components of the solution, the concentration of the solution, salts and molecules in the aqueous phase that can compete for adsorption sites, the adsorption time, the pH of the solution that determines the electric charge of the solid surface (*Bansal, 2005*). Positive, negative and neutral functional groups can coexist on the surface. At  $\text{pH} < \text{pH}_{\text{pzc}}$  (pH of zero charge) the positive groups predominate over the negative ones, i.e. although the surface has a net positive charge, some negative groups are still present. At the  $\text{pH}_{\text{pzc}}$  the number of positive groups equals the number of negative ones and as the pH increases, the number of negative groups increases (*Cornell, 2003; Bansal, 2005*). The adsorption of a nonpolar solute will be higher on a nonpolar adsorbent. Since there is competition between the solute and the solvent, the solvent should be polar in nature for the solute to be adsorbed preferentially. Other factors that also determine the adsorption from solutions are the hydrogen bonding and the steric arrangement or the chemical structure of the adsorbate molecule. As the AC have a highly microporous structure, some of the pores may be inaccessible to larger molecules of the adsorbate (*Bansal, 2005*).

Each test started generating a sample by diluting the considered pollutant with osmotic water or tap water. The pH of the water was not changed to improve the adsorption as reported in literature (*Chun, 2001; Dobiàs, 2005; Higgins, 2006*) since these values were (i) in the correct range for a biological treatment of a WWTP (*Metcalfe & Eddy, 2003*), (ii) already compatible with the ones allowed for discharge according to Italian regulation 152/2006 (between 5.5 and 9.5). Moreover, in real WWTP the pH can not be changed without a significant increase of costs. Then, the concentration of the pollutant

was measured. The initial sample was divided in three/five equal jars and different amounts of powder were added. As reported in Figure 2.3.a (a), each subsample was mixed for 10 minutes (about 60 rpm) to allow the adsorption of the pollutant on the adsorbent particles. After the adsorption step the powder separation step Figure 2.3.a. (d) was carried out immediately for 10 minutes or, if the coagulant  $\text{FeCl}_3 \cdot 6\text{H}_2\text{O}$  was added as shown in Figure 2.3.a (b), after 2 minutes of rapid mixing and 5 minutes sedimentation (Figure 2.3.a (c)) and lasted only 5 minutes. In the last case, the filtration system was filled only with the clarified part of the suspension. Finally, the concentration of the pollutants remaining in the treated water was measured.

Hach-Lange and Nanocolor tubes-tests have been used to measure the pollutants concentration before and after each test (<http://www.Hach-Lange.com>; [www.mn-net.com](http://www.mn-net.com)). The procedures of the tube-tests are reported in Appendix II. A particular care was kept in maintaining tubes and samples at a temperature between 20 °C and 25 °C for the correct kinetic of the chemicals reactions. For the same reason it was always verified that the pH of the samples was between 4 and 9. A Hach-Lange spectrophotometer DR2800 was used to evaluate the solutes concentrations; the measured optical absorbance was converted to the concentration value using an experimentally determined calibration curve. The error on the measures produced by the residual powders after the filtration was taken into account by measuring the absorbance of filtered samples made only by distilled water and the used powders, i.e. without pollutants.

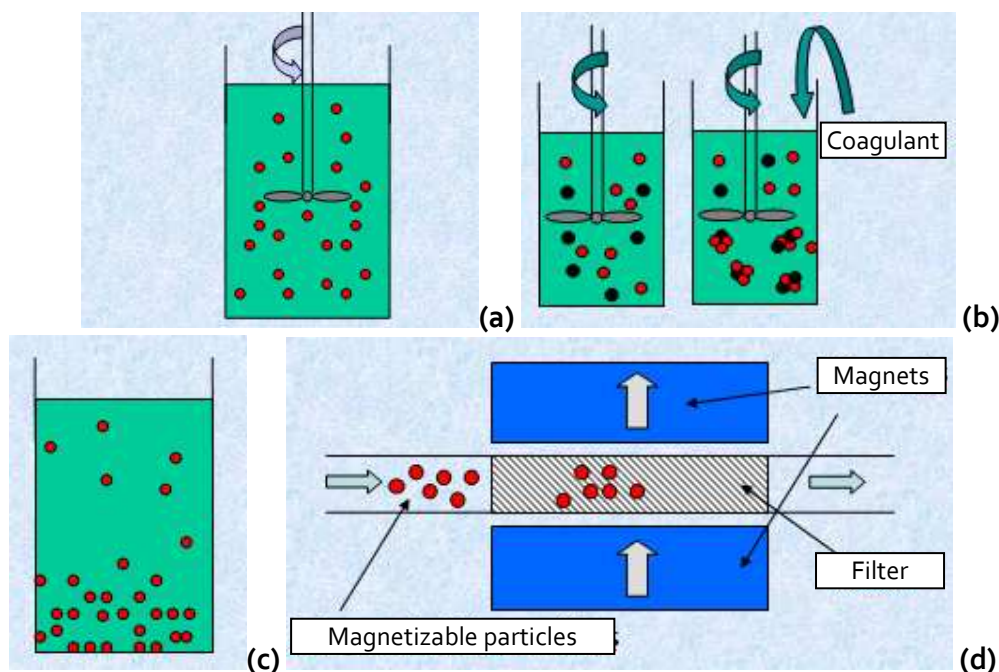


**Figure 2.3.a.** 10 minutes adsorption step (a) eventually followed by the addition of Ferric chloride, 2 minutes of rapid mixing (b) and a 5 minutes sedimentation step (c). Filtration with or without addition of coagulant and sedimentation, lasting 5 or 10 minutes respectively (d).

In addition to the separations carried out during the adsorption tests, many sets of powder/water mixtures with and without ferric chloride were prepared and their turbidity vs. time was measured using a turbidity meter (Hanna Instruments 93703). Each separation test started creating a sample of tap water and adding to it 0.5 g/l of MACs or 0.5 g/l of zeolite and 0.25 g/l of magnetite. After an ultrasonic bath of 30 s in order to break powder aggregates, the mixture was homogenised using a magnetic stirrer. In all the tests with the addition of ferric chloride ( $\text{FeCl}_3 \cdot 6\text{H}_2\text{O}$ ), an amount of 15 mg/l (corresponding to 3 mg/l of Fe(III)) was added and followed by 2 minutes of rapid mixing in order to destabilize the solution and to allow the Fe(III) ions oxidation and deposition. This concentration of the coagulant is acceptable for water treatment. Thus, the samples were subjected to sedimentation or filtration or both. In the last case, the filtration system was filled only with the clarified part of the suspension. The filtration was carried out using continuous-flow magnetic filtration devices.

## 2.4 Filtration experimental setups

Two experimental setups (Borghi, 2014a) significantly different in terms of size, external flux density field, water flow rate and average velocity in the filter, were manufactured and tested (Figure 2.4.a and Figure 2.4.b). Both magnetic filtration devices consisted of a tank, input and output rubber pipes, a magnetic separation unit and a pump. Thus, the fluid circulated inside a closed-cycle system. The flow started from a tank filled with a mixture of water, pollutant, adsorbent powder (and eventually ferric chloride) and returned to the same reservoir after passing through the magnetic filter located between two permanent magnets (or on one permanent magnet in setup #1) which provided the external flux density field in the filter volume, mainly orthogonal to the fluid flow. The generated magnetic force was able to capture and withhold the powder particles against the drag force of the surrounding fluid and the effects of Brownian motion.

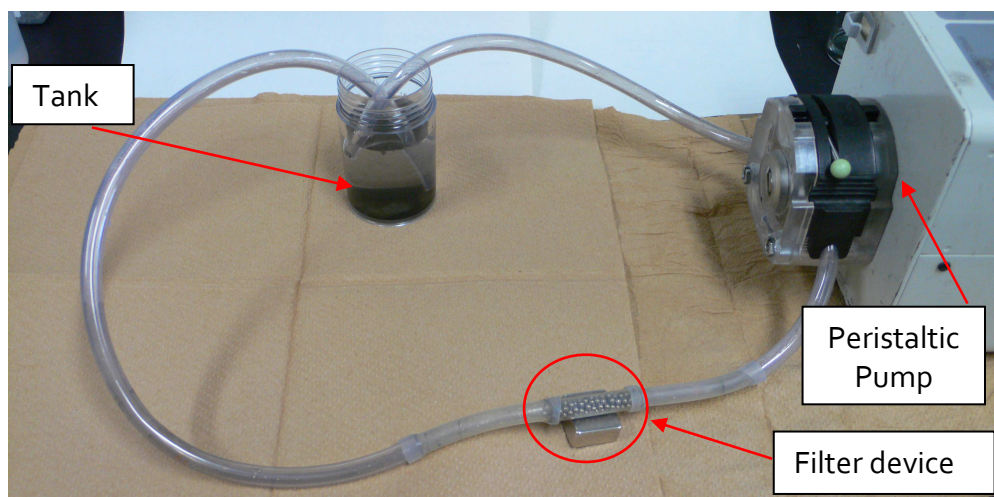


Figure 2.4.a. Experimental setup #1.

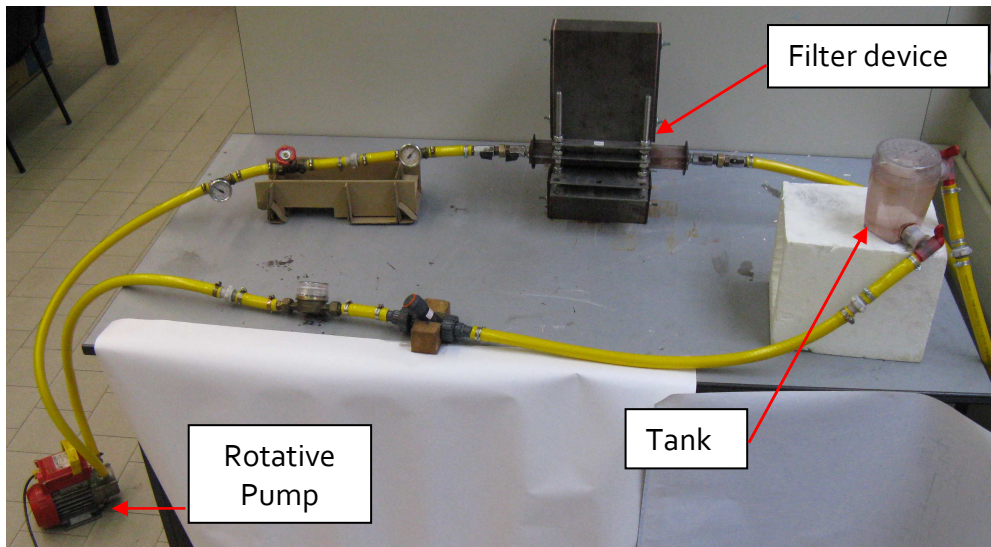


Figure 2.4.b. Experimental setup #2.

The filter was made of tightly packed stainless steel spheres that are commercial bearings produced by Koyo Italia S.r.l (Figure 2.4.c). The filter progressively clogged reducing its filtration efficiency and requiring a periodic wash or a substitution. Table 2.4.a shows the main parameters of the two systems with the steel spheres filter and the symbol used. The effective susceptibility  $\chi_{s,eff}$  of the steel takes into account the spheres demagnetizing factor (Fiorillo, 2004; Mariani, 2009). The average fluid velocity  $u_o$  was calculated on the free water section (evaluated using the section filling factor). The applied external magnetic flux density field is relatively uniform in the filter volume; the values reported in Table 2.4.a refer to the maximum value in the centre and the lowest one on the inlet and outlet sections. The direction and the intensity of the magnetic flux density field are not constant in each cross section of the filter with a prevalence of the component normal to the flow velocity. Figure 2.4.d reports the magnetization curve of the steel spheres showing the correlation between the magnetic flux density  $\mathbf{B}$  and the magnetic field  $\mathbf{H}$ ; the asymptote represents the spheres saturation level.

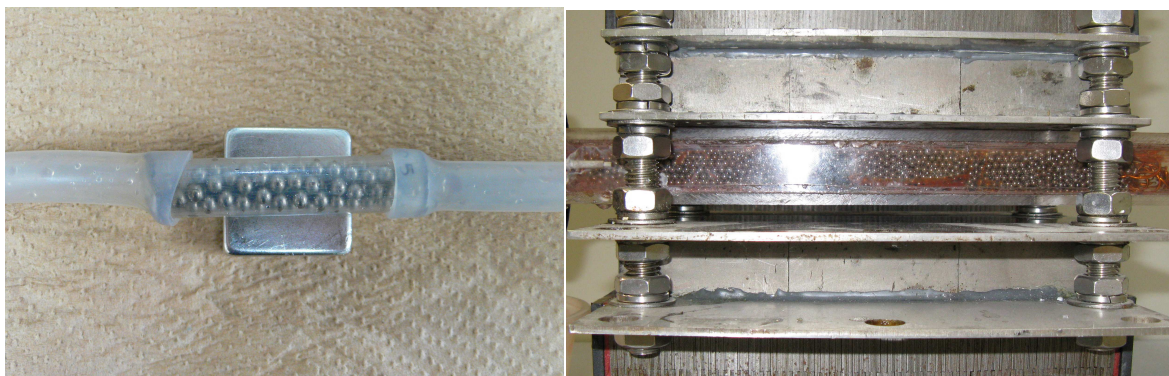
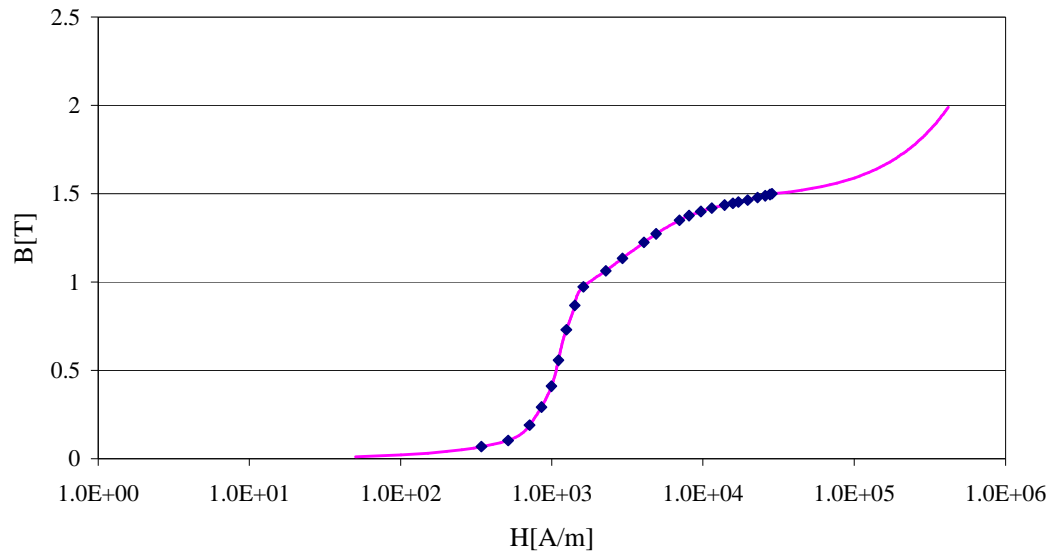


Figure 2.4.c. Zoom of the filter device of setup #1 (left) and setup #2 (right) filled with spheres on a Nd-Fe-B permanent magnet and between two Sm-Co permanent magnets respectively.

**Table 2.4.a.** Magnetic filtration systems data.

	<b>Experimental setup #1</b>	<b>Experimental setup #2</b>
<b>Filter data</b>		
<b>Material</b>	SUS440C	SUS440C
<b>Saturation Magnetization</b>	1.1 T	1.1 T
<b>Spheres Number</b>	100	6900
<b>Relative permeability</b>	200	200
<b>Effective Susceptibility <math>\chi_{s,eff}</math></b>	2.9	2.9
<b>Diameter, <math>d_s</math></b>	3 mm	3 mm
<b>Volume Filling Factor</b>	55%	55%
<b>Section Filling Factor</b>	78%	78%
<b>Cross Section</b>	Circular, 64 mm <sup>2</sup>	Rectangular, 37 mm × 23 mm
<b>Lenght</b>	40 mm	210 mm
<b>Average Fluid Velocity, <math>u_o</math></b>	0.16 m/s	1.3 m/s
<b>Circuit data</b>		
<b>System Volume, <math>V</math></b>	0.1 l	2.5 l
<b>Flow Rate, <math>q</math></b>	2.24 cm <sup>3</sup> /s	240 cm <sup>3</sup> /s
<b>Tubes inner diameter</b>	7 mm	18 mm
<b>Fluid velocity inside tubes</b>	5.8 cm/s	94 cm/s
<b>Filtration time</b>	10-20 min	10-20 min
<b>Pump</b>	Roller	Rotative
<b>Fluid Viscosity, <math>\eta</math></b>	1 mPa.s	1 mPa.s
<b>Magnet -to-filter gap</b>	1-2 mm	5-6 mm
<b>External Magnet data</b>		
<b>Ingot Dimensions</b>	25 mm × 25 mm × 12 mm	70 mm × 70 mm × 30 mm
<b>Ingot Material</b>	1 Nd-Fe-B ingot	6 Sm-Co ingots
<b>Remanence</b>	0.4 T	1.05 T
<b>Magnetic circuit</b>	absent	C-shaped
<b>Applied Flux Density Field, <math>B_o</math></b>	50-100 mT	450-500 mT



**Figure 2.4.d.** Magnetic **B-H** characteristic of the stainless steel SUS440C.

## Chapter 3

### Adsorbents Removal

#### 3.1 Magnetic Activated Carbons (MACs)

MACs were separated using the magnetic filtering device of both the setups described in section 2.4. A turbidity meter (HI 93703) was used to evaluate the MACs concentration in the systems. The MACs concentration was deduced using an interpolating curve based on the values reported in Table 3.1.a.

**Table 3.1.a.** Correlation values between turbidity and MACs concentration.

<b>MACs concentration</b>	0.01 g/l	0.03 g/l	0.05 g/l	0.1 g/l	0.5 g/l
<b>Turbidity</b>	4.7 FTU	8.6 FTU	15 FTU	26 FTU	47 FTU

Figures 3.1.a and 3.1.b shows experimental MACs residuals for setups #1 and #2 respectively, defined as

$$\text{Residual (\%)} = \frac{C_r}{C_0} \times 100 \quad (3.1.1)$$

where  $C_0$  and  $C_r$  are the initial and the residual MACs concentration, i.e. before and after the filtration. Figure 3.1.a reports the results obtained for setup #1, showing that the experimental removal of MACs after 10 minutes filtration was  $93 \pm 6\%$ . The residual was nearly constant after 5 minutes of filtration. Figure 3.1.b reports the same results for setup #2. The experimental removal of MACs after 10 minutes filtration was  $98 \pm 2\%$ . The removal was very fast at the beginning of filtration and then slowly decreased. In both cases filtration without external field, i.e. mechanical filtration, led to worse and spread results; the effect of the magnetic flux density field on the filter's performance can be clearly seen since without external field the MACs residual was much larger. The relatively small capture obtained with the mechanical filtration may be due to the residual magnetization of the spheres, which were reused from previous experiments.

Moreover, in order to analyze the behaviour of a synthetic magnetically-modified powder with the addition of a coagulant, a series of filtration and/or sedimentation tests with and without the addition of Ferric Chloride was made on MACs. The results in terms of residual percent turbidity defined as

$$\text{Residual Turbidity (\%)} = \frac{\text{FTU}_r}{\text{FTU}_0} \times 100 \quad (3.1.2)$$

where  $\text{FTU}_0$  and  $\text{FTU}_r$  are the initial and the residual MACs turbidity, i.e. before and after the filtration, are reported in Figure 3.1.c. The initial turbidity values were always between 40 and 70 FTU. All the data have an error of about  $\pm 7\%$  and  $\pm 3\%$  during the sedimentation and

filtration, respectively. The turbidity after 10 minutes filtration is in the range 3 FTU - 7 FTU and reaches 0.5 FTU - 5 FTU after 20 minutes. It can be seen that the main decrease occurs in the first minute of filtration. The Italian regulation 152/2006 sets limits on TSS (Total Suspended Solids) but these are not easily correlated with the turbidity because the relationship depends on the type of suspended solid. However the turbidity values obtained at the end of the magnetic filtration process are about 5 FTU; this value corresponds to the limpidity of the drinking water recommended in (*WHO, 2006*). Anyway, this does not imply that this water can be drinkable without further toxicological analysis on MACs.

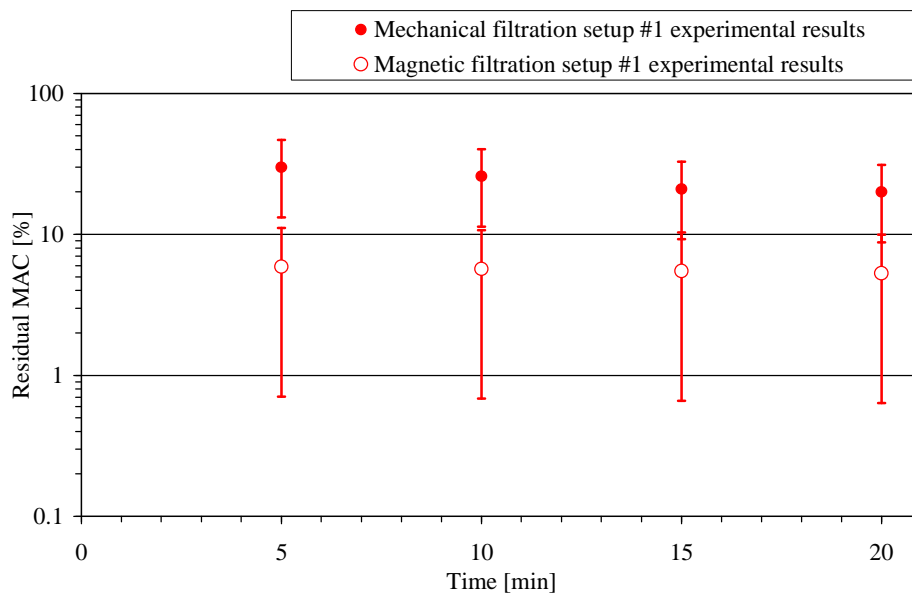


**Figure 3.1.a.** Comparison between the MACs residuals after the filtration in setup #1 with and without the application of the magnetic field produced by the permanent magnet.

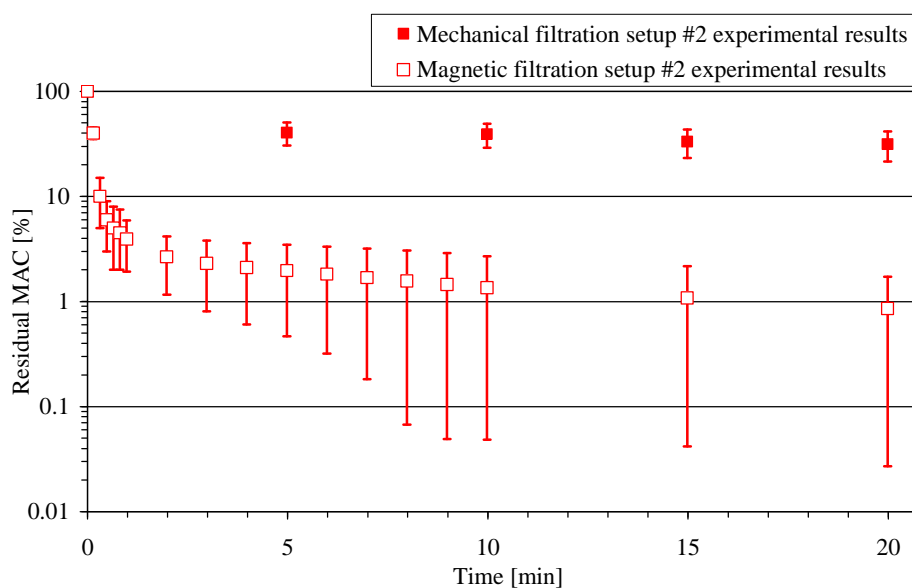


**Figure 3.1.b.** Comparison between the MACs residuals after the filtration in setup #2 with and without the application of the magnetic field produced by the permanent magnets.

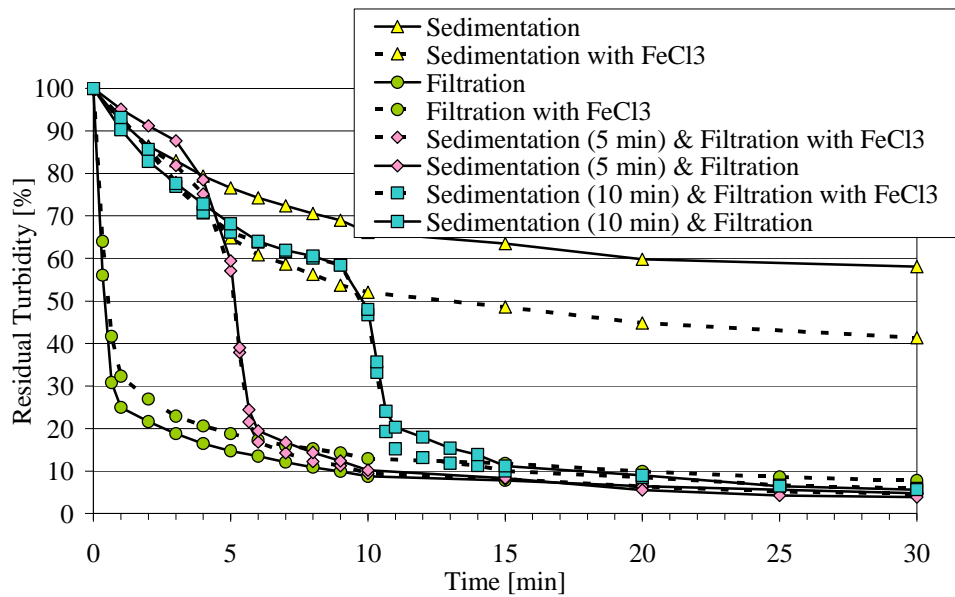


**Figure 3.1.c** Percent reduction of the turbidity vs. time for MACs sedimentation and/or filtration with (dashed lines) and without addition of ferric chloride.

All the test reported in Figure 3.1.a, 3.1.b and 3.1.c were performed using 0.5 g/l of MACs because this concentration was usually sufficient to capture near all the studied pollutants in (Borghini, 2014a; Borghini, 2014b). The results show that the behaviour of the MACs with and without coagulant is very similar, as expected because they are already magnetic. Its addition improved the sedimentation of MACs of about 15-20% but did not improve the filtration significantly. Because the Fe(III) ions generated by the addition of ferric chloride could also remain in solution, the Fe(III) residual was checked after every test resulting under the limit of 20 µg/l of the tube test. This value is well below the MCL level of 0.3 mg/l recommended by the Secondary Drinking Water Standards (EPA).

### 3.2 Zeolite-Magnetite mixtures

Zeolite-magnetite mixtures were separated using only the magnetic filtering device of setup #2. The turbidity meter (HI 93703) was used to evaluate the turbidity. Test with and without a preliminary sedimentation and with and without the addition of ferric chloride were performed. These tests helped the evaluation of the applicability of the magnetic seeding technique to a non magnetic adsorbent. The results reported in Figure 3.2.a show the residual percent turbidity (defined in (3.1.2)) without ferric chloride addition. The initial turbidity values were always between 150 and 200 FTU. In Figure 3.2.b are shown the results with the addition of the coagulant.

The coagulant addition effects on the efficiency of the separation varying the sedimentation times. Different tests were performed in order to find the best combination of sedimentation and filtration times with the aim to reduce spaces and times of the treatment. The magnetic filtration was applied immediately or after 5, 10, 15 minutes of

sedimentation. All the reported data have an error of about  $\pm 7\%$  and  $\pm 3\%$  during the sedimentation and filtration, respectively. All the tests were made with a 2:1 (mass ratio) mixture zeolite-magnetite. This proportion was chosen to have a significant magnetization in the aggregates without generating too much sludge. It can be seen in Figure 3.2.b that the turbidity after 20 minutes is in the range 3 FTU - 10 FTU, close to the WHO suggestions. Anyway, this does not imply that this water can be drinkable without further toxicological analysis on the zeolite-magnetite mixtures (WHO, 2006).

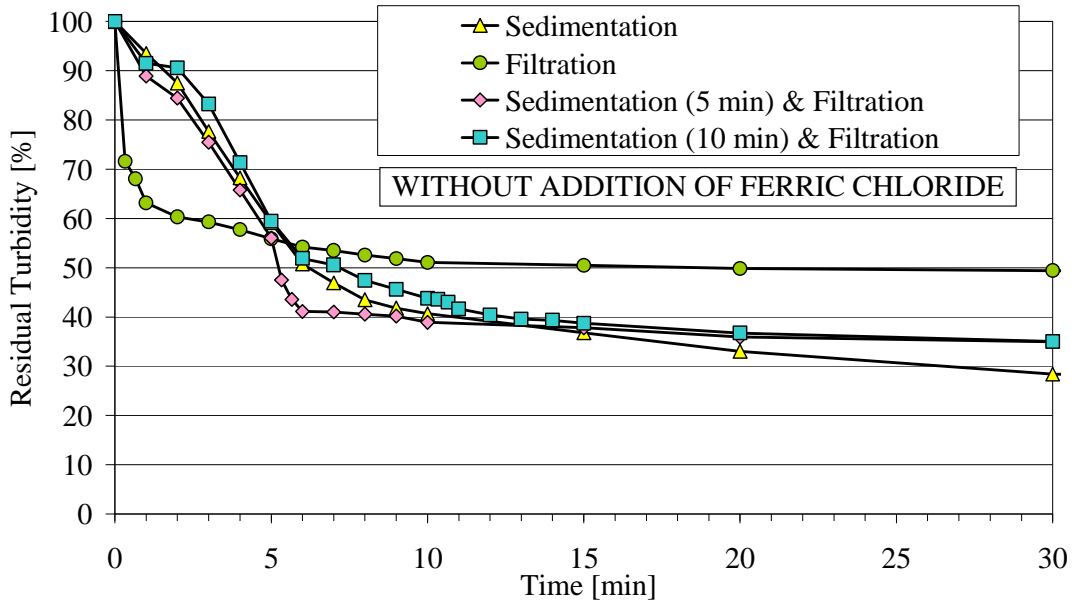


Figure 3.2.a. Percent reduction of the turbidity vs. time for Magnetite-zeolite mix sedimentation and/or filtration without addition of ferric chloride.

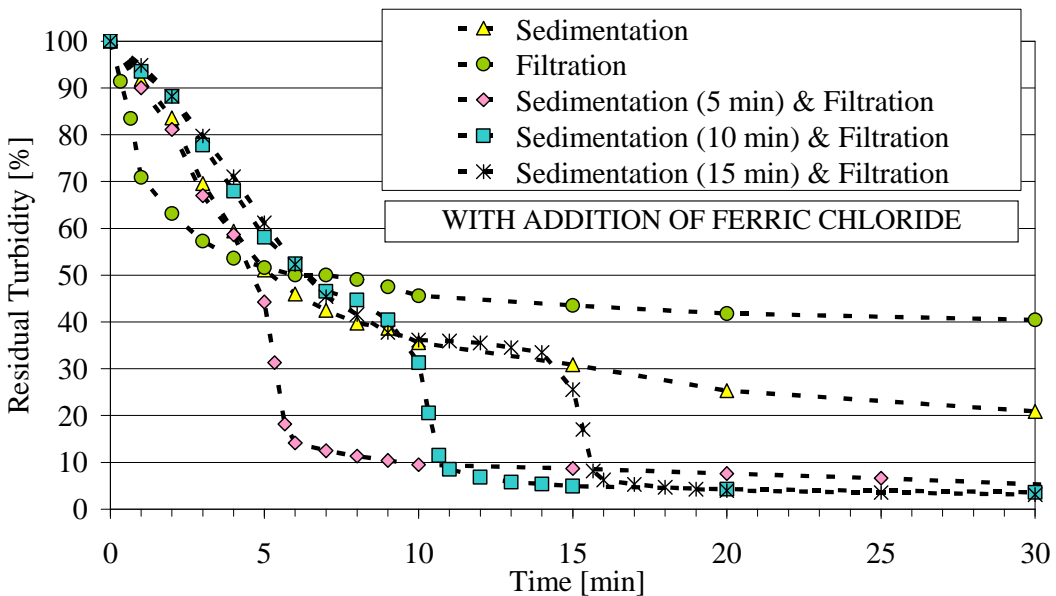


Figure 3.2.b. Percent reduction of the turbidity vs. time for Magnetite-zeolite mix sedimentation and/or filtration with addition of ferric chloride.

It can be seen in Figure 3.2.a that all the curves without ferric chloride addition behaved essentially in the same way during the sedimentation phase. However, if the filtration was applied immediately the percent turbidity residuals were larger than the corresponding sedimentation ones after 10 minutes while in the first minutes were smaller. This was probably due to the rapid removal of the magnetite fraction inside the filter while all the zeolite content was not captured and maintained in suspension by the pump. Moreover, the curves which report the results of sedimentation followed by filtration show that after 5 minutes there was still a fraction of magnetite in the suspension that was rapidly captured by the filter and that after 10 minutes sedimentation was completely removed. The reduction of the percent turbidity with respect to the immediate filtration case can be due to the reduction of the zeolite content during the previous sedimentation phase.

Figure 3.2.b shows the importance of the coagulant and its critic effect on the filtration efficiency. The generated Fe(III) ions promoted the formation of micrometric or millimetric aggregates of the two powders that are magnetic and easier to remove than the original zeolite-magnetite mix. Comparing Figure 3.2.a and 3.2.b it can be seen that the addition of the ferric chloride improve the sedimentation of about 10%, as expected. All the curves behave essentially in the same way during the sedimentation phase, as in Figure 3.2.a. Again, if the filtration was applied immediately the percent turbidity residuals were larger than the corresponding sedimentation ones after 10 minutes while in the first minutes were smaller. The reason may be that there was not enough time for the formation of the aggregates and therefore the rapid removal of the magnetite fraction inside the filter leaved in suspension almost only zeolite. However, the curves which report the results of sedimentation followed by filtration show that with at least 5 minutes of sedimentation there was a floccs formation which included magnetite. This can be seen from the strong decrease of the percent turbidity at the beginning of the filtration. Increasing the time of sedimentation to 10 and 15 minutes lead to an enlargement of the floccs (*Kawamura 2000; Metcalf & Eddy 2003; Amirtharajah, 2005*). This has beneficial effects on sedimentation and reduces the total amount of powders introduced in the filter. Moreover, the magnetic filter efficiency is increased by the larger dimensions of the aggregates allowing getting a lower final turbidity (*Borghini, 2014a*).

It can be seen from Figure 3.2.b that the percent residual turbidity after 10 or 15 minutes of filtration was almost the same. Anyway, even if the total time is the same, reducing the filtration time can have a positive effect on the process and maintenance costs. In fact the reduced content of powder in the filter allows enlarging the times between ultrasonic cleaning. The conclusion can be that the best compromise between sedimentation and filtration is of 15 minutes sedimentation followed by 5 minutes of filtration. Because the Fe(III) ions generated by the addition of ferric chloride could also remain in solution, the Fe(III) residual was checked after every test resulting under the limit of 20 µg/l of the tube test (like during the tests with MACs and ferric chloride).

## CHAPTER 3: ADSORBENTS REMOVAL

## Chapter 4

### Numerical Modelling

A statistical study of the interaction particle-filter elements of a control volume at the centre of the filter (cell) was developed with periodicity conditions. The solutions of the magnetostatic problem and the fluid dynamics in the cell were obtained by an integral approach. The analysis of a small portion of the filter, but statistically representative, eliminates the need to model the entire device on the micrometer scale, with unacceptable computational costs, and constitutes the basis for the analysis of the efficiency of the proposed magnetic filtration process. The aim of the model is to provide indications regarding the influence of design parameters on separation efficiency.

#### 4.1 The spheres filter

The spheres filters of setup #1 and setup #2 were made of tightly packed SUS440C stainless steel spheres with a diameter of 3 mm. In three-dimensional Euclidean space, the densest packing of equal spheres is achieved by a family of structures called close-packed structures. Two simple arrangements within the close-packed family correspond to regular lattices (see Figure 4.1.a).

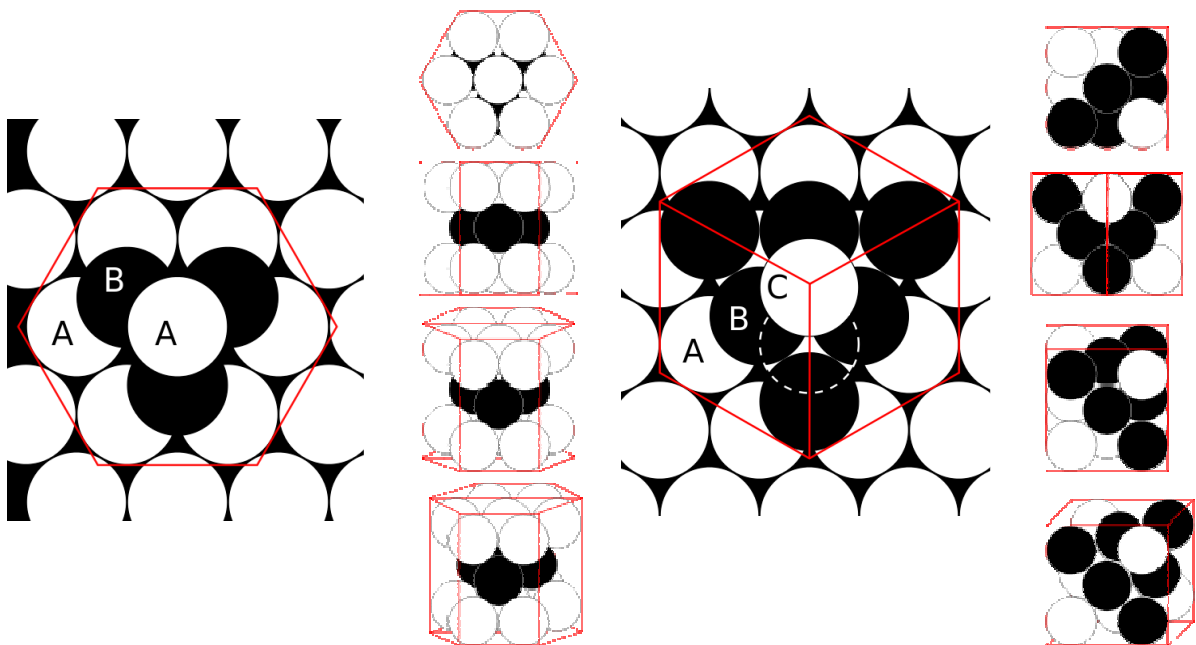


**Figure 4.1.a.** Hexagonal close packing (left) and cubic close packing or face centred cubic FCC (right).

The one on the right in Figure 4.1.a is called cubic close packing (or face centred cubic), the layers are alternated in the ABCABC... sequence. The one on the left is called hexagonal

close packing and the layers are alternated in the ABAB... sequence. But many layer stacking sequences are possible (ABAC, ABCBA, ABCBAC, etc.), and still generate a close-packed structure. As reported in *Borghi, 2014a* the model of the spheres filters was developed by modelling the simplest close-packed structure: the face-centred cubic (FCC) lattice created by the spheres.

Modelling one elementary cell allows deducing the filter capture efficiency for the two experimental setups and the scaling up to larger filters also. The main hypothesis of the model is that each particles' aggregate is spherical, suspended in the fluid, and subjected to the magnetic and fluid-dynamic forces. The gravitational force and the interaction among magnetized particles' aggregates are neglected.

The elementary cell was chosen as  $1/8$  of the FCC cell lattice in order to reduce the computational effort in evaluating the flux density and the water velocity fields. Assuming tightly packed spheres with 3 mm diameter, the elementary cell is cubic and has a side of 2.12 mm. It contains four octants of sphere centred on opposite corners as shown in Figure 4.1.b(a). The complementary volume shown in Figure 4.1.b(b) is the physical domain for the water flow and the particles inside it. A right handed Cartesian coordinate system Oxyz, with the origin defined in the left-down corner of the elementary cell shown in Figure 4.1.b and the axes parallel to the cell edges, was considered. The inlet section for the water flow was assumed to be in the  $y = 0$  plane. The external flux density field  $B_0$  was assumed to be uniform in the cell and directed along the z axis.

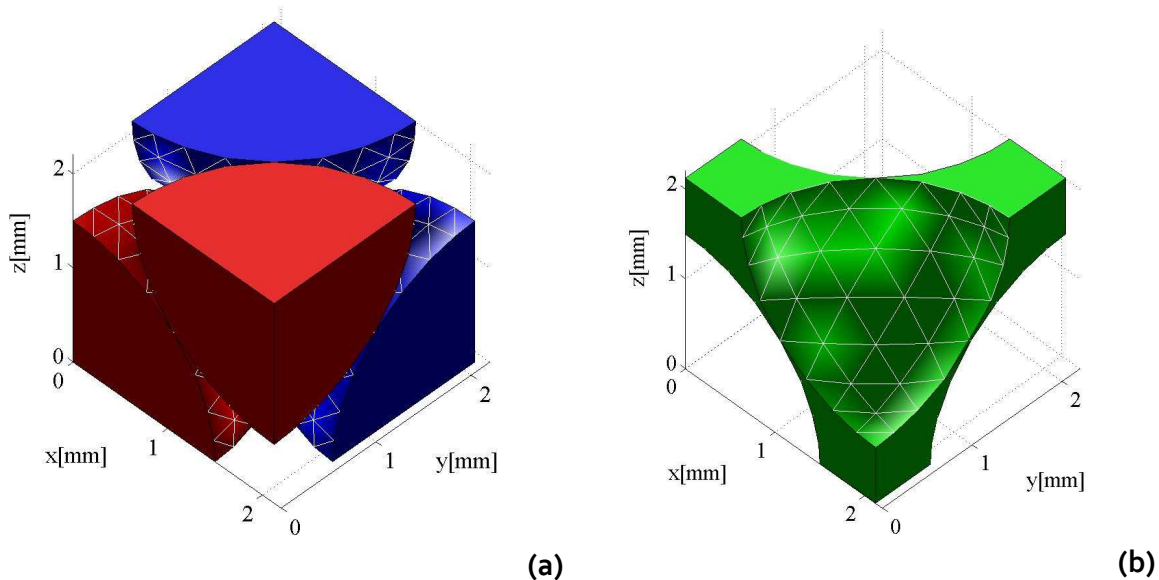
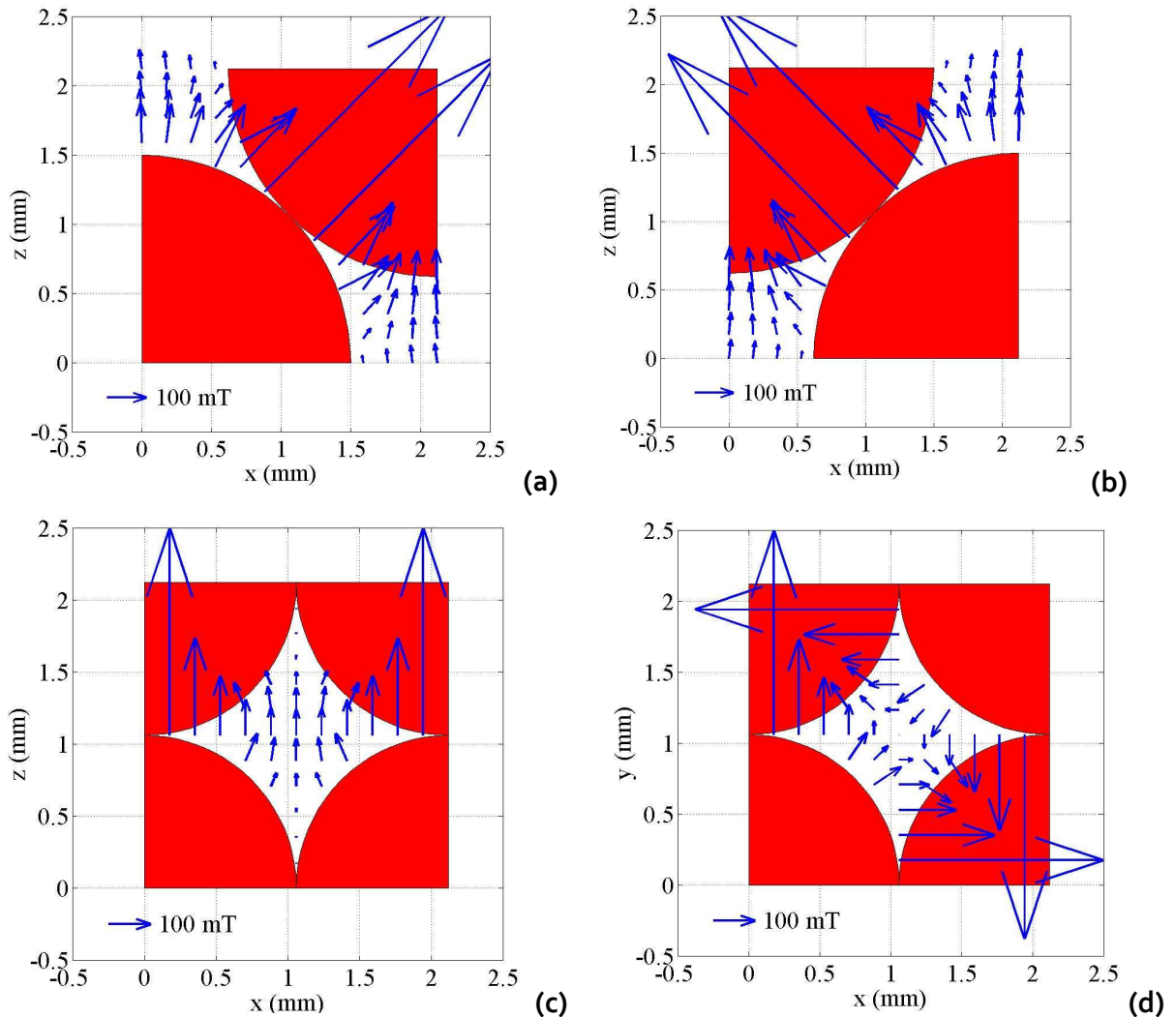


Figure 4.1.b. Spheres filter elementary cell: (a) steel and (b) water.

The flux density field  $\mathbf{B}$  inside the cell is assumed to be stationary. The water velocity field  $\mathbf{u}$  inside the cell is assumed to be stationary and laminar. The effect of filter clogging is not taken into account. The flux density  $\mathbf{B}(\mathbf{x})$  and the water velocity  $\mathbf{u}(\mathbf{x})$  fields are defined as point-dependent functions in the pre-processing stage through the volume integral equation method (*Fabbri, 2008; Mariani, 2010; Morandi, 2010; Borghi, 2014a*). This method

lead to calculate the field's sources (in a  $3 \times 3 \times 3$  array of cells surrounding the studied one) which are defined inside the discretized spheres. Each sphere is discretized with 512 tetrahedrons. Thus the flux density field  $\mathbf{B}(\mathbf{x})$  and the water velocity  $\mathbf{u}(\mathbf{x})$ , when evaluated outside the spheres, i.e. inside the water, do not suffer of singularities or discontinuities and are continuous and differentiable functions of the point  $\mathbf{x}$ . This complies well with the numerical integration of particle's trajectories where the gradients of the fields are needed in order to evaluate the forces. The distributions of magnetic flux density on the input, output and middle  $y$ -sections and on the middle  $z$ -section of the elementary cell are shown in Figure 4.1.c, for an external  $z$ -directed uniform field of 100 mT. The maximum values of the magnetic flux density are obtained near the tangency points among the upper and lower spheres.



**Figure 4.1.c.** Magnetic flux density field distributions on the input (a), output (b) and middle (c)  $y$ -sections and on the middle (d)  $z$ -section of the elementary cell.

The magnetization distribution in one octant and in one elementary cell is shown in Figure 4.1.d. Note that the magnetization is strongly non-uniform inside the spheres. The

magnetic force takes the maximum values near the tangency point where is nearly radial and inward directed. The magnetic force distribution in the elementary cell is reported in Figure 4.1.e.

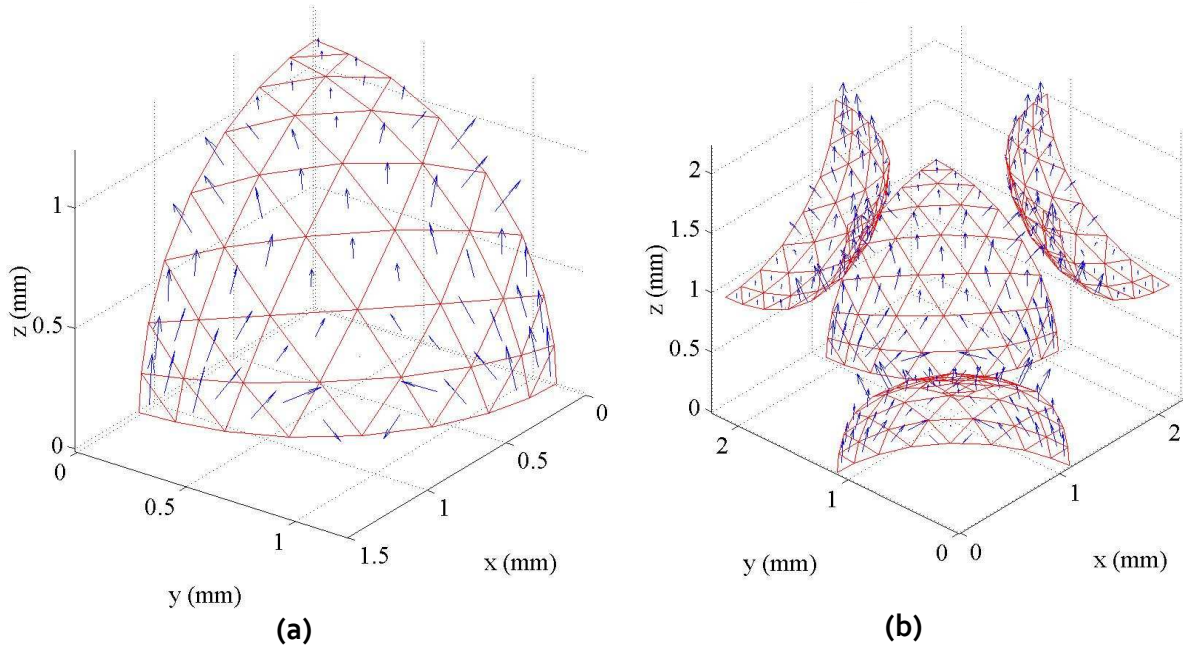


**Figure 4.1.d.** Magnetization distribution in one octant (a) and in the elementary cell (b). As an aid for visualization the triangles show the sections of the volume elements through each barycentre, where the magnetizations are displayed.

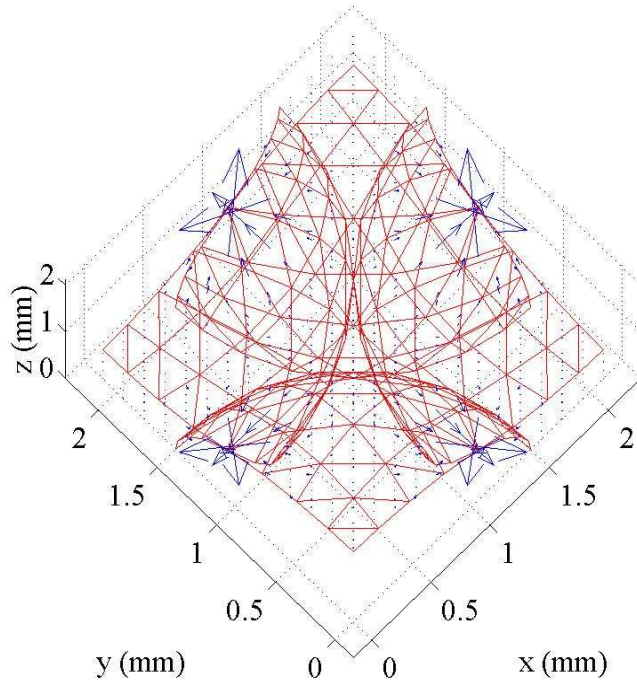


**Figure 4.1.e.** Magnetic force distribution in the elementary cell.

The distributions of water velocity on the lower, upper, middle z-sections and on the middle y-section of the elementary cell are shown in Figure 4.1.f, for an average y-directed velocity of 0.16 m/s. As expected, the water velocity field is nil on the spheres' surfaces, in particular at the tangency points. As shown in Figures 4.1.c and 4.1.f the fields  $\mathbf{B}$  and  $\mathbf{u}$  are fully 3D; moreover their distributions on opposite faces of the cell are geometrically similar but reversed. The available symmetries (reflections of the components of flux density and water velocity fields in the planes orthogonal to the coordinate axes through the vertices) allow reconstructing the fields in a larger domain, if needed.

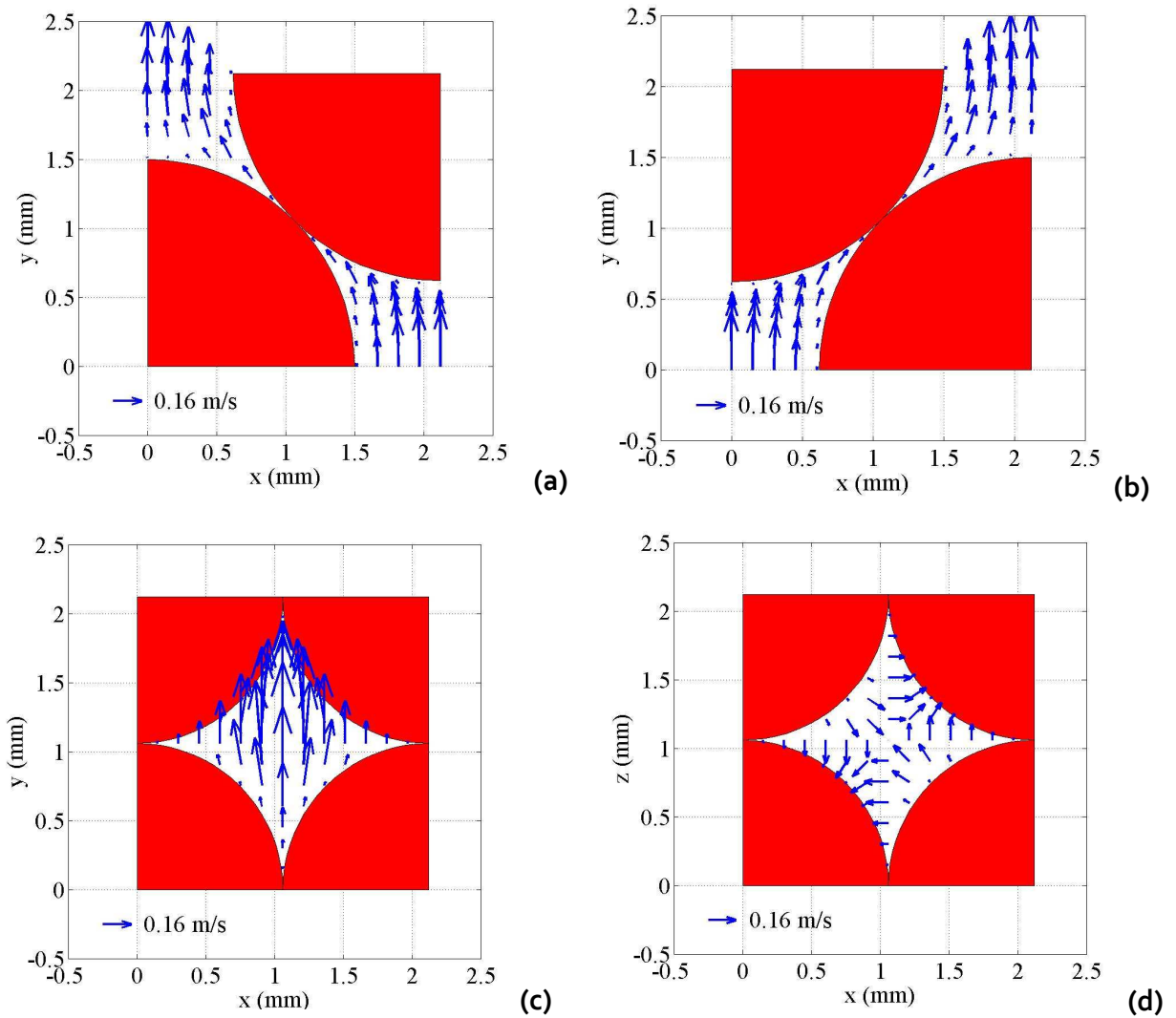


**Figure 4.1.f.** Water velocity field distributions on the lower (a), upper (b), middle (c) z-sections and on the middle (d) y-section of the elementary cell.

The trajectory of each particles' aggregate is assumed to be independent from all the others. It is obtained by integrating numerically the dynamic motion equations where the effects of the surrounding fluid, the magnetic field, the constraints due to the filter geometry and the thermal fluctuations are taken into account, as follows:

$$\begin{cases} \frac{d\mathbf{x}_p}{dt} = \mathbf{v}_p \\ m_p \frac{d\mathbf{v}_p}{dt} = \mathbf{F}_{mag} + \mathbf{F}_{drag} + \mathbf{F}_{add.m} + \mathbf{F}_{lift} + \mathbf{F}_{grad.p} + \{\mathbf{F}_{th} + \mathbf{F}_{coll}\} \end{cases} \quad (4.1.1)$$

where  $\mathbf{x}_p$  is the time-dependent position of the particles' aggregate,  $\mathbf{v}_p$  the time-dependent velocity of the particles' aggregate and  $m_p$  is its mass. Among the considered forces, described in the following, the leading ones are the drag force ( $\mathbf{F}_{drag}$ ) and the magnetic force ( $\mathbf{F}_{mag}$ ).

The force due to the interaction with the surrounding fluid is the sum of different terms, i.e. drag, added mass, Saffman's lift and pressure gradient (Meng, 1991; Clift, 2005). The drag force is evaluated in the following form:

$$\mathbf{F}_{drag} = -\frac{S_p \rho_w C_D}{2} |\mathbf{v}_p - \mathbf{u}(\mathbf{x}_p)| (\mathbf{v}_p - \mathbf{u}(\mathbf{x}_p)) \quad (4.1.2)$$

where  $S_p$  is the aggregate cross section and  $\rho_w$  the water density.  $C_D$  is the drag coefficient, depending on the relative Reynolds number, defined as  $Re_p = \rho_w |\mathbf{v}_p - \mathbf{u}| d_p / \eta$ , where  $d_p$  is the aggregates' diameter and  $\eta$  the water dynamic viscosity. The Schiller-Nauman  $C_D = 24 \cdot (1 + 0.15 Re_p^{0.687}) / Re_p$  correlation for smooth spherical particles, which recover the Stokes' law in the limit of small relative Reynolds number, is used (Clift, 2005).

The added mass force, i.e. the force required to accelerate the water surrounding the particle, is considered in the following form (Meng, 1991):

$$\mathbf{F}_{add.m} = -\frac{V_p \rho_w}{2} \left( \frac{d\mathbf{v}_p}{dt} - \mathbf{v}_p \cdot \nabla \mathbf{u}(\mathbf{x}_p) \right) \quad (4.1.3)$$

where  $V_p$  is the aggregate volume, and the first term in the parenthesis is moved in the left hand side of (4.1.1) for the numerical integration. The spatial derivatives are discretised with finite-differences using  $d_p$  as step size, centred in  $\mathbf{x}_p$ .

The expression for the Saffman's lift force used in (4.1.1), which is valid for small particle Reynolds number, is taken from (Li, 1992):

$$\mathbf{F}_{lift} = 2K \frac{V_p (\eta \rho_w)^{1/2}}{d_p (\mathbf{D} : \mathbf{D})^{1/4}} \mathbf{D} \cdot (\mathbf{u}(\mathbf{x}_p) - \mathbf{v}_p) \quad (4.1.4)$$

where  $K = 2.594$  is the constant coefficient of Saffman's lift force and the deformation tensor  $\mathbf{D}$  is defined as  $D_{ij} = (\partial u_i / \partial x_j + \partial u_j / \partial x_i) / 2$  with  $i, j = 1, 2, 3$  (Note that the deformation tensor is half of the shear rate gamma dot.). The double dot defines the summation on both indices of the tensor, i.e.  $\mathbf{D} : \mathbf{D} = \sum_{ij} D_{ji} D_{ij}$ . The pressure gradient force is considered in the following form (Meng, 1991):

$$\mathbf{F}_{grad.p} = V_p (\rho_w \mathbf{v}_p \cdot \nabla \mathbf{u}(\mathbf{x}_p) - \eta \nabla^2 \mathbf{u}(\mathbf{x}_p)) \quad (4.1.5)$$

The second order derivatives are discretised using a centred-difference approximation with  $d_p$  as step size, centred in  $\mathbf{x}_p$ .

The magnetic force  $\mathbf{F}_{mag}$  is evaluated taking the scalar product of the magnetic moment of the particles' aggregate times the spatial gradient of the magnetic flux density field applied to the particle (Mariani, 2010), as follows:

$$\mathbf{F}_{mag} = V_p \mathbf{M}_p(\mathbf{B}) \cdot \nabla \mathbf{B}(\mathbf{x}_p) \quad (4.1.6)$$

The magnetization  $\mathbf{M}_p$  of particles' aggregates is function of the applied field  $\mathbf{B}$ . In evaluating  $\mathbf{B}$ , the contribution due to the magnetic moments of all the other particles is neglected with respect to the fields generated by the external permanent magnets and the steel spheres.

The force  $\mathbf{F}_{th}$  related to the thermal fluctuations can be modelled as an isotropic Gaussian random process with zero mean and constant variance (<https://www.sharcnet.ca/Software/Fluent12/pdf/th/flth.pdf>). In order to simplify the calculation the thermal force is formally time-integrated and subtracted to the particle momentum. Thus the particle velocity is written as a sum of an average term and an isotropic thermal fluctuation, as follows:

$$\mathbf{v}_p = \langle \mathbf{v}_p \rangle + \mathbf{u}_{th} \quad (4.1.7)$$

The standard deviation of the resulting thermal velocity is  $\sqrt{3kT/m_p}$ , where  $k$  is the Boltzmann constant and  $T$  the room temperature. The components of the thermal fluctuation are evaluated at the beginning of each time step of integration of (4.1.1) using pseudo-random numbers (Fishman, 1990). This allows the use of a deterministic 5<sup>th</sup> order Runge-Kutta method for the integration of (4.1.1). At the considered mass flow rates the thermal kinetic energy  $3kT/2$  is negligible with respect to the kinetic energy of the particles' aggregate  $m_p \langle v_p \rangle^2 / 2$ . Thus, the randomizing effects of Brownian motion at room temperature are negligible for the aggregates in the water stream. However, in the capture regions, which are near the tangency points among spheres, the fluid is almost at rest and the thermal fluctuations play a role against the particle retention.

Finally, in order to take into account the collisions between particles and spheres, the constraints force  $\mathbf{F}_{coll}$  is considered. This force acts only when the distance between the aggregate centre and the nearest sphere surface is lower than half of the aggregate diameter  $d_p$ . In the code when this condition is fulfilled at one integration step, in the next one the velocity is updated using the momentum conservation (the tangential component is conserved and the normal one is reversed). The breaking of the aggregates during collisions is possible, but this is not considered since it would require the modelling of the interactions between the hydrophobic and magnetic forces that stabilize the aggregate. Thus, only elastic collisions are considered.

Figure 4.1.g shows some of the trajectories in the elementary cell as seen from two different viewpoints where one of the octants has been removed for easing the visualization. The particles' starting positions are calculated applying (4.1.1) to a zero flux density field cell with a uniform input distribution. The number of trajectories considered in each run is about 400. It can be seen that the particles tend to move near the spheres surfaces. In particular,

the tangency point among the spheres is the capture zone where the particles can stop. The trajectory calculation is stopped when the particle goes out of the cell or its average velocity vanishes. The CPU time required for the simulation of one cell is about 16 hours on CPU i7-2600@3.4GHz (RAM 3.4 GB) excluding the pre-processing time for the velocity and flux density fields definition.

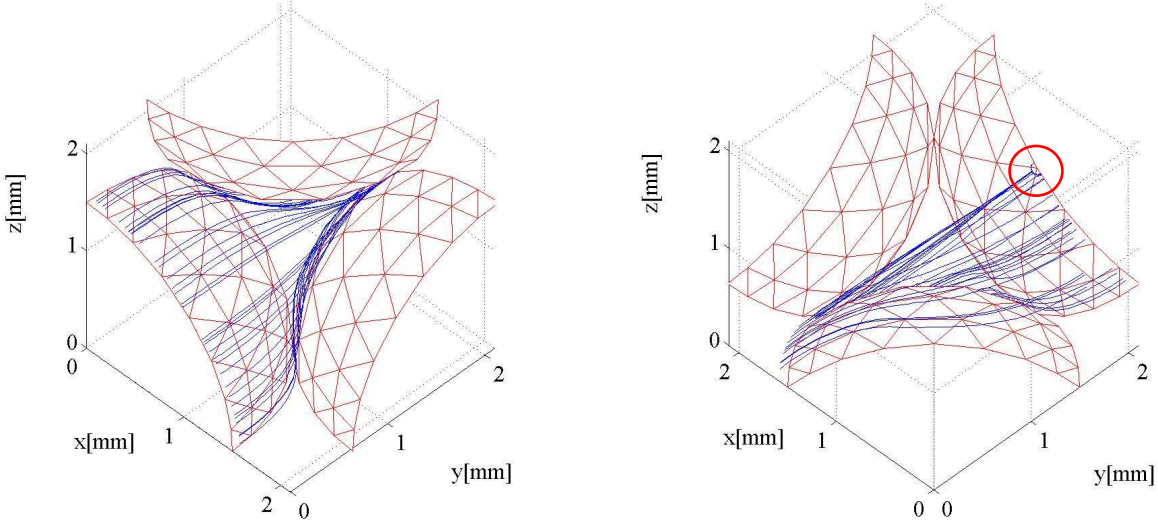


**Figure 4.1.g.** Trajectories sample in the elementary cell as seen from two different viewpoints (inlet section seen from above on the left, outlet section seen from below on the right) where one of the octants has been removed for easing visualization. The red circle highlight the tangency point were the particles could stop.

The results obtained integrating equation (4.1.1) are summarized in Figure 4.1.h, where the elementary cell capture efficiency vs. the capture parameter  $\Omega$  is plotted. The capture efficiency  $\sigma$  is defined as the ratio between the numbers of captured and entering particles, as follows:

$$\sigma = \frac{N_{input}^{particles} - N_{output}^{particles}}{N_{input}^{particles}} \quad (4.1.8)$$

The same definition applies also to the filter capture efficiency. The parameter  $\Omega$  is defined as the ratio between the estimated magnitudes of the magnetic force and drag force (in the low velocity limit, i.e.  $F_{drag} \sim 3\pi d_p \eta u_0$ ) as follows:

$$\Omega = \frac{d_p^2 M_{ps} \chi_{s,eff} B_0}{36\eta u_0 d_s} \quad (4.1.9)$$

where  $d_p$  and  $M_{ps}$  are the diameter and the saturation magnetization of the particles' aggregates,  $u_0$  the average fluid velocity,  $\eta$  the fluid dynamic viscosity,  $B_0$  the external flux density field,  $\chi_{s,eff}$  the effective susceptibility of the steel spheres and  $d_s$  their diameter. The magnitude of the magnetic force used in (4.1.9) is  $F_{mag} \sim (\pi d_p^3/6)(M_{ps} \chi_{s,eff} B_0/2)/d_s$ . It is obtained assuming that a particle in the capture zone is fully magnetised. The local flux

density field in the capture zone is estimated as  $\chi_{s,eff} B_o$ . A variation of the particle' magnetic energy of the order  $M_{ps} \chi_{s,eff} B_o/2$  at a distance equal to the steel spheres diameter is considered.

The choice to use  $\Omega$  as the capture parameter is clearly incomplete since there are other competing forces besides the drag and the magnetic ones. Therefore, there are different possible sets of values for the system parameters that correspond to the same value of  $\Omega$ , but lead to different capture efficiencies. The elementary cell capture efficiency shown in Figure 4.1.h is obtained averaging the different outcomes for similar  $\Omega$  for about 100 sets of system parameters. All the parameters involved in the definition of  $\Omega$  are varied. Also the fluid viscosity is varied, since a suspension has an effective viscosity larger than the surrounding fluid (*Landau, 2011*). Moreover, in certain cases there is evidence in ferrofluids of an increase of the viscosity with magnetic field (*Odenbach, 1998*).

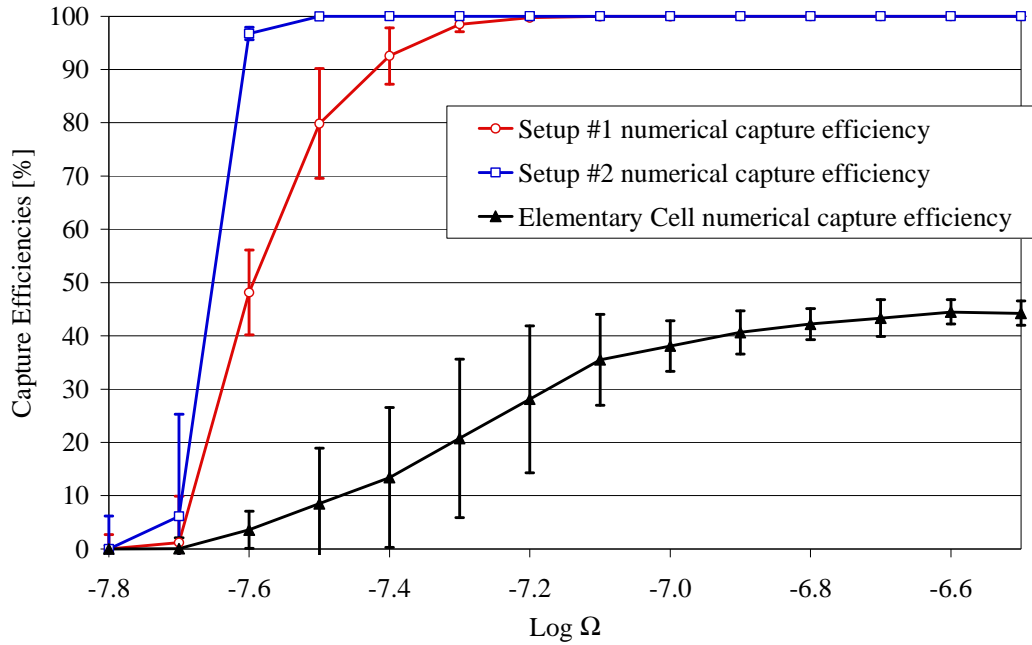


**Figure 4.1.h.** Filters and elementary cell capture efficiencies vs. the capture parameter  $\Omega$ .

In order to calculate the filters efficiencies ( $\sigma_f$ ) from the elementary cell one ( $\sigma_c$ ), each filter is assumed to consist of N subsequent layers with equal thickness, each made of elementary cells, orthogonal to the filter axis. In this way the model is scalable and allows studying also larger devices. For each experimental setup the number of layers is evaluated as the ratio between the filter length and the cell side (18 for setup #1 and 94 for setup #2). Assuming that all the cells are statistically independent, the particle balance on the filter leads to the following relation between the filter capture efficiency and the cell one:

$$1 - \sigma_f = (1 - \sigma_c)^N \quad (4.1.10)$$

The filter capture efficiencies shown in Figure 4.1.f are deduced from the cell one using (4.1.10).

Figure 4.1.h shows that the capture efficiency increases by increasing the capture parameter  $\Omega$ ; considering the definition of  $\Omega$  given in (4.1.9), the increasing of the magnetic force against the drag obviously leads to an increase of the particles retention. Thus, increasing the external field or the particles magnetization has approximately the same effect of reducing the average fluid velocity or viscosity. The increase of the particle's aggregates diameter, which influence both magnetic and drag force, leads to a more efficient capture. Finally, from (4.1.10) it can be deduced that increasing the filter length, i.e. the number of layers, increases the overall capture efficiency. In fact Figure 4.1.h shows that experimental setup #2, which is longer than #1, has higher capture efficiency. Anyway in both cases the thinner fraction of the powder is weakly captured.

If the particles initial size distribution is known, the calculated capture efficiency can be used to evaluate the time evolution of the particles concentration in the system, as follows. The mass balance of the particles with similar diameters, labelled populations, leads to the following equation:

$$d(C_k V) = -C_k q dt + (1 - \sigma_{f,k}) C_k q dt \quad (4.1.11)$$

where  $C_k$  is the particle's concentration for population k made of particles with similar diameter,  $V$  is the system volume and  $q$  is the volume flow rate.  $\sigma_{f,k}$  is the filtering efficiency for population k, deduced from Figure 4.1.h. Solving (4.1.11) leads to exponential time decay for each population:

$$C_k(t) = C_k(0) \exp(-\sigma_{f,k} q t / V) \quad (4.1.12)$$

## 4.2 Numerical results

For MACs tests the initial concentration  $C_k(0)$  for population k was deduced from the experimental distribution shown in Figure 2.2.1.b. and the total concentration at any given time was obtained summing up the concentration for all the populations, as follows:

$$C_{TOT}(t) = \sum_k C_k(t) \quad (4.2.1)$$

Figure 4.2.a and 4.2.b show the time dependence of the residuals calculated using (3.1.1) and (4.2.1). The error bars were obtained considering a mass redistribution up to 4% of the powder in the populations of particles with diameter lower than 3  $\mu\text{m}$ . This can be justified considering the ultrasonic washing applied after MACs addition to the pollutant-water samples. Another possibility of redistribution can be the breaking of the aggregates during filtration because of collision with the spheres. The overall comparison of numerical results with laboratory tests is satisfying for both experimental setups but the correspondence is better for setup #2. This may be due to the larger number of spheres constituting the filter in setup #2 with respect to #1. In fact in setup #1 the possible positioning errors while realizing the filter itself, the larger non uniformity of the applied field and the larger fraction of spheres placed on the filter surface are all source of variability on the results (as shown by the larger error bars of Figure 4.2.a with respect to Figure 4.2.b).

The experimental results and the numerical ones shown in Figure 4.2.b well agree at the beginning of the filtration. As shown in Figure 4.1.h the capture efficiency of setup #2 for all the particles with the diameter larger than about  $0.5 \mu\text{m}$  (corresponding to  $\text{Log } \Omega \cong -7.6$ ) is near 100%. In this case (4.1.12) shows that the initial slope of the MACs residual depends only from the ratio between flow rate and system volume. For what concern the time behaviour of the filter after 10 minutes, it can be seen that setup #2 shows a weak decrease of the MACs residual that is not present in setup #1. This can be explained since the setup #2 has larger capture efficiency than #1 for the thinner fraction of the powder, as shown in Figure 4.1.h Figure 4.2.c reports some pictures of the tank of setup #2 during MACs filtration.

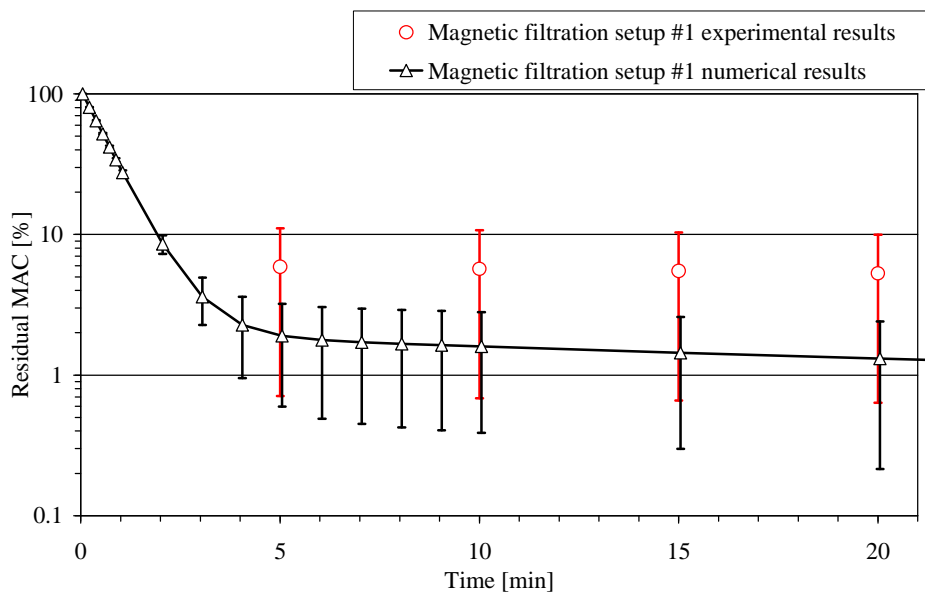


Figure 4.2.a. Numerical and experimental results on MACs removal with setup #1.

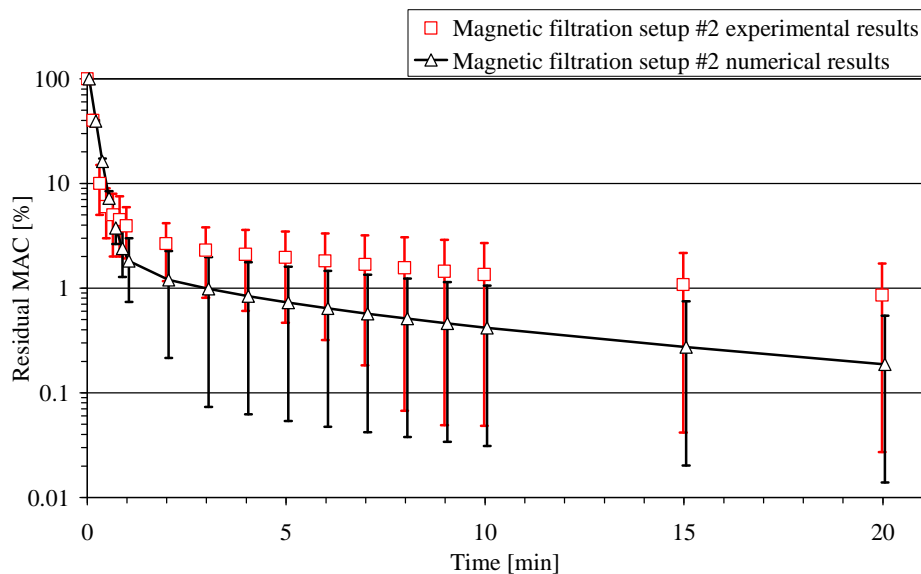
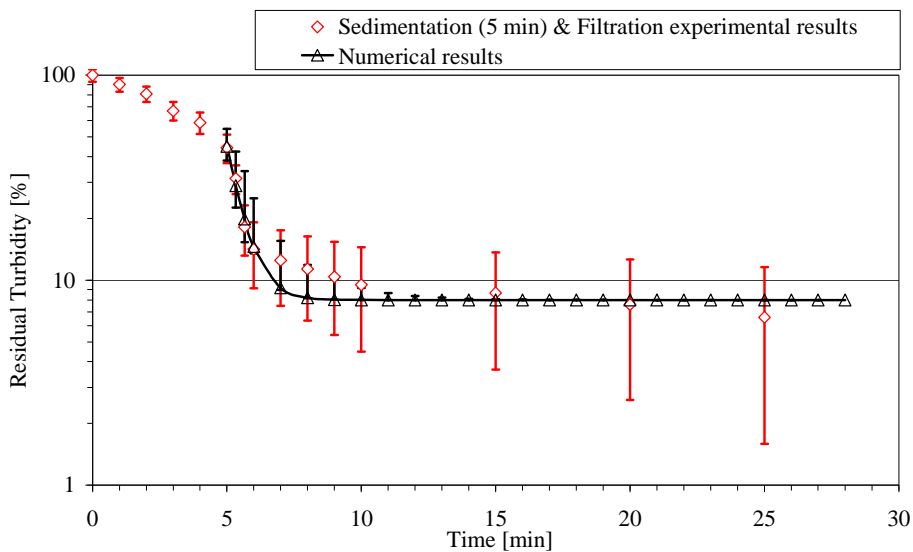


Figure 4.2.b. Numerical and experimental results on MACs removal with setup #2.



**Figure 4.2.c.** Pictures of the tank of setup #2 at the beginning of MACs filtration (a), after 10 seconds (b) and after 30 seconds (c).

Considering zeolite-magnetite mixtures, the initial size distribution of the aggregates and their composition depended on the sedimentation step and was unknown. Only experimental and numerical tests with setup #2 were performed. Figure 4.2.d, Figure 4.2.e and Figure 4.2.f show the time dependence of the residuals during the filtration step calculated using (4.1.12) and (3.1.2) introducing different values for  $\sigma_f$ . The turbidity values were used instead of the concentration ones. Figure 4.2.d, Figure 4.2.e and Figure 4.2.f report the best interpolation of the experimental data, i.e.  $\sigma_f$  of 0.3 with error bars of  $\pm 0.2$ .



**Figure 4.2.d.** Numerical and experimental results on zeolite-magnetite mixtures removal with setup #2. These results regard the tests performed applying 5 minutes of sedimentation followed by filtration.

According to Figure 4.1.h, these values of  $\sigma_f$  are on the rapid slope of the filter capture efficiency curve; thus a small increase of  $\Omega$  could speed up the removal. A possibility could be the increasing of the magnetite fraction but this would lead to a higher production of sludge. Another possibility could be the use of a magnetite powder with a smaller average diameter; the finer magnetite particles could bond with the finer particles of zeolite that

tend to remain in suspension, increasing the final capture efficiency. Considering that the values reported in Figure 4.2.d, Figure 4.2.e and Figure 4.2.f are close the lower limit of the slope of the filter capture efficiencies reported in Figure 4.1.h, a decreasing of the magnetite fraction would not lead to an acceptable final turbidity.

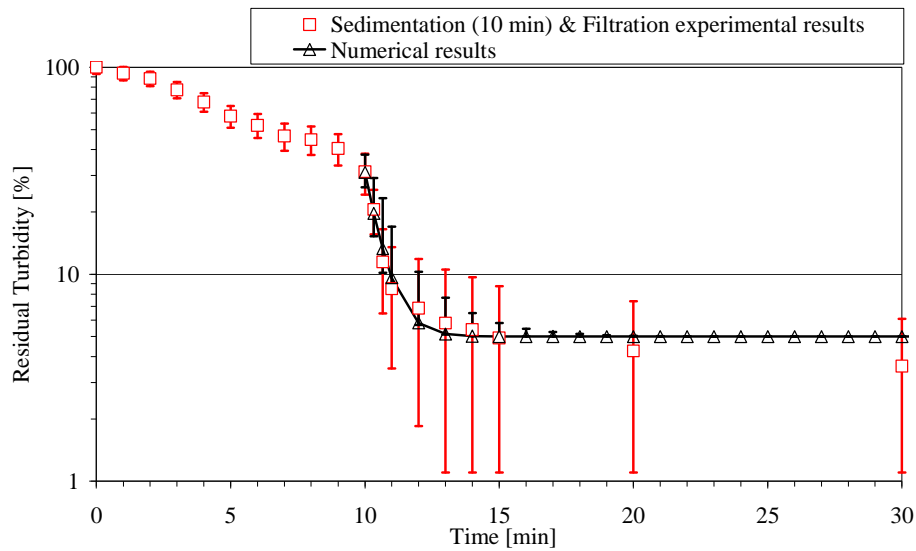


**Figure 4.2.e.** Numerical and experimental results on zeolite-magnetite mixtures removal with setup #2. These results regard the tests performed applying 10 minutes of sedimentation followed by filtration.

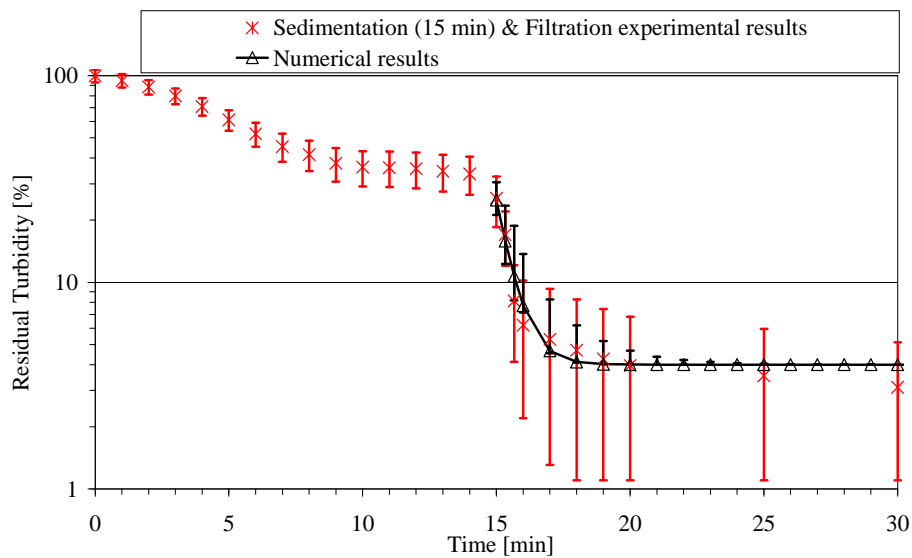


**Figure 4.2.f.** Numerical and experimental results on zeolite-magnetite mixtures removal with setup #2. These results regard the tests performed applying 15 minutes of sedimentation followed by filtration.

## CHAPTER 4: NUMERICAL MODELLING

## Chapter 5

### Pollutants adsorption results

The aim of the pollutant adsorption tests performed was not to reach the equilibrium but to remove as quickly as possible the maximum amount of pollutants. The tests led to positive results for almost all the tested substances. The reproducibility of the data was checked doing at least two times all the tests. The results obtained are all reported in terms of residual as defined in (3.1.1) where  $C_0$  and  $C_r$  are the initial and the residual pollutant concentrations in the solutions. The residual was always reported varying the amount of adsorbent powder used. Some tests were made also with an adsorption time of 30 minutes to analyse the adsorption potential.

#### 5.1 Adsorption on Magnetic Activated Carbons (MACs)

MACs were used to adsorb surfactants, endocrine disruptors and cations. Because of MACs composition the predominant adsorbents are, due to their large area, a microporous structure and a high degree of surface reactivity, the porous ACs (*Bansal, 2005*). The adsorption capacity of ACs is influenced both by the physical or porous structure and the chemical structure of the carbon surface. They have carbon atoms with unpaired electrons and residual valences that are highly reactive. The adsorption involves two types of forces: physical forces that may be dipole moments, polarization forces, dispersive forces, or short range repulsive interactions and chemical forces that are valency forces arising out of the redistribution of electrons between the solid surface and the adsorbed atoms. Depending upon the nature of the forces involved, the adsorption is of two types: physical adsorption and chemisorption. In the case of the physical adsorption, the adsorbate is bound to the surface by relatively weak van der Waals forces. Chemisorption, on the other hand, involves exchange or sharing of electrons between the adsorbate molecules and the surface of the adsorbent resulting in a chemical reaction (*Metcalf&Eddy, 2003; Bansal, 2005; Gaspard, 2008*).

##### 5.1.1 Surfactants

Surfactants can be adsorbed on the ACs part of MACs mainly by hydrogen bonding and hydrophobic and van der Waals interactions, secondly by electrostatic attraction; the shortest is the polar tail the better is the adsorption (*Gonzalez-Garcia, 2001; Basar, 2004; Gonzalez-Garcia, 2004a; Gonzalez-Garcia, 2004b; Duman, 2010; Soria-Sanchez, 2010*). During all the experiments performed the pH of the samples was always higher than  $\text{pH}_{\text{pzc}}$  (that is about 4) where the negative groups predominate over the positive ones. The surfactants concentration range was always lower than the CMC (Critical Micelle

## CHAPTER 5: EXPERIMENTAL RESULTS

Concentration) value for all surfactants. The CMC is defined as the concentration of surfactants above which micelles form and all additional surfactants added to the system go to micelles (a micelle is an aggregation of surfactants with the hydrophilic head towards the water and the hydrophobic tails in the centre of the aggregate). Considering that magnetite in MACs is around 1/3 and the small porosity and specific surface of magnetite compared to the ACs it can be assumed that the adsorption on the iron oxide was negligible; adsorption on iron oxides and magnetite properties are described in (Borghini, 2011). The tests led to positive results with regard to all surfactants. Various initial surfactant concentrations were considered and for some tests an increasing in the adsorption time or the addition of ferric chloride was evaluated. The adsorption of all surfactants led to concentration below the 0.5 mg/l limit for water reuse in agriculture (according to Italian legislation), using at most 0.5 g/l of MACs.

Figure 5.1.1.a shows the results for all the tests concerning SDS; the data have an error of  $\pm 5\%$ . With 0.01 g/l of MACs appreciable variations are possible on the outcome but the whole session of experiments showed that regardless of the initial condition (concentration, adsorption time, ferric chloride addition) it was possible to capture about  $95 \pm 5\%$  of the surfactant with 0.5 g/l of MACs and smaller concentrations of surfactant were easier to remove. Increasing the adsorption time led to better removals showing that the amount of powder added was not saturated after 10 minutes. It can be seen that the coagulant slightly increased the SDS removal. The coagulant addition allowed reaching the EPA Drinking Water Standard for foaming agents (0.5 mg/l) for SDS with 0.1 g/l of MACs without increasing the adsorption time.

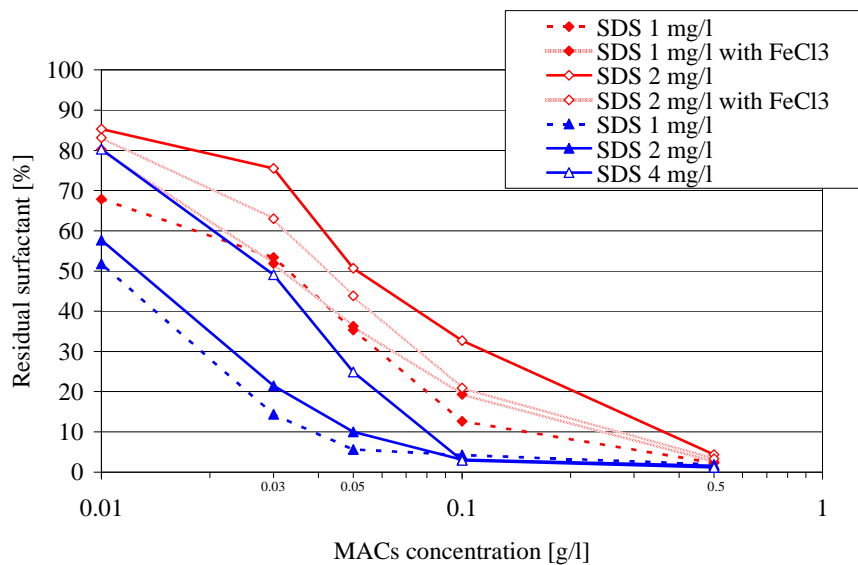


**Figure 5.1.1.a.** Percent residual of anionic surfactant SDS vs. MACs concentration. The red-rhomboidal curves represent results after 10 minutes of adsorption (with different initial concentration and with or without the addition of ferric chloride). The blue-triangular ones represent results after 30 minutes of adsorption (with different initial concentration).

The residual Fe (III) was checked after the filtration of every sample and was below the MCL level for MACs concentration above 0.1 g/l consistently with the results shown in Table 5.1.3.a.

Figure 5.1.1.b shows the results for all the tests concerning the cationic surfactants DDAB and Kemfluid EQ18; the data have an error of  $\pm 5\%$ . With the exception of the DDAB test without the addition of ferric chloride the whole session of experiments showed that regardless of the initial condition (concentration, adsorption time, and ferric chloride addition) it was possible to capture about  $95 \pm 5\%$  of the surfactant with 0.5 g/l of MACs and smaller concentrations of surfactant were more difficult to remove. Increasing the adsorption time for Kemfluid EQ18 did not lead to appreciable better removals suggesting that the amount of powder added was already almost saturated after 10 minutes adsorption but, it can be seen that the coagulant significantly increased the cationic surfactants removal. This suggests an electrostatic interaction related to the ferric ions. The ferric chloride addition allowed reaching the EPA limit for both DDAB and Kemfluid EQ18 with 0.05 g/l of MACs without increasing the adsorption time. The residual Fe (III) was checked after the filtration of every sample and was below the MCL level for MACs concentration above 0.1 g/l consistently with the results shown in Table 5.1.3.a.

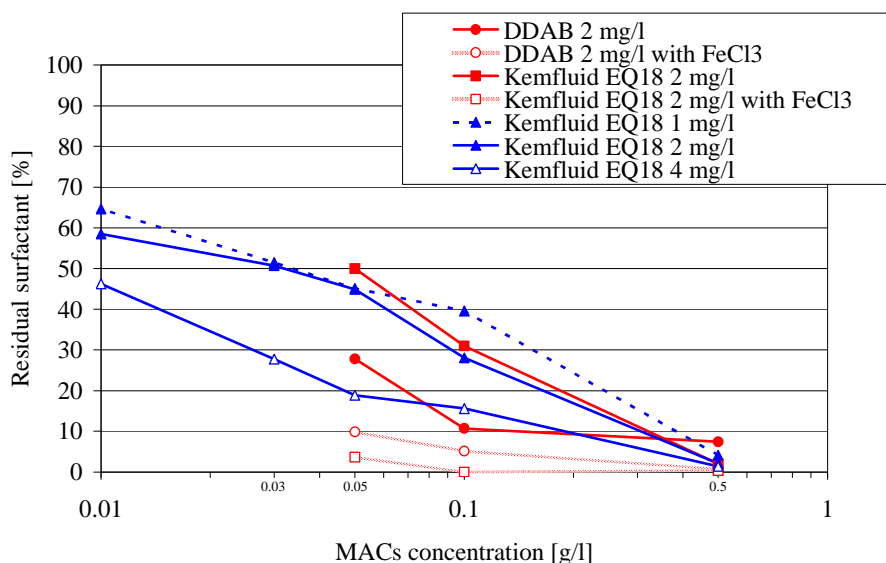


**Figure 5.1.1.b.** Percent residual of cationic surfactants Kemfluid EQ18 and DDAB vs. MACs concentration. The red-circular and the red-square shaped curves represent the results after 10 minutes of adsorption of DDAB and Kemfluid EQ18 respectively (with different initial concentration and with or without the addition of ferric chloride). The blue-triangular ones represent results after 30 minutes of adsorption of Kemfluid EQ18 (with different initial concentration).

Figure 5.1.1.c shows the results for all the tests concerning the non ionic surfactants TRITON X-100 and IGEPAL CO-630, precursors of 4-tert-OP and branched 4-NP respectively; the data have an error of  $\pm 5\%$ . With the exception of the TRITON X-100 test

with initial concentration of 10 mg/l the whole session of experiments showed that regardless of the initial condition (concentration, adsorption time, and ferric chloride addition) it was possible to capture about  $95 \pm 5\%$  of the surfactant with 0.5 g/l of MACs and smaller concentrations of surfactant were easier to remove. Increasing the adsorption time for TRITON X-100 led to significantly better removals suggesting that the amount of powder added was not saturated after 10 minutes adsorption. Considering the same initial conditions TRITON X-100 achieved better captures than IGEPAL CO-630. An increase of the oxyethylene length originates a decrease in the adsorption because of the excluded area created by the polyoxyethylene chain directed to the solution (*Soria-Sanchez, 2010; Gonzalez-Garcia, 2004a*). IGEPAL CO-630 and TRITON X-100 have the same polyoxyethylene chain bonded to a benzene ring but they have a different branched alkyl chain that during the 10 minutes of adsorption produced a slightly better adsorption of TRITON X-100.

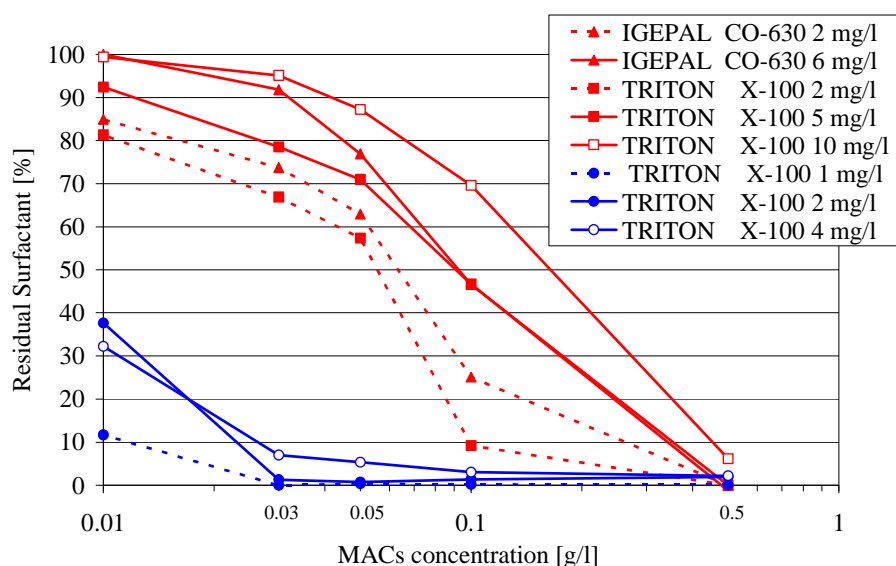


**Figure 5.1.1.c.** Percent residual of non ionic surfactants IGEPAL co-630 and TRITON X-100 vs. MACs concentration. The red-triangular and the red-square shaped curves represent the results after 10 minutes of adsorption of IGEPAL co-630 and TRITON X-100 respectively (with different initial concentration). The blue-circular ones represent results after 30 minutes of adsorption of TRITON X-100 (with different initial concentration).

The results achieved suggested the predominance of hydrophobic interactions over all. The pH conditions were less important for the capture. In fact the cationic Kemfluid EQ18 was the one that achieved the worst removal also if the pH condition were always higher than the  $pH_{pzc}$ , with the negative groups predominating over the positive ones (and increasing the electrostatic interactions). The smaller capture of cationic than anionic ones, despite the pH conditions were always over the  $pH_{pzc}$ , could be explained with the different steric hindrance and the competition between the charged head and the predominance of

the hydrophobic interactions over all (Gonzalez-Garcia, 2001; Basar, 2004; Gonzalez-Garcia, 2004a; Gonzalez-Garcia, 2004b; Duman 2010; Soria-Sanchez, 2010; Borghi, 2011).

### 5.1.2 Octylphenols and Nonylphenols

The relative affinity of alkylphenols (APs) and alkylphenols ethoxylated (APEs) toward the carbon surface is believed to be due to (i) the  $\pi$ - $\pi$  dispersion interaction between ACs basal planes and the phenolic ring, (ii) electrostatic attraction-repulsion interactions, (iii) hydrogen bonding between adsorbate and carbon surface, (iv) the donor-acceptor complexes formed between the basic sites on the carbon surface and the organic ring of the phenol, (v) oligomerization of phenols on ACs surfaces in the presence of dissolved oxygen (Bansal, 2005; Lu, 2007; Soria-Sanchez, 2010; Mohan, 2011).

Figure 5.1.2.a shows the residual of 4-OP and 4-n-NP with different initial concentration (5-10 mg/l for 4-OP and 6 mg/l for 4-n-NP, corresponding to 23.6-47.2  $\mu$ M and 27.3  $\mu$ M respectively). The experiments showed that it is possible to capture  $95 \pm 5\%$  of both APs with 0.1 g/l of MACs. Smaller concentrations of AP were found to be easier to remove and 4-OP achieved slightly better captures than 4-n-NP for concentrations of MACs smaller than 0.1 g/l. This difference could be ascribed to the small molecular structure difference between 4-OP and 4-n-NP which consist of one more methyl group on the alkyl chain. It can be seen from Figure 5.1.2.a that the adsorption capacity of 4-n-NP on MACs is about 60 mg/g after 10 minutes, while (Nakahira, 2006) reports an equilibrium adsorption capacity of 270 mg/g. This shows that the MACs potential is not fully exploited.

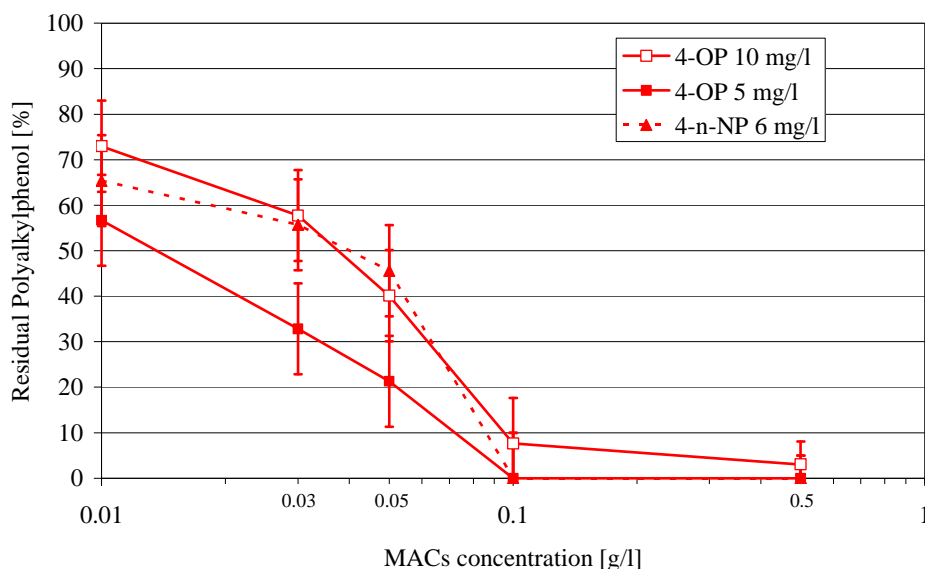


**Figure 5.1.2.a.** Percent residual of APs vs. MACs concentration. The different curves refer to different initial concentrations of the tested polyalkylphenols.

However, the aim of these tests was not to reach the equilibrium but to remove as quickly as possible the maximum amount of pollutants. The current Italian regulation D.Lgs

152/2006 states limits of 0.5 mg/l for the total phenols in surface water; concentration that was achieved with 0.1 or 0.5 g/l of MACs, depending on the initial concentration of the AP.

Both 4-OP and 4-n-NP have the phenolic benzene ring and a linear alkyl chain. Unlike the APEs, they do not have the steric hindrance of the oxyethylene chain that could decrease the adsorption (Soria-Sanchez, 2010; Gonzalez-Garcia, 2004a). Beside the effects due to the size of the molecules also the solubility is important for the adsorption. The adsorption of a nonpolar solute is higher on a nonpolar adsorbent: 4-n-NP and 4-OP, deprived of the polar polyoxyethylene chain, were less soluble and more affine to the ACs than the tested APEs (Bansal, 2005; Lu, 2007; Soria-Sanchez, 2010). In fact, despite the higher molar concentrations of APs than APEs, 4-n-NP was better adsorbed than IGEPAL CO-630 and 4-OP was better adsorbed than TRITON X-100 (Figure 5.1.1.b). At  $\text{pH} > \text{pH}_{\text{pzc}} \cong 4$  the negative groups predominate over the positive ones, i.e. although the surface has a net negative charge, some positive groups are still present (Bansal, 2005; Borghi, 2011). Since all the samples were found to have a pH in the range between 7 and 8.5, its effect on the adsorption should have been relatively small according to (Mohan, 2011); in order to obtain much larger phenols removal the pH value should have been reduced below 4 which could be difficult to manage in a real WWTP (Kawamura, 2000; Metcalf&Eddy, 2003).

### 5.1.3 Cations

The adsorption efficiency of Fe(III) on MACs was investigated both because is a parameter of interest in drinking water quality both to evaluate if the ferric chloride added in the magnetic seeding tests left Fe(III) ions in solution at the end of the treatment. Samples of Fe(III) of 1 mg/l or 3 mg/l were generated introducing ferric chloride in distilled water, MACs were added mixing for 10 minutes to allow the adsorption and filtrated for 10 minutes. The results reported in Table 5.1.3.a show that 0.1 g/l of MACs are enough to reach the recommended Secondary Drinking Water Standard (EPA) of 0.3 mg/l in both conditions.

**Table 5.1.3.a.** Residual of Fe(III) ions after adsorption on MACs (Initial Fe(III) 1-3 mg/l).

MACs concentration (g/l)	0.01	0.03	0.05	0.1	0.5
Residual %	36±10	22±10	10±5	4±2	<2

The adsorption efficiency of Mn(II) on MACs was investigated both because is a parameter of interest in drinking water quality both to compare the results with the one obtained with the zeolite-magnetite mixtures. Samples of Mn(II) of 1 mg/l were generated introducing manganese chloride in distilled water, MACs were added mixing for 10 minutes to allow the adsorption and filtrated for 10 minutes. The results reported in Table 5.1.3.b show that 1 g/l of MACs was not enough to reach the recommended Secondary Drinking Water Standard (EPA) of 0.05 mg/l. The results obtained, considering the same amount of adsorbent, were better than the ones obtained with the natural zeolite-magnetite mixtures

and worst than the ones obtained with the Na-activated zeolite-magnetite mixtures (See section 5.2).

**Table 5.1.3.b.** Residual of Mn(II) ions after adsorption on MACs (Initial Mn(II) 1 mg/l).

MACs concentration (g/l)	0.05	0.1	0.3	0.5	1
Residual %	100	90±10	70±10	50±5	30±5

The adsorption efficiency of Ca(II) and Ca(II) chelated with EDTA (Ethylenediaminetetraacetic acid) on MACs was investigated both because hardness is a parameter of interest in drinking water quality both to compare the results with the one obtained with the zeolite-magnetite mixtures. The Ca(II) was chelated with the intent to improve the adsorption of Ca(II). The initial samples had a concentration of 150-300 mg/l (corresponding to a hard/very hard water). To chelate the Ca(II) 0.8 g/l of EDTA were added; this was the maximum amount of EDTA soluble in the used distilled water. In Figure 5.1.3.a the correlation between the amount of EDTA and the pH of the solution is reported; for larger concentrations than 0.8 g/l of EDTA the pH stays unvaried. The removal achieved was low both for Ca(II) and the chelate Ca(II). Considering 0.5-1 g/l of MACs, after 10 minutes adsorption and the filtration only 5-10% of Ca(II) was removed. Moreover, the experiments on the chelated Ca(II) did not show a significative capture. Thus, the addition of EDTA did not improve the hardness removal.

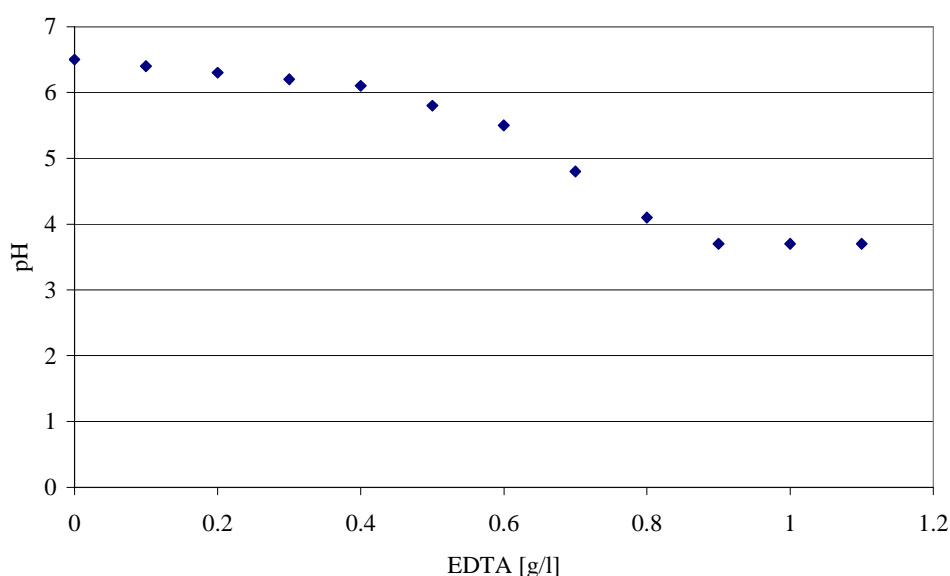


**Figure 5.1.3.a.** Correlation curve between the EDTA concentration and the pH of the solution.

## 5.2 Adsorption on Zeolite-Magnetite mixtures

The use of natural zeolites in water treatment is one of the oldest and the most perspective areas of their application. The efficiency of water treatment by using natural

and modified zeolites depends on the type and quantity of the used zeolite, the size distribution of zeolite particles, the initial concentration of contaminants, pH value of solution, ionic strength of solution, temperature, pressure, contact time of system zeolite/solution and the presence of other organic compounds and anions. A very unique property of natural zeolites is their selectivity towards cationic. The presence of heavy metals (Zn, Cr, Pb, Cd, Cu, Mn, Fe, etc.) in water is a serious environmental problem and their removal by natural zeolites has been extensively studied. The efficiency of removing metal ions from waters depends on many factors such as initial concentration of metal ions in wastewater, the pH value of the system, the possibility of formation of metal hydroxyl anion, previous chemical and thermal modification of zeolite and the amount of water that should be purified (*Margeta, 2013*).

### 5.2.1 Cations

The adsorption efficiency of Mn(II) was studied as in (*Taffarel, 2009*) both on natural zeolite-magnetite mix and Na-activated zeolite-magnetite mix. These tests were carried out in order to check if the adsorption improvement due to Na-activation was affected by the addition of the coagulant ferric chloride. Figure 5.2.1.a reports the percent residuals of Mn(II) using zeolite-magnetite mix with the addition of ferric chloride, both for zeolite ZEOVER and Na-activated zeolite. All the data have an error of  $\pm 5\%$ . It can be seen from Figure 5.2.1.a that Mn(II) adsorption on Na-activated zeolite roughly doubles as reported in (*Taffarel, 2009*). Thus, the effect of the coagulant on the adsorption is not detectable. The comparison with the zeolite-magnetite mixtures without coagulant was not carried out because the residual turbidity was too high for a correct measurement with the spectrophotometer. Increase in Mn(II) uptake by Na-activated zeolite is probably due to the decrease in Ca(II), Mg(II) and K(I) concentration and to the higher concentration of more easily exchangeable Na(I) (*Taffarel, 2009*).

A major use of zeolites as ion exchange agents is for water softening applications in the detergent industry and substitute use of phosphates. The best Si/Al ratio for water softening is  $\leq 2$  (*Kogelbauer, 2001; Payra, 2003*). The adsorption efficiency of Ca(II) on natural zeolite-magnetite mix and Na activated zeolite-magnetite mix was investigated. The initial samples had a concentration of 150-300 mg/l (corresponding to a hard/very hard water). The removal achieved was low considering 0.25-0.75 g/l of zeolite (both natural and Na-activated) mixed with 0.25 g/l of magnetite, after 10 minutes adsorption, the addition of the coagulant and the filtration, only 5-10% of Ca(II) was removed. The Ca(II) was also chelated with the intent to improve the adsorption of Ca(II). To chelate the Ca(II) 0.8 g/l of EDTA were added as in zeolite-magnetite adsorption tests. The experiments on chelated Ca(II) did not show a significative removal. Thus, also with zeolite-magnetite mix (both natural and Na-activated), the addition of EDTA did not improve the hardness removal. The

poor results obtained could be explained by Si/Al ratio of the used zeolite (2.5), too high for water softening (Kogelbauer, 2001; Payra, 2003).

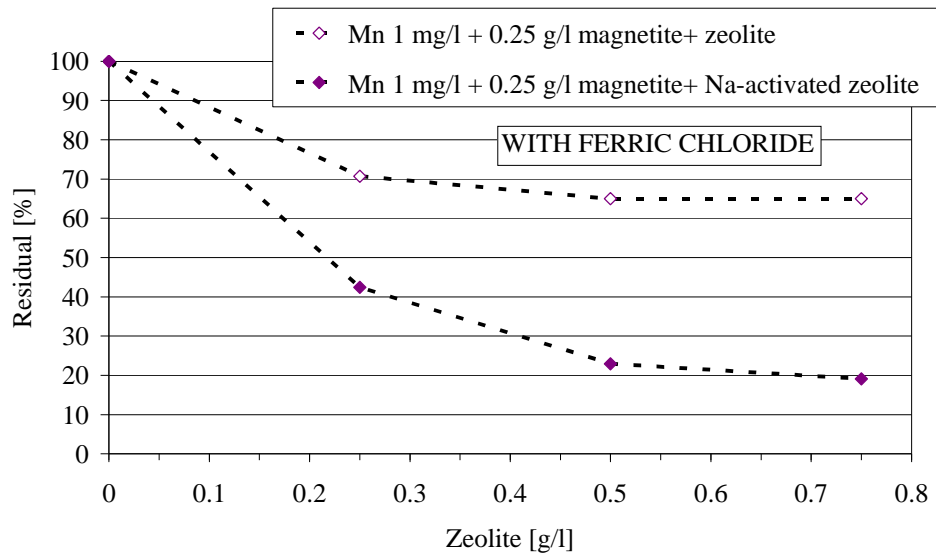


**Figure 5.2.1.a.** Removal of Mn(II) by adsorption on natural zeolite and Na-activated zeolite (filled dots) mixed with 0.25 g/l magnetite and the addition of  $\text{FeCl}_3$ .

## CHAPTER 5: EXPERIMENTAL RESULTS

## Chapter 6

# Sustainability and applicability of the process

## 6.1 Filter and adsorbent reuse

For a full-scale application is necessary to analyze the entire cycle of the powder and the possible techniques for reusing both the adsorbent and the filtering element present in the filtration plant. The filter progressively saturates capturing the powders and hence reducing its filtering capacity. Thus a washing section is needed. The saturation was calculated in laboratory for MACs adding increasing amounts of powder while measuring the turbidity after the filtration. The turbidity was converted in mg/l and considering the TSS lower limit (Italian legislation) of 35 mg/l, the saturation was of 1.3 mg MACs/sphere. As shown in Figure 6.1.a the filter performance decreases with the MACs mass held on the spheres. Moreover, no increase of the pressure drop on the filter was detected. This is probably due to the large void fraction of the filter and to the localized magnetic traps near the tangency points between spheres. This has positive effect on the hydraulic losses and the piping.

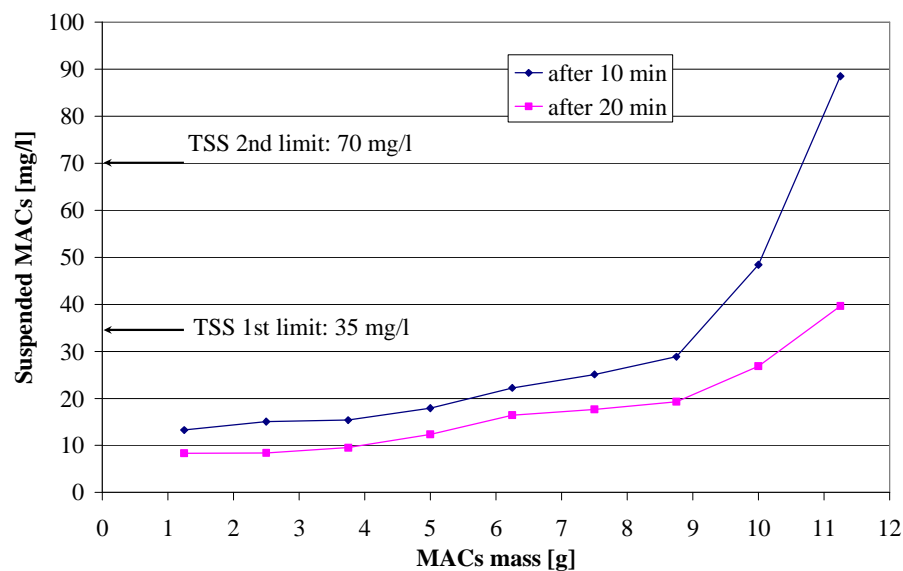


**Figure 6.1.a.** Filter saturation curve calculated measuring the residual MACs after a progressive addition to the filter. The residuals were measured both after 10 and 20 minutes of filtration.

In (Mariani, 2009; Mariani, 2010; Borghi, 2011) and in the Appendix I a magnetic filter using steel wool as filtering element was analysed. Despite its good capture efficiency, the wool filter has shown two main problems: firstly the needed periodic washing was difficult to achieve and secondly a careful wool fixing was required. In order to solve both these problems, stainless steel spheres were chosen as filtering elements (Abbasov, 2007, Borghi

2014a, Borghi 2014b). This choice allows an easier washing with an ultrasonic bath and a simpler assembling of the filter. Moreover, the spheres, with respect to meshes or wools, are relatively insensible to the local direction of the external magnetic field and lead to larger filling factors (thus requiring a lower applied field to be magnetized). Considering the sustainability of the process, It is important to highlight that the spheres used are commercial bearings and not a specific product that has to be manufactured exclusively for the treatment.

A sustainable process needs also a regeneration and reactivation section of the adsorbent powder. A possible solution for MACs regeneration is the decomposition using  $H_2O_2$  exploiting the catalytic properties of magnetite (Do, 2011). This process has been already tested successfully for the regeneration of MACs after the adsorption of COD (<http://www.ms-engineering.co.jp/eng/technical/mac/index.htm>). An alternative solution presented in literature is ultrasound regeneration (Lim, 2005). This method seems interesting since the steel spheres already need an ultrasonic treatment. Thus enhancing that phase a regeneration of both the filter and the adsorbent could be achieved. Finally, if the wastewater contains almost only surfactants as could be in detergent industry or car-washing station discharges, the sludge may be used itself as a more effective adsorbent for other contaminants like dyes and natural organic matter (NOM) (Wang, 2007; Ding, 2010; Shariati, 2011). A solution for zeolites regeneration is desorption using different solutions of  $HNO_3$ , NaCl, KCl, EDTA,  $NH_4Cl$ , etc. with various molar concentrations. Recent studies of desorption efficiency of metal ions and regeneration of natural zeolites indicate that the adsorption process is reversible in most cases (Li, 2007; Katsou, 2011). If the pollutant adsorbed on the zeolite is not an ion a thermal regeneration might be possible (Sannino, 2012).

## 6.2 Large scale application

For what concern the scalability of the proposed magnetic separation technique to a real WWTP, the analysis of the magnetic filtration process does not impose limits on the dimensions of the spheres filter; the main limit is due to the possibility to create a rather uniform field in the filter volume using permanent magnets (PMs). As shown in (Fabbri, 2013) is possible to realize a field of about 0.5 T using actual Sm-Co magnets in Halbach array configuration up to a filter volume of 30cm × 30cm × 120cm (Figure 6.2.a(A)). In the same conditions used in our laboratory scale setup these PMs would allow to treat a volume flow rate of about 90 m<sup>3</sup>/h which is compatible with the treated flow rates of an average size WWTP that has flow rate from 15 m<sup>3</sup>/h to 160 m<sup>3</sup>/h (Metcalf&Eddy, 2003). To treat a flow rate of 15 m<sup>3</sup>/h a configuration of volume 15cm × 15cm × 120cm is needed (Figure 6.2.a(B)). A comparison of the two devices is reported in the following.

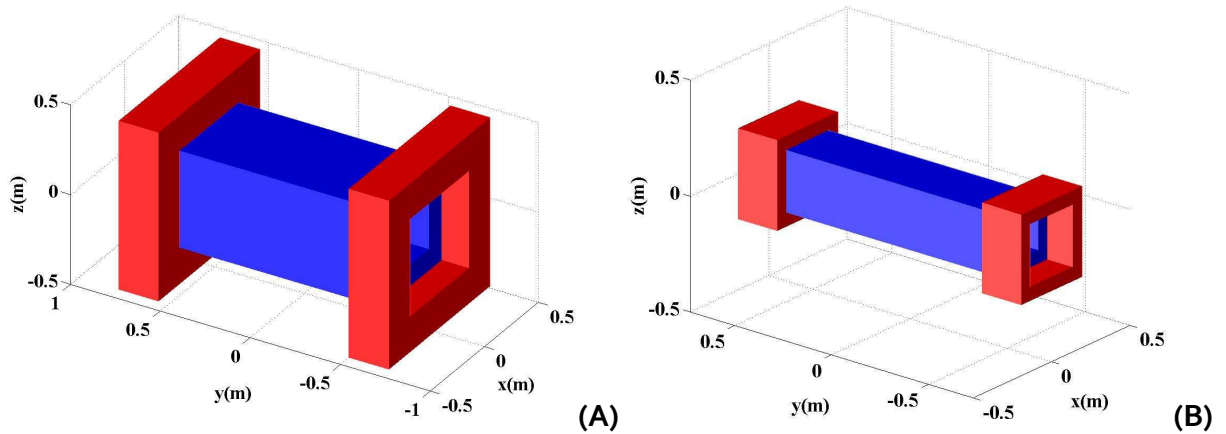


**Figure 6.2.a.** Overall view of permanent magnets arrays used as the flux density field source for a magnetic filtration unit of 30cm × 30cm × 120cm (A) and 15cm × 15cm × 120cm (B).

The direction of the magnetization in each PM, shown in Figure 6.2.b, was chosen in order to provide an almost uniform field (within 10% of the average) on each cross section of the channel. The geometrical dimensions of the PMs of the two configurations are given in Table 6.2.a. Considering both configurations, the main array generates a background field with a value at the center of the channel of about 0.46-0.47 T, transversal to the conduit axis.

**Table 6.2.a.** Geometrical dimensions of the PMs. The (A) columns refer to the 30cm × 30cm × 120cm configuration and the (B) refer to the 15cm × 15cm × 120cm configuration.

	Main PMs(A)	Heads PMs(A)	Main PMs(B)	Heads PMs(B)
a [cm]	30	54	15	27
b [cm]	12	20	6	6
c [cm]	120	-	120	-
w [cm]	-	22	-	20
s [cm]	-	106	-	106

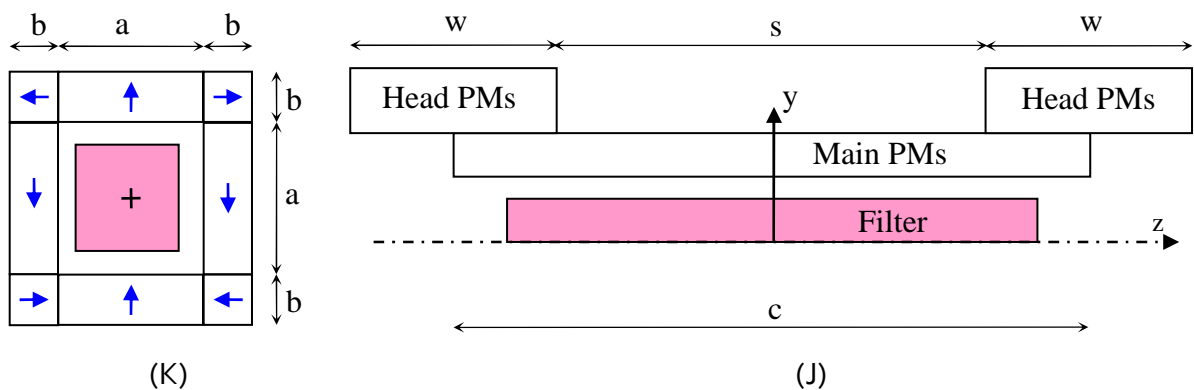


**Figure 6.2.b.** Transversal (K) and longitudinal (J) sections of the permanent magnets arrays. The arrows in (K) show the directions of the magnetization inside each element of the array. The same arrangement is used for the headings and the main PMs array.

The background field produced on the axis by the main PMs array is shown in Figure 6.2.c. In order to compensate the field decrease near the channel ends, two further arrays of PMs (heads) were placed near the ends for increasing the field up to 0.51-0.52 T. The field profile produced on the channel axis by the main PMs array and the heads is nearly uniform on each cross section and varies along the axis between 0.41 T and 0.51-0.52 T, as shown in Figure 6.2.c.

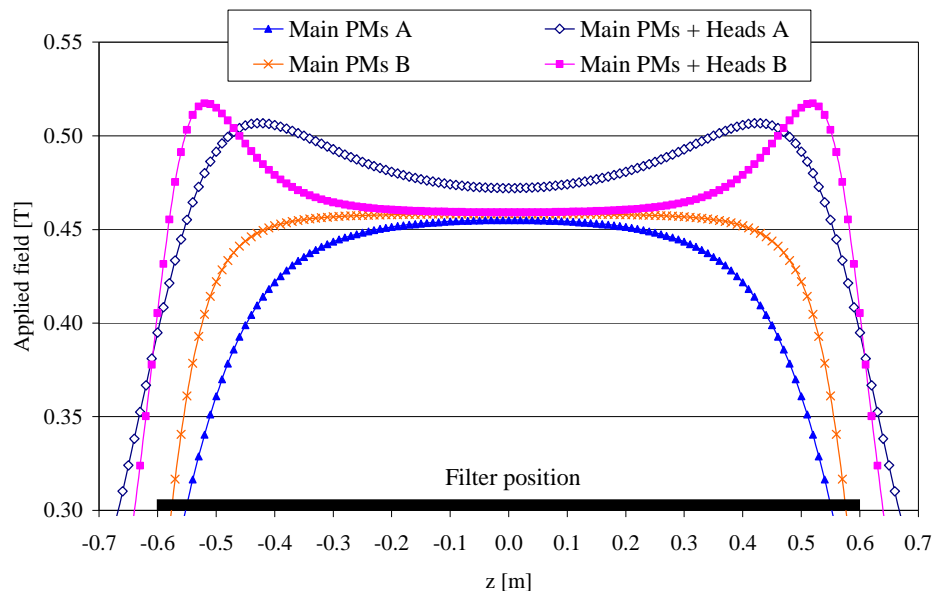


**Figure 6.2.c.** Profiles of flux density produced by main PMs and Heads in both the analyzed configurations (a and b) on the channel cross section along the axis. The non-uniformity on the cross section is lower than 10%.

In (Fabbri, 2013) commercial Sm-Co brick magnets grade XGS-26 with a remanence of 1 T were considered. To evaluate the costs of the described configurations also commercial Nd-Fe-B brick magnets grade N33EH with a remanence of 1 T are considered. These are low grade, i.e. cheap materials. Higher grades of Nd-Fe-B like N35H with a remanence of 1.4 T lead to a more compact layout. However, the reduced amount of material is more than compensated by the higher price of N35H. The volumes of the arrays are given in Table 6.2.b. The Nd-Fe-B magnets are easier to realize than the Sm-Co ones and are more performing (they can achieve higher fields). Nd-Fe-B cannot work at elevated temperatures, in hydrogen rich atmospheres and they corrode in an aqueous environment ([www.vacuumschmelze.com](http://www.vacuumschmelze.com); <http://www.mceproducts.com>). This last disadvantage is the only one that should be taken into account for the water treatment application. Considering that they can be efficiently coated to avoid the humidity problem ([www.vacuumschmelze.com](http://www.vacuumschmelze.com); <http://www.mceproducts.com>), the difference of cost (2012 quotation <http://www.saimag.com>). shown in Table 6.2.b (the Sm-Co cost is almost double) make Nd-Fe-B coated PMs the most advantageous choice for a real water treatment process. Moreover, for water treatment applications is important to remember that

permanent magnets do not require an electrical power supply and have smaller footprint with respect to superconductive magnets (*Mitsuhashi, 2003; Ihara, 2004; Svoboda, 2004; Nishijima, 2006; Ishiwata, 2010*).

**Table 6.2.b.** Volumes and costs of the PMs arrays.

	Main PMs (A)	Heads PMs (A)	Main PMs (B)	Heads PMs (B)	Total cost (A)	Total cost (B)
<b>Volume</b>	192 dm <sup>3</sup>	156 dm <sup>3</sup>	60.5 dm <sup>3</sup>	31.7 dm <sup>3</sup>	-	-
<b>Sm-Co Cost (4.2 k€/ dm<sup>3</sup>)</b>	1016 k€	1094 k€	254 k€	133 k€	2110 k€	387 k€
<b>Nd-Fe-B Cost (2.35 k€/ dm<sup>3</sup>)</b>	568.5 k€	612 k€	142 k€	74.5 k€	1180.6 k€	216.6 k€

The data reported in Table 6.2.c refer to the construction costs of water treatment plants, wastewater treatment plants and municipal wastewater filtration sections. These costs are evaluated using the algorithms reported in (WRC, 1974, EPA, 1983) and actualizing them as indicated by the Federal Reserve Bank of Minneapolis (<http://www.minneapolisfed.org/>). The design flow used in these algorithms is the average daily flow.

**Table 6.2.c.** Extrapolated construction costs for a water treatment plant, a wastewater treatment plant and a filtration section of a wastewater treatment plant. The extrapolation was made considering the two different flow rates mentioned above.

	Water treatment plant			Wastewater treatment plant			Wastewater filtration section		
	medium	max	min	medium	max	min	medium	max	min
<b>Q= 15 m<sup>3</sup>/h</b>	272.2	347.1	98.1	1300.8	2746.8	689.8	172.6	206.8	149.6
	k€	k€	k€	k€	k€	k€	k€	k€	k€
<b>Q= 90 m<sup>3</sup>/h</b>	1004.3	1173.7	743.3	4690.3	8962.1	2573.9	505.3	553.9	462.4
	k€	k€	k€	k€	k€	k€	k€	k€	k€

Comparing the values reported in Table 6.2.c with the costs of the magnets shown in Table 6.2.b it is possible to deduce that:

- 1) Considering the water treatment the magnetic filtering seems inapplicable, in fact the cost of the plant is less than that of the magnets. However, in case an additional removal of contaminants is necessary (for example the introduction a new regulation regarding emerging pollutants and/or concentration limits) the introduction of a new treatment section could be the only possible solution. In this case, especially if the

space available for the filtration is limited, the magnetic filtering could be competitive also in terms of cost to the others commercially available technologies.

- 2) With regard to the wastewater treatment plants the cost of the magnet is relatively small (around 10 % considering Nd-Fe-B PMs). In this case, the magnetic filtration could be considered as an addition or alternative to existing technologies.

It is important to highlight that this estimate is based on an extrapolation which considers only the change in value of the currency; the laws of the market and the costs of new technologies, higher or lower than the old ones, are not taken into account. In addition, this estimate considers only the cost of the magnets, neglecting the cost of all the parts necessary for its operation (powder, spheres, pumps, ultrasounds, manufacturing, etc). As a possible element of comparison Siemens Water Technologies S.r.l states on its website that its CoMag<sup>TM</sup> and BioMag<sup>TM</sup> reduce footprint and capital cost of primary and tertiary treatments (<http://www.water.siemens.com>). However, the cost is not the only possible criterion for making a choice. The choice of a given process depends on several considerations: the intended destination for the treated effluent, the characteristics of the water, the compatibility between different operations or processes, the resources available for the disposal of residual pollutants, environmental and economic feasibility (*Metcalf & Eddy, 2003*). It should be noted that in some circumstances the economic feasibility may not be a limiting factor for the purposes of the design of a system of advanced treatment, in particular in cases where the specific security requirements of the environment necessitates the need to remove certain pollutants and/or if there is no space available for a plant expansion. In fact, the compactness of the magnetic filter and the time (and consequently the spaces) for the sedimentation may be an important element of evaluation. Thus, the issues relating to the magnetic filtration process introduction in the treatment plant must be evaluated case by case.

## Conclusions

After a short review of the state of the art of water treatment and magnetic separation a numerical and experimental study of the magnetic separation of pollutants from water by means of a continuous-flow magnetic filter subjected to a field gradient produced by permanent magnets was presented. The removal of both Magnetic Activated Carbons (MACs) and zeolite-magnetite mix with the addition of a coagulant was investigated. Adsorption tests of different pollutants (surfactants, endocrine disruptors, Fe(III), Mn(II), Ca(II)) on these adsorbents were also performed achieving good results. It is important to remember that in real water and wastewater the pollutants are not pure, there is a mixture of different pollutants with competition and synergies. Thus, the studied process needs to be tested on real samples to confirm the adsorption results. However, Activated Carbons and zeolites are already used in real treatment with good results, suggesting that MACs and zeolite-magnetite mix can achieve efficient captures also of mixtures of pollutants. The possibility to bond magnetite with any conventional adsorbent gives the chance to choose the better adsorbent for the specific polluted water that have to be treated, can avoid the characterization of the new adsorbent and allows the introduction of the technique in any powder adsorption process. The numerical results concerning the adsorbent removals well reproduced the experimental ones obtained from two different experimental setups. This confirmed that the discretization of the filter in elementary cells, evaluating the efficiency of the whole filter from the removal capacity of a single cell, allows using the model to predict the efficiency of larger scale devices. Because of the permanent magnets available on the market, in real situations the treatable flow rates are up to  $90 \text{ m}^3/\text{h}$  ( $\sim 2000 \text{ m}^3/\text{d}$ ). The costs of permanent magnets are relevant but necessities of achieving higher removals and/or smaller footprints can make the magnetic separation a competitive choice, especially for wastewater treatment.



## Appendix I

### Previous work at LIMSA

The experimental investigations made during my master thesis (*Borghini, 2010*) on the adsorption of detergents and pure surfactants on iron oxides powders (magnetite and hematite) and the filtration through a HGMS steel wool filter were deepened during the first six months of my PhD Course (*Borghini, 2011*). The results obtained show the limitations of the iron oxides powders and the wool filter. The removal using only magnetite and hematite technique lead to good results but without the possibility of improvement. Moreover, the important amounts of sludge generated by the powders and the necessity of disposal of the wool filter after each usage were problems that needed to be solved to have a sustainable process.

This filter was modeled and manufactured in laboratory by the former PhD student of LIMSA team Giacomo Mariani (*Mariani, 2009; Mariani, 2010*).

For laboratory experiments artificial samples were prepared by mixing tap water with commercial detergents and osmotic water with pure surfactants; Table I.I reports the surfactants of the detergents and the pure ones with whom they have been simulated (all the pure surfactants were purchased by Sigma-Aldrich S.r.l but Kemfluid EQ18 and the Cocamidopropyl Betaine that were a gift from Biochimica S.p.A). In commercial detergents several substances are added in addition to surfactants: isothiazolinones as antimicrobials, perfumes (limonene, linalool, hexyl cinnamaldehyde, lily aldehyde...), sodium salts as cleaning agents, etc.

In order to investigate the adsorption of these surfactants and detergents on iron oxide powders, two hematite ( $\alpha\text{-Fe}_2\text{O}_3$ , CAS 1309-37-1) powders with different average diameter, labeled #48100 and #48651, and one magnetite ( $\text{Fe}_3\text{O}_4$ , CAS 1317-61-9) powder, labeled #48800, were purchased from Kremer Pigmente GmbH. Micrometric powders of magnetite and hematite are easy available since they are actually used as pigments; they are non-toxic for humans and the environment, and in addition they have a relatively low cost, i.e. 1-10 Euro/kg (<http://kremer-pigmente.de>). The main features of the powders are listed in Table I.II (<http://kremer-pigmente.de>; *Okada, 2002; Cornell, 2003*). The  $\text{pH}_{\text{pzc}}$  were obtained by mass titration (*Reymond, 1999*) and are comparable with the literature values although it is extremely sensitive to the presence of traces of impurities on the oxide surface (*Fuerstenau, 2002; Cornell, 2003; Ji, 2007*). Figure I.I shows the frequency of the particle size distribution of each powder measured using Fritsch Laser-Particle-Sizer "Analysette 22".

APPENDIX I: PREVIOUS WORK AT LIMSA

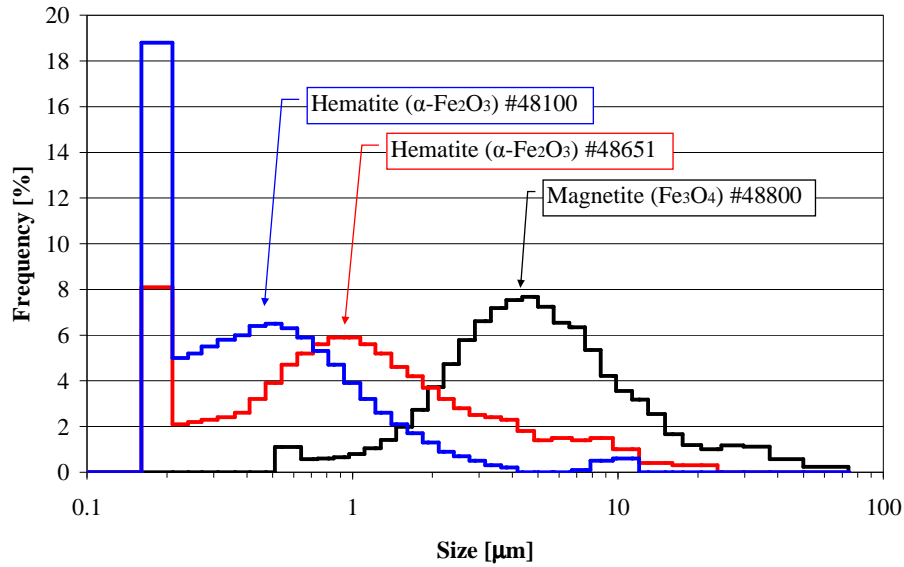


**Figure I.I.** Experimental size distributions for the two hematite powders #48100 and #48651 and the magnetite powder #48800.

**Table I.I.** Tested detergents and surfactants.

	<b>Prevailing Surfactant</b>	<b>Secondary Surfactant</b>
Dishwashing Detergent (DD)	Sodium Alkyl Ether Sulphate (5-15%) (anionic) CAS 68584-34-2	Cocamidopropyl Betaine (5%) (amphoteric) CAS 61789-40-0
<i>Simulated with</i>	Sodium Dodecyl Sulphate SDS (anionic) CAS 151-21-3	Cocamidopropyl Betaine CB (amphoteric) CAS 61789-40-0
Floor Degreaser (FD)	Monobutyl Ether (5%) (non ionic) CAS 111-76-2	-
<i>Simulated with</i>	Imbentin AGS/35 (non ionic) CAS 68937-03-1	-
Washing machine Softener (WS)	Alkyl Ester Ammonium (15-30%) (cationic)	Didecyldimethylammonium chloride (0.1-0.5%) (cationic) CAS 7173-51-5
<i>Simulated with</i>	Kemfluid EQ18 (cationic) CAS 91995-81-2	Didecyldimethylammonium bromide DDAB (cationic) CAS 2390-68-3
Surface Cleaner (SC)	Alcol Ethoxylate (5-15%) (non ionic) CAS 68439-46-3	-
<i>Simulated with</i>	Triton X-100 (non ionic) CAS 9002-93-1	-

Table I.II. Properties of the iron oxide powders.

	Magnetite #48800	Hematite #48651	Hematite #48100
Content Fe <sub>3</sub> O <sub>4</sub> (wt %)	98.5	-	-
Content Fe <sub>2</sub> O <sub>3</sub> (wt %)	-	81.0	96.5
Content SiO <sub>2</sub> + Al <sub>2</sub> O <sub>3</sub> (wt %)	1.2	7.5	< 4.0
Content CaO + MgO (wt %)	0.14	4.3	-
CAS number	1317-61-9	1309-37-1	1309-37-1
Specific Gravity (ISO 787/10)	5.1 g/cm <sup>3</sup>	5.3 g/cm <sup>3</sup>	5.3 g/cm <sup>3</sup>
Tamped Density (ISO 787/11)	1.4 g/cm <sup>3</sup>	0.81 g/cm <sup>3</sup>	0.84 g/cm <sup>3</sup>
Specific Surface (Σ <sub>A</sub> )	2 m <sup>2</sup> /g	15 m <sup>2</sup> /g	19 m <sup>2</sup> /g
pH <sub>pzc</sub>	8.1±0.3	8.3±0.2	7.9±0.3
Most representative particle size	5 μm	1 μm	0.5 μm
Magnetism	ferrimagnetic	antiferromagnetic	antiferromagnetic
Bulk magnetic susceptibility	3.8	2E-3	2E-3

Each test started generating a sample by mixing the detergents or the surfactants with tap water or osmotic water, respectively. Then, the concentration of surfactants was measured with an Hach-Lange tube test (see Appendix II). The initial sample has been divided in three/four equal jars and the iron oxide powder was added. For the considered process the iron oxide concentration ranged typically between 1 and 51 g/l. Also lower and higher concentrations have been tested in some cases. Each subsample was mixed for 10 minutes (about 60 rpm) to allow the adsorption of surfactants on the iron oxide particles and then the powder separation step was carried out. Finally, after the separation step, the concentration of the surfactants remaining in the treated water was measured through the Hach-Lange tube test. The separation step depended on the type of oxide used because of the different particle sizes and magnetic susceptibility of the three powders. In the case of hematite #48100 and #48651 the magnetic filtering device used was the setup #2 reported in section 2.4 with the steel wool filter shown in Figure I.II instead of the spheres filter.

As shown in Figure I.II, the wool filter was made of AISI434 wool obtained from GMT Inc., with fibres of effective diameter of the order of 10 micron and a packaging factor of about 3.5E-3. Each filtering element was made rolling the wool around a circular drilled tube and placed inside the rectangular filtering section. The holes, with a diameter of 1 mm, were arranged in nine series of three equally spaced holes each. The flow was constrained to pass radially through the wool; in its working configuration the wool fibres were disposed orthogonally to the magnetic flux density field and, on average, to the mixture flow. A detailed description of the wool filter is reported in (Mariani,2009; Mariani, 2010).

## APPENDIX I: PREVIOUS WORK AT LIMSA

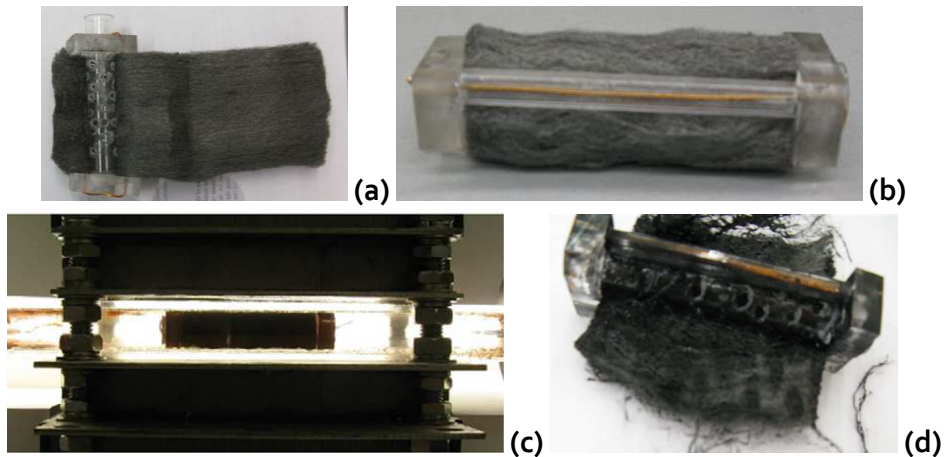


**Figure I.II.** Zoom of the wool filter opened showing the drilled tube (a), rolled (b), between two Sm-Co permanent magnets (c) and opened after the filtration (d).

In order to avoid damage to the laboratory device because of the high amount used, magnetite #48800 was separated only by sedimentation. The sedimentation was fast but the finer fraction of the powder floated on the surface; 10 minutes near the magnet allowed attracting the ferrimagnetic particles of magnetite cleaning the water. Figure I.III shows an optical microscope image of the chains of magnetized particles on the surface film.

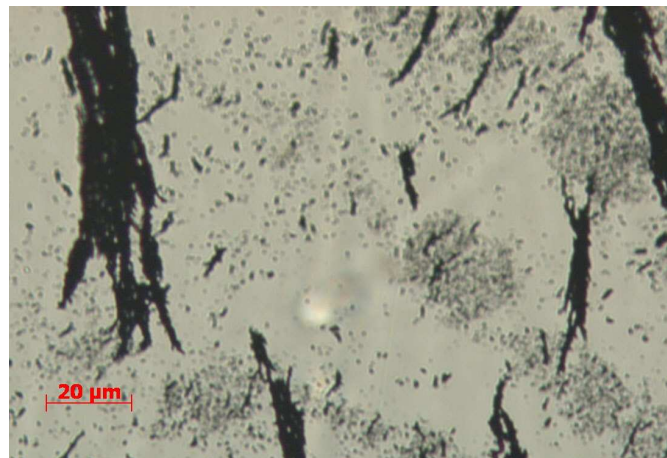


**Figure I.III.** Structure of the magnetite #48800 fine fraction floating on the water surface.

The capture efficiency of the wool filter  $\sigma$ , defined as the ratio between the numbers of captured and entering particles, has been characterized in (Mariani, 2009; Mariani 2010) by a statistical analysis of the particle's trajectory over randomly generated wool geometry. It depends on the adimensional parameter  $\Omega$  (defined as in section 4.1). With reference to the bulk susceptibility values reported in Table I.II, the effective susceptibility for hematite is unchanged, while for magnetite takes a value of about 1.7. Figure I.IV reports the calculated capture efficiency of the filter. The error bars are due to the stochastic nature of the model. Figure I.IV, for given magnetic filter, shows the dependence of the particle diameter and susceptibility on the capture efficiency. Magnetite powder with its large diameter and

ferromagnetic behaviour lead to a  $\text{Log } \Omega$  values in the range 0.5 - 4.4 implying a fast capture by the steel wool. In facts, as shown in Table I.III, one passage through the filter is sufficient to completely remove the magnetite #48800. On the contrary, for the hematite  $\text{Log } \Omega$  ranges between -3.4 and 0.5 and many passages through the filter are required to completely remove the hematite powder. Since the capture is more effective for the larger particles sizes the mass retention is different from the particle one.

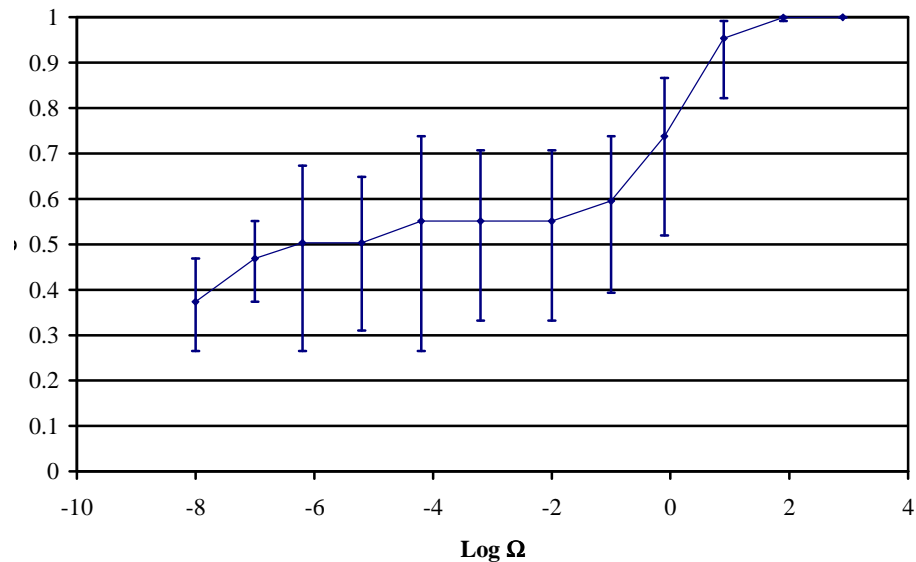


**Figure I.IV.** Calculated capture efficiency of the used wool filter. The error bars are due to the statistical nature of the model.

**Table I.III.** Particle and mass retention for 1 g sample of the iron oxides powders as a function of the number of passages through the wool magnetic filter.

Number of passages	Magnetite #48800		Hematite #48651		Hematite #48100	
	Particle Retention [%]	Mass Retention [%]	Particle Retention [%]	Mass Retention [%]	Particle Retention [%]	Mass Retention [%]
1	99.8	99.9	53.9	86.1	48.2	83.6
2	99.9		77.7	97.1	72.8	96.6
3			89.0	99.2	85.6	98.9
4			94.4	99.7	92.4	99.6
5			97.2	99.9	95.7	99.8
6			98.5		97.8	99.9
7			99.2		98.8	
8			99.6		99.4	

Moreover, the size distribution of the suspended powder changes during the process, as shown in Figure I.V for hematite #48100. As shown in Table I.III, the mass capture was

above 99% after the 4<sup>th</sup> passage and the particle capture was above 99% after the 8<sup>th</sup> passage. Figure I.VI shows a sample of hematite #48100 suspended in water before and after the filtration with the wool magnetic filter.

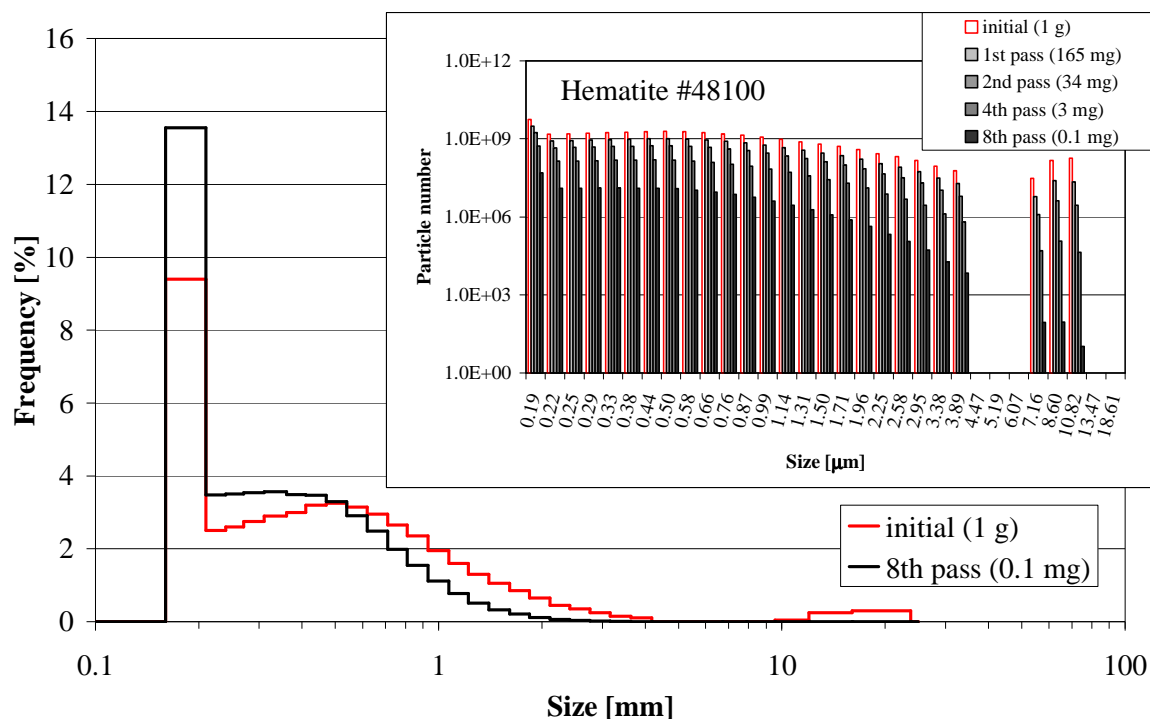


**Figure I.V.** Calculated size distributions for the hematite powder #48100 after eight passages through the wool magnetic filter. The insert shows the evolution of the particle number distribution with the number of passages through the filter for a 1 g sample of hematite #48100.



**Figure I.VI.** Sample of a water suspension of hematite #48100 before (left) and after (right) 10 minutes filtration in the wool magnetic filter.

The laboratory adsorption tests led to positive results with regard to all surfactants but using large amount of powders. Various initial surfactant concentrations was considered, the reproducibility of the data was checked several times, leading to an average variation of about 10% on the measures.

The results are reported in terms of residual as defined in (3.1.1), where  $C_0$  and  $C_r$  are the initial and the residual concentration in the solutions. For each detergent and surfactant the residual (%) is plotted as a function of the concentration of powder used (in g/l).

Furthermore, the same data were used to plot the adsorption isotherms, showing the surface excess vs the residual concentration. The surface excess was calculated as follows:

$$\Gamma_s = \frac{C_0 - C_r}{C_A \Sigma_A} \quad (I)$$

where  $C_A$  and  $\Sigma_A$  are the concentration and the specific area of the adsorbent. A larger mixing times of 20 minutes produced no changes on the final surfactants concentration, while a 2-5 minutes mixing caused roughly the doubling of the final surfactants concentration. We have not used an adsorption model because our experimental points are insufficient to draw conclusions, especially in cases where the final concentration is constant with the adsorbent producing no defined slope. However, since the iron oxides surface is certainly impure, for pure surfactants a Langmuir type model is not certainly applicable.

Figures I.VII and I.VIII show the behaviour of non-ionic surfactants in SC, FD and the pure surfactants Triton X-100 and Imbentin AGS/35. There is few adsorption for magnetite #48800 and a quite good capture by both hematites. A difference in removal between pure surfactants and detergents could be explained by the presence of other species in the aqueous phase that can compete for adsorption sites at that pH. Figure I.IX and Figure I.X show the results for cationic surfactants in WS, simulated with Kemfluid EQ18 and the DDAB behaviour respectively. The DDAB was analyzed separately with higher concentrations than the softener ones (0.1-0.5% V/V) because of the limits of our spectrophotometer. All cationics seem to have a good removal (80-90%) and the same trend of adsorption. This satisfying results could be explained because at  $\text{pH} > \text{pH}_{\text{pzc}}$  the negative groups on the iron oxide surface predominate over the positive ones generating a relevant electrostatic attraction to the hydrophilic positive head of the surfactant. Figure I.XI shows the results obtained using the three iron oxides on samples generated diluting the DD and the pure surfactant SDS alone and with the CB. We did not analyze the CB alone because the tube tests cannot measure amphoteric surfactants. The hematite, finer than magnetite and porous, removes larger amount of all types of surfactants. Furthermore, a lower amount of powder was required to achieve the same result or better values.

APPENDIX I: PREVIOUS WORK AT LIMSA

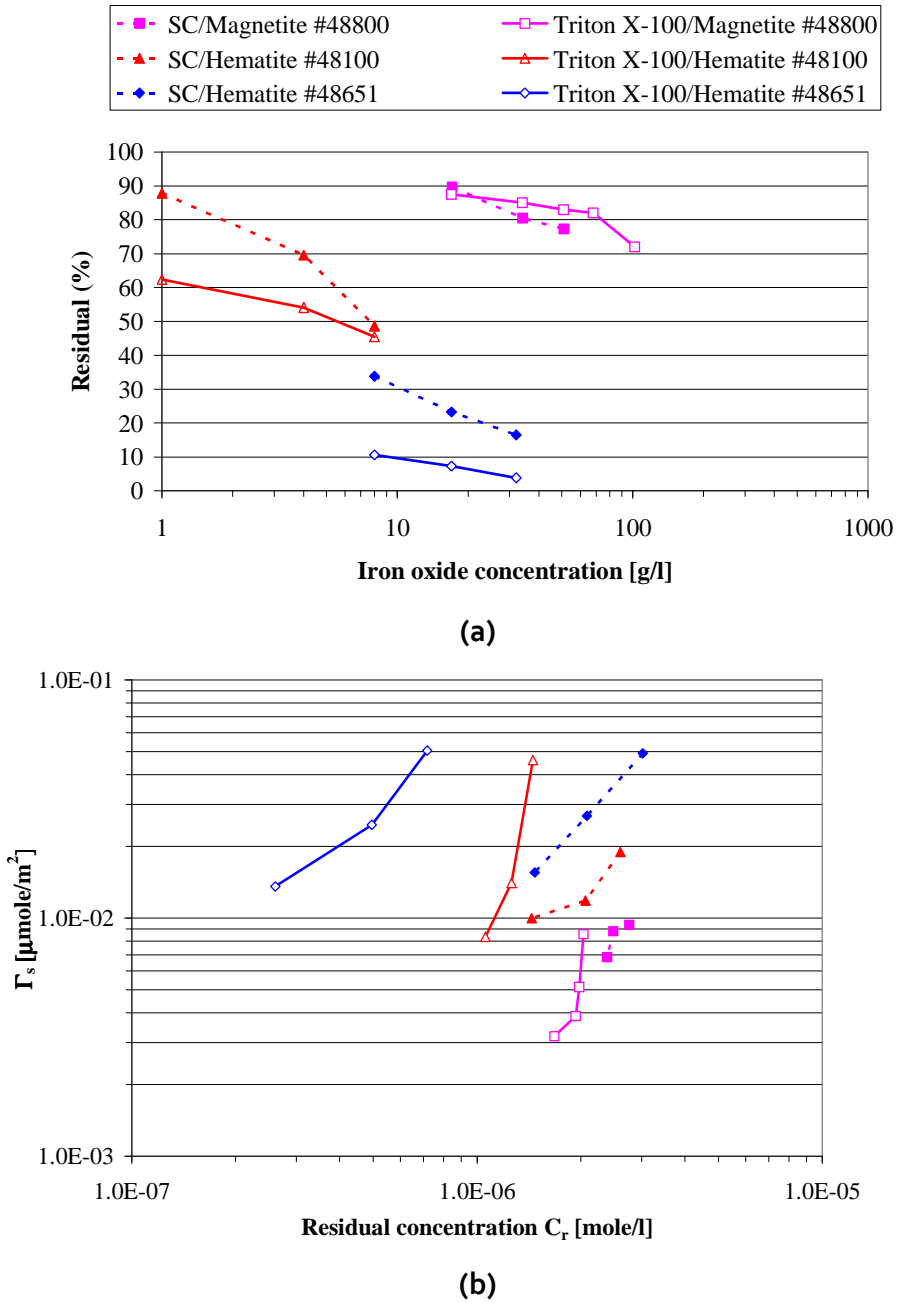
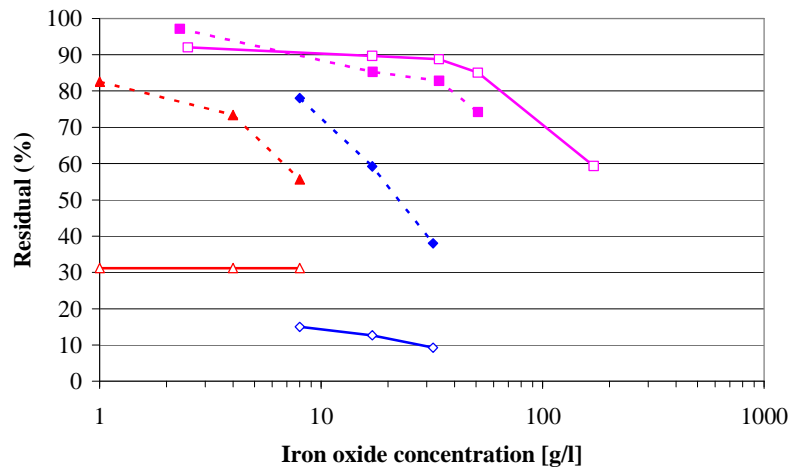
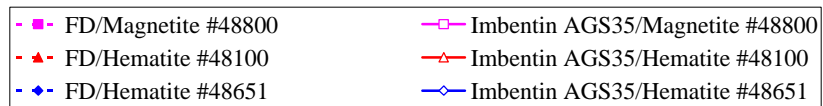
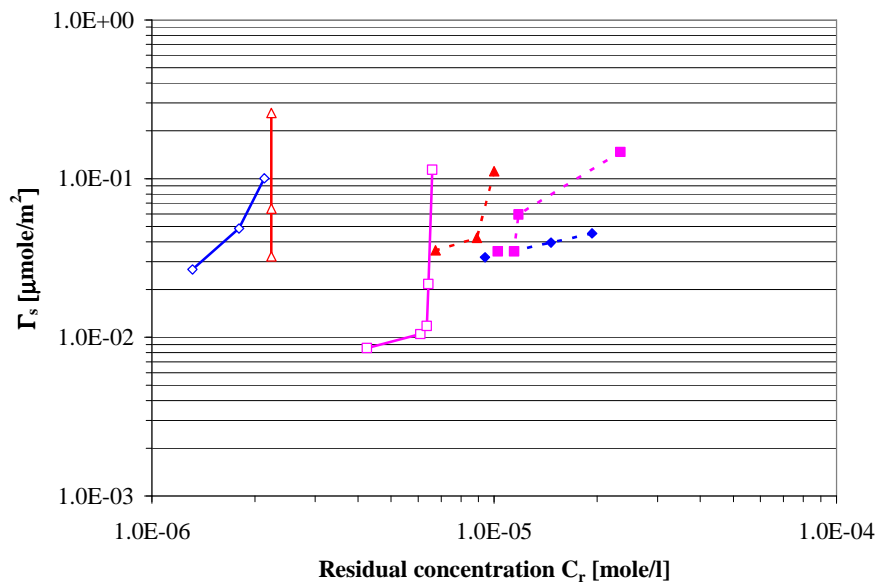


**Figure I.VII.** Residual of SC and Triton X-100 after adsorption on the three iron oxides (a) and adsorption isotherms of SC and Triton X-100 on the three iron oxides (b). The initial concentration of the surfactants ranges between 1.4 and 4.2 mg/l.



(a)



(b)

**Figure I.VIII.** Residual of FD and Imbentin AGS35 after adsorption on the three iron oxides (a) and adsorption isotherms of FD and Imbentin AGS35 on the three iron oxides (b). The initial concentration of the surfactants ranges between 1.5 and 2.9 mg/l.

APPENDIX I: PREVIOUS WORK AT LIMSA

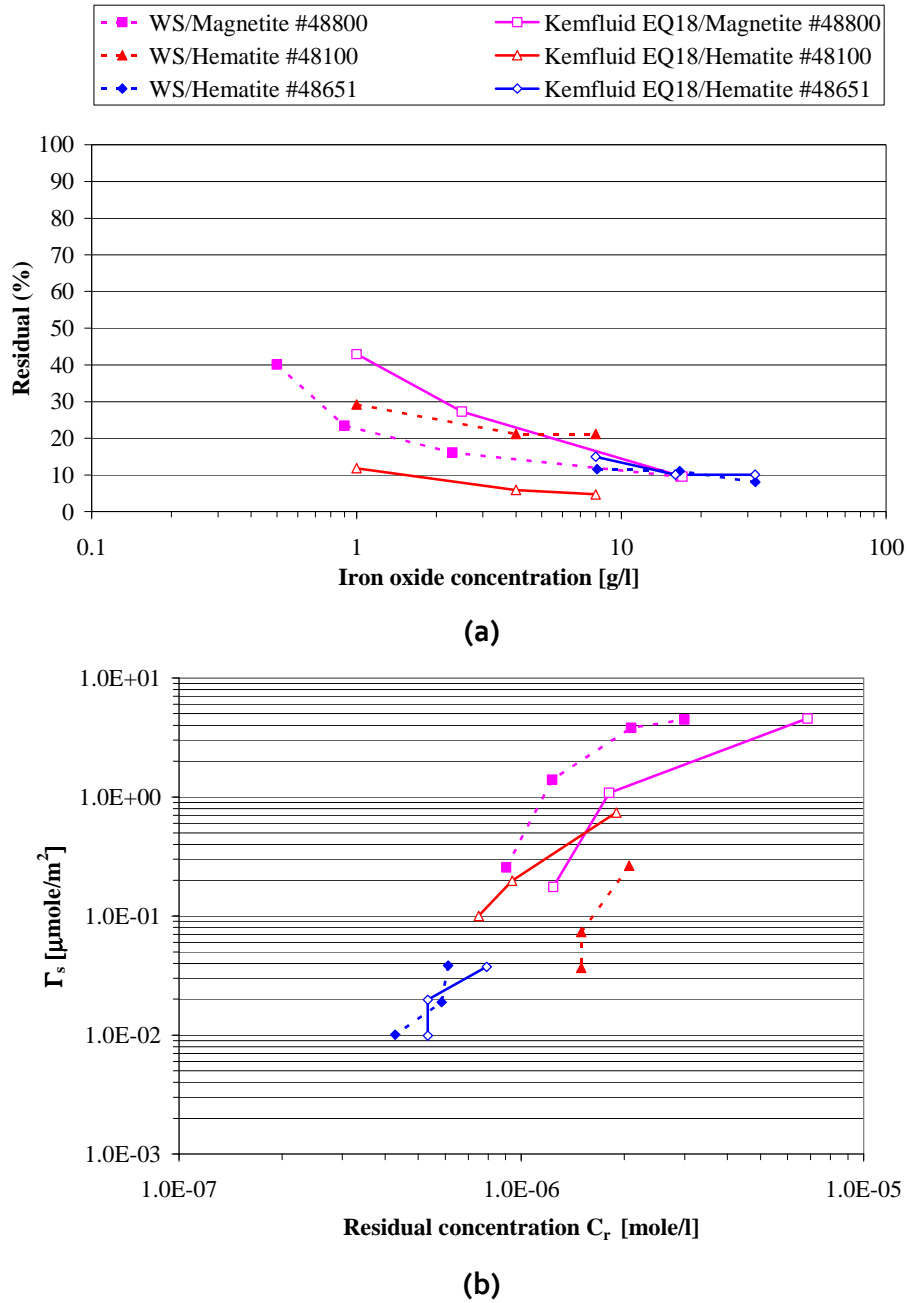
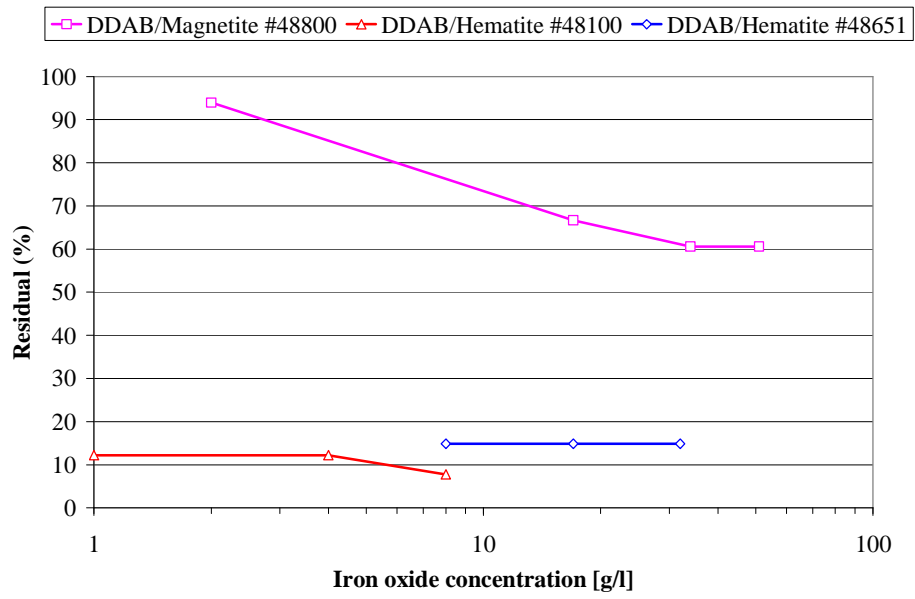
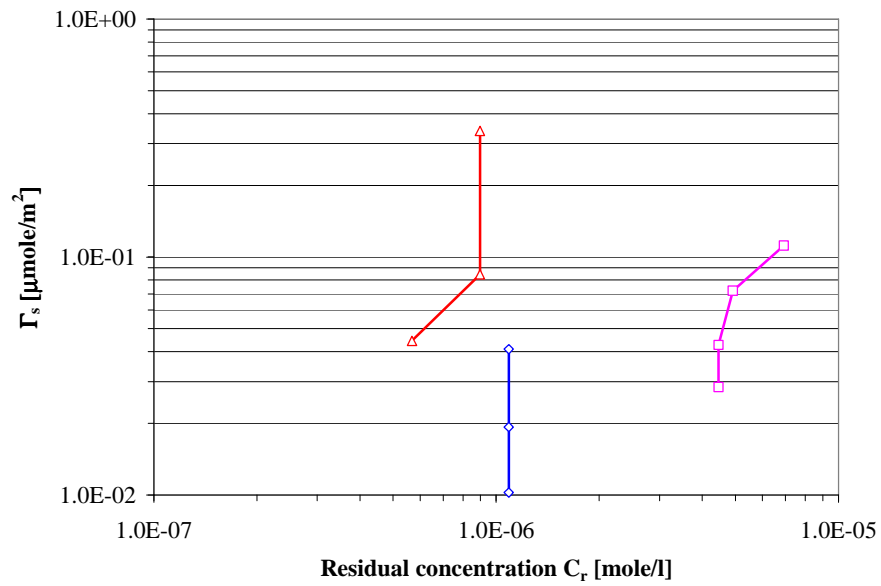


**Figure I.IX.** Residual of WS and the Kemfluid EQ18 after adsorption on the three iron oxides (a) and adsorption isotherms of WS and Kemfluid EQ18 on the three iron oxides (b). The initial concentration of the surfactants ranges between 1.2 and 3.6 mg/l.



(a)



(b)

**Figure I.X.** Residual of DDAB after adsorption on the three iron oxides (a) and adsorption isotherms of DDAB on the three iron oxides (b). The initial concentration of the surfactant was 3 mg/l.

APPENDIX I: PREVIOUS WORK AT LIMSA

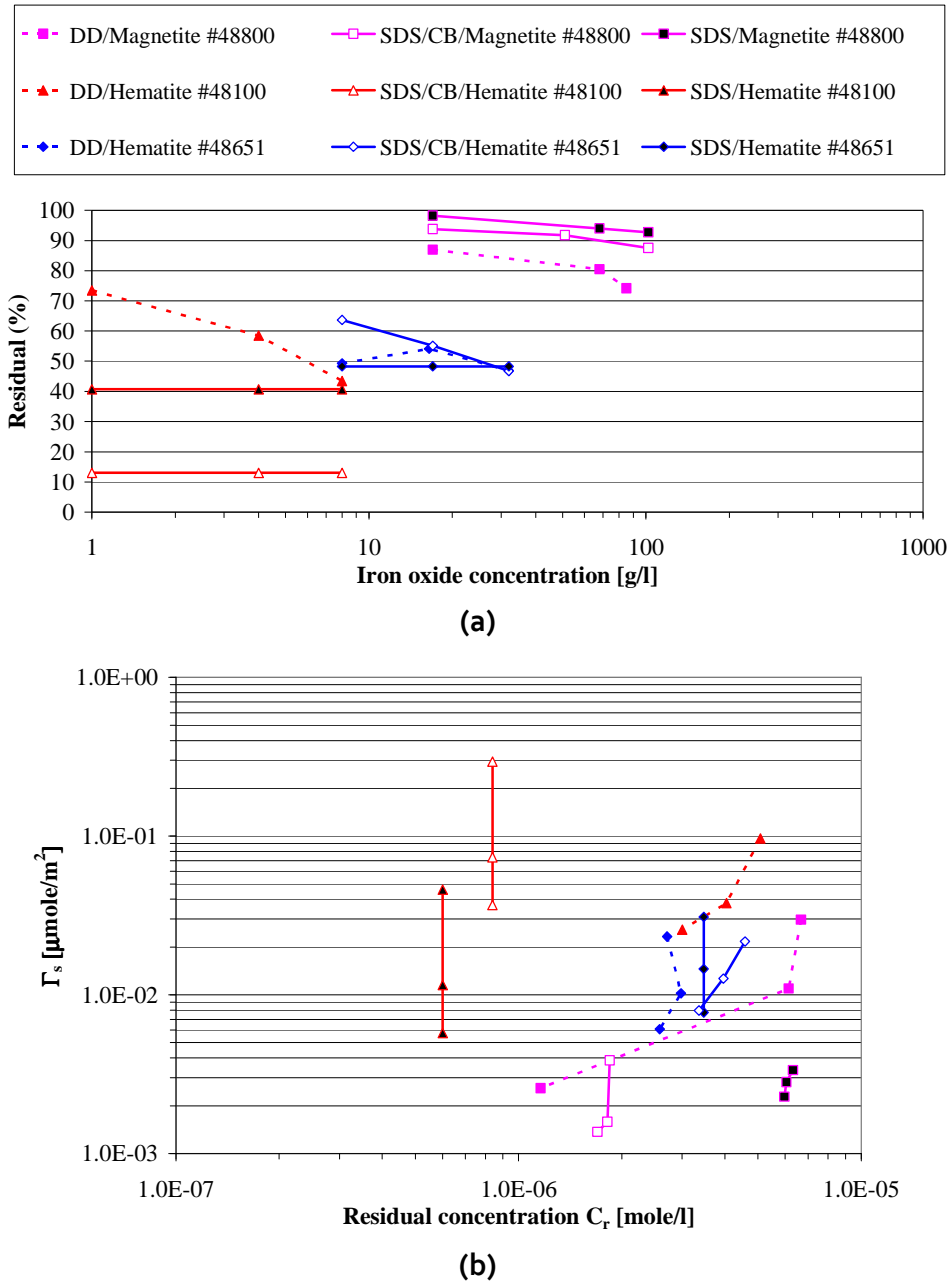


**Figure I.XI.** Residual of DD and SDS, alone and with CB, after adsorption on the three iron oxides (a). Adsorption isotherms of DD and SDS, alone and with CB on the three iron oxides (b). The initial concentration of the surfactants ranges between 0.2 and 2.1 mg/l.

## Appendix II

### Tube tests procedures

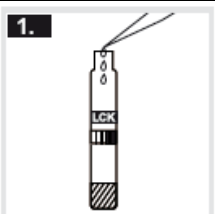
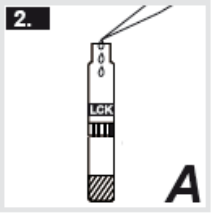
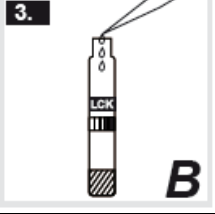
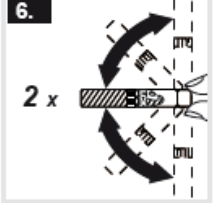
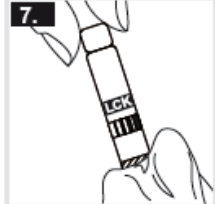
The measure of the initial and final concentration of the tested pollutants was carried out using Hach-Lange and Nanocolor tube tests. The spectrophotometer Hach-Lange DR2800 (shown in Figure II.I) was compatible with all the Hach Lange tube tests. The cuvettes of the Nanocolor tests were not compatible with the spectrophotometer. Thus, the content of the cuvette was decanted in Hach-Lange empty cuvettes and the correct wave length reported on the test procedure was set to read the corresponding absorbance. A concentration-absorbance correlation curve was always created reading the absorbance of different sample of the same pollutant with known concentration. All measure took from 5 to 20 minutes and at least two measures are necessary to have a point on the curves reporting the residual pollutant after the treatment. So laboratory tests to evaluate the absorption of contaminants and to verify the residual concentrations have occupied much of the time of the research. All the tube tests procedures are reported in the following.



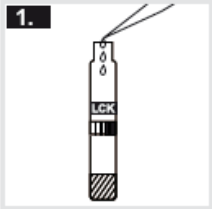
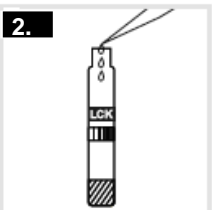
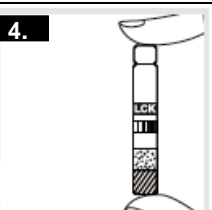
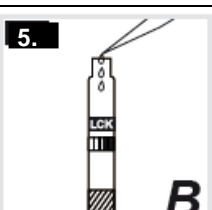
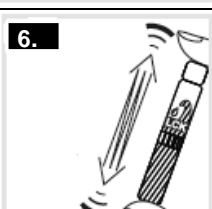
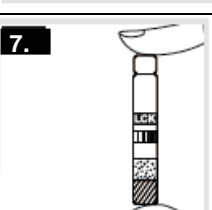
**Figure II.I.** Hach-Lange spectrophotometer DR2800.

## APPENDIX II: TUBE TESTS PROCEDURES

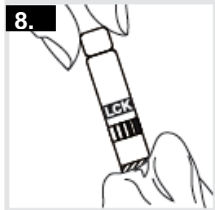
Procedure for cationic, anionic and non ionic surfactants:

	<b>Cationic surfactants (lck 331) Hach-Lange</b>	<b>Anionic surfactants (lck 332) Hach-Lange</b>	<b>Non-ionic surfactants (lck 333) Hach-Lange</b>
<b>1.</b> 	Pipette 4 ml of sample	Pipette 3.5 ml of sample	Pipette 2.5 ml of sample
<b>2.</b> 	Pipette 0.4 ml of reagent A	Pipette 0.4 ml of reagent A	-
<b>3.</b> 	Pipette 0.2 ml of reagent B	Pipette 0.2 ml of reagent B	-
<b>4.</b> 	Close the cuvette and shake it for 2 minutes	Close the cuvette and shake it for 60 seconds	Close the cuvette and shake it for 2 minutes
<b>5.</b> 	Leave the cuvette standing upright for 30 seconds	Leave the cuvette standing upright for 30 seconds	Leave the cuvette standing upright for 2 minutes
<b>6.</b> 	Invert the cuvette twice carefully	Invert the cuvette twice carefully	-
<b>7.</b> 	Thoroughly clean the outside of the cuvette and evaluate	Thoroughly clean the outside of the cuvette and evaluate	Thoroughly clean the outside of the cuvette and evaluate

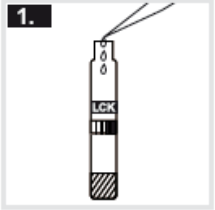
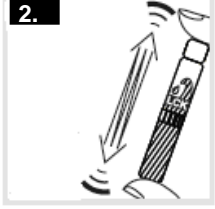
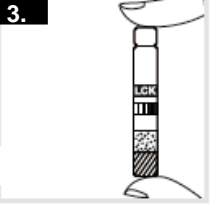
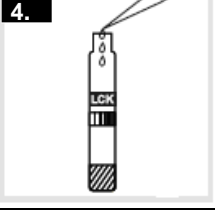
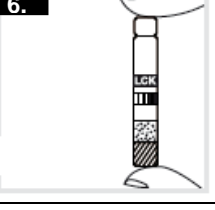
Procedure for phenols, iron (FeIII) and organic complexing agents (EDTA):

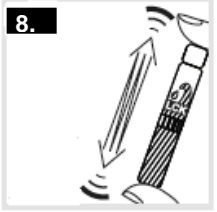
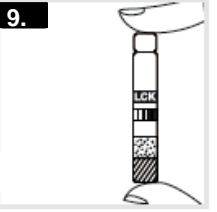
	Phenols (lck 345) Hach-Lange	Iron (REF 985037) Nanocolor	Organic complexing agents (REF 985052) Nanocolor
1. 	Pipette 2 ml of sample	Pipette 4 ml of sample	Pipette 4 ml of sample
2. 	Pipette 0.2 ml of reagent A	Introduce NANOFIX R <sub>2</sub> reagent	Introduce NANOFIX R <sub>2</sub> reagent
3. 	Close the cuvette and shake it for 30 seconds	Close the cuvette and shake it for 30 seconds	Close the cuvette and shake it for 30 seconds
4. 	Leave the cuvette standing upright for 2 minutes	Leave the cuvette standing upright for 10 minutes	Leave the cuvette standing upright for 5 minutes
5. 	Pipette 0.2 ml of reagent B	-	-
6. 	Close the cuvette and shake it for 30 seconds	-	-
7. 	Leave the cuvette standing upright for 2 minutes	-	-

APPENDIX II: TUBE TESTS PROCEDURES

	<p>Thoroughly clean the outside of the cuvette and evaluate</p>	<p>Thoroughly clean the outside of the cuvette and evaluate</p>	<p>Thoroughly clean the outside of the cuvette and evaluate</p>
---	---	---	---

Procedure for hardness (Call, dH) and manganese (MnII):

	<p><b>Hardness (lck 327) Hach-Lange</b></p>	<p><b>Manganese (REF 985058) Nanocolor</b></p>
	<p>Pipette 4 ml of reagent A</p>	<p>Pipette 4 ml of sample</p>
	<p>Close the cuvette and shake it for 30 seconds</p>	<p>Close the cuvette and shake it for 30 seconds</p>
	<p>Leave the cuvette standing upright for 2 minutes and introduce it in the spectrophotometer</p>	<p>-</p>
	<p>Pipette 0.2 ml of sample</p>	<p>Pipette 0.5 ml of reagent R2</p>
	<p>Close the cuvette and shake it for 30 seconds</p>	<p>Close the cuvette and shake it for 30 seconds</p>
	<p>Leave the cuvette standing upright for 30 seconds and introduce it in the spectrophotometer</p>	<p>Leave the cuvette standing upright for 1 minute</p>

	<p>Pipette 0.2 ml of reagent B</p>	<p>Introduce NANOFIX R<sub>3</sub> reagent</p>
	<p>Close the cuvette and shake it for 30 seconds</p>	<p>Close the cuvette and shake it for 30 seconds</p>
	<p>Leave the cuvette standing upright for 30 seconds</p>	<p>Leave the cuvette standing upright for 5 minutes</p>
	<p>Thoroughly clean the outside of the cuvette and evaluate</p>	<p>Thoroughly clean the outside of the cuvette and evaluate</p>

## APPENDIX II: TUBE TESTS PROCEDURES

## References

- Abbasov T.** (2007), "Theoretical magnetic filtration with magnetized granular beds: basic principles and filter performance", *China Particuology* 5, pp. 71-83.
- Alvarez-Bastida C. et al.** (2013), "The corrosive nature of manganese in drinking water", *Science of The Total Environment* 447, pp. 10-16.
- Amirtharajah A.** and Casey Jones S. (2005), "Drinking Water Treatment" in: *Environmental System and Management*, CRC Press, New York, chapter 88.
- Anastassakis G.N.** (2002), "Separation of fine mineral particles by selective magnetic coating", *Journal of Colloid and Interface Science* 256, pp. 114-120.
- Anderson N. J. et al.** (1982), Water and wastewater treatment with reusable magnetite particles, *Water Science and Technology* 14, pp. 1545-1546.
- Anderson N. J. et al.** (1983), "Colour and turbidity removal with reusable magnetite particles-VI", *Water Research* 17(10), pp. 1235-1243.
- Asimakopoulos A.G. et al.** (2012), "Recent trends in biomonitoring of bisphenol A, 4-t-octylphenol, and 4-nonylphenol", *Toxicology Letter* 210, pp. 141-154.
- Baban A.** and Talinli I. (2009), "Modeling of organic matter removal and nitrification in sewer systems - an approach to wastewater treatment", *Desalination* 246, pp. 640-647.
- Bansal R.C.** and Goyal M. (2005), *Activated Carbon Adsorption*, CRC Press, New York.
- Basar C.A. et al.** (2004), "Removal of Surfactants by Powdered Activated Carbon and Microfiltration", *Water Research* 38, pp. 2117-2124.
- Borghì C.C.** (2010), *Studio sperimentale sulla separazione di tensioattivi mediante adsorbimento su ossidi di ferro per il trattamento di acque reflue urbane*, Master Thesis (Italian version), University of Bologna, Bologna, Italy.
- Borghì C.C., Fabbri M., Fiorini M., Mancini M. and Ribani P.L.** (2011), "Magnetic removal of surfactants from wastewater using micrometric iron oxide powders", *Separation and Purification Technology* 83, pp. 180-188.
- Borghì C.C., Akiyama Y., Fabbri M., Nishijima S. and Ribani P.L.** (2014a), "Magnetic separation of Magnetic Activated Carbons for water treatment and reuse", *COMPEL Journal* 33(1/2), pp. 445-462.
- Borghì C.C. and Fabbri M.** (2014b), "Magnetic recovery of modified Activated Carbon powder used for removal of endocrine disruptors present in water", *Environmental Technology*, DOI: 10.1080/09593330.2013.858776, in press.
- Bouwer H.** (2005), "Adverse Effects of Sewage Irrigation on Plants, Crops, Soil, and Groundwater" in: Lazarova V. and Bahri A., *Water Reuse for Irrigation, Agriculture, Landscapes and Turf Grass*, CRC Press, New York, pp. 235-263.
- Cavalli L.** (2004), "Surfactants in the Environment Fate and Effects of Linear Alkylbenzene Sulfonates (LAS) and Alcohol-Based Surfactants" in: *Handbook of Detergents: Environmental Impact, part B*, U. Zoller Ed. CRC Press, pp. 373-427.
- Chaturvedi S. and Dave P.N.** (2012), "Removal of iron for safe drinking water", *Desalination* 303, pp. 1-11.
- Chun C. and Park J.** (2001), "Oil Spill Remediation Using Magnetic Separation", *Journal of Environmental Engineering*, pp. 443-449.

**Clift R. et al.** (2005), *Bubbles, drops, and particles*, Academic Press, Dover Publications Inc., New York, pp. 110-112.

**Cornell R.N.** and Schwertmann U. (2003), *The Iron Oxides: Structure, Properties, Reactions, Occurrences and Uses*, 2nd edition, WILEY-VCH GmbH & Co. KGaA. S.

**Ding C.** and Shang C. (2010), "Mechanisms Controlling Adsorption of Natural Organic Matter on Surfactant-Modified Iron Oxide-Coated Sand", *Water Research* 44, pp. 3651-3658.

**Do M.H. et al.** (2011), "Activated Carbon/Fe<sub>3</sub>O<sub>4</sub> Nanoparticle composite: Fabrication, Methyl Orange Removal and Regeneration by Hydrogen Peroxide", *Chemosphere* 85, pp. 1269-1276.

**Dobiàs B.** and Stechemesser H. (2005), *Coagulation and Flocculation*, Second Edition, CRC Press, New York, pp. 663-765.

**Duman O.** and Ayaranci E. (2010), "Adsorptive Removal of Cationic Surfactants from Aqueous solutions onto High-area Activated Carbon Cloth Monitored by in Situ UV Spectroscopy", *Journal of Hazardous Materials* 174, pp. 359-367.

**Duncan R.R. et al.** (2009), *Turfgrass and Landscape Irrigation Water Quality: Assessment and Management*, CRC Press, New York, pp. 13-38.

**EPA** (1983), *Construction costs for municipal wastewater treatment plants: 1973-1982*. Environmental Protection Agency, Washington DC, EPA/430/9-83-004.

**EPA** (2005), *Aquatic life ambient water quality criteria-nonylphenol final*. Environmental Protection Agency, Washington DC, EPA-822-R-05-005.

**Fabrizi M.** (2008), "Magnetic flux density and vector potential of uniform polyhedral sources", *IEEE Transactions on Magnetics* 44(1), pp. 32-36.

**Fabrizi M., Morandi A.** and Ribani P.L. (2013), "DC induction heating of aluminium billets using static permanent magnets", in *HES-13*, F. Dughiero, M. Forzan, E. Sieni (Ed.s), SGE ED, Padova, ISBN 978-88-89884-25-6, 2013, pp. 355-362.

**Fiorillo F.** (2004), *Measurements and characterization of magnetic materials*, Elsevier-Academic Press, Amsterdam, pp. 9-16.

**Fishman G.S.** (1990), "Multiplicative congruential random number generators with modulus  $2^*b$ : an exhaustive analysis for  $b = 32$  and a partial analysis for  $b = 48$ ", *Mathematics of Computation* 189, pp. 331-344.

**Frassinetti S. et al.** (1996), "Bacterial Attack of Non-Ionic Aromatic Surfactants: Comparison of Degradative Capabilities of New Isolates from Nonylphenol Polyethoxylate Polluted Wastewaters", *Environmental Technology* 17(2), pp. 199-205.

**Fuerstenau D.W.** (2002), "Equilibrium and Nonequilibrium Phenomena Associated with the Adsorption of Ionic Surfactants at Solid-Water Interfaces", *Journal of Colloid and Interface Science* 256, pp. 79-90.

**Gang Z.Y. et al.** (2010), "Synthesis, characterization and properties of ethylenediamine-functionalized Fe<sub>3</sub>O<sub>4</sub> magnetic polymers for removal of Cr(VI) in wastewater", *Journal of Hazardous Material* 182, pp. 295-302.

**Gao X.** and Chorover J. (2010), "Adsorption of Sodium Dodecyl Sulfate (SDS) at ZnSe and  $\alpha$ -Fe<sub>2</sub>O<sub>3</sub> Surfaces: Combining Infrared Spectroscopy and Batch Uptake Studies", *Journal of Colloid and Interface Science* 348, pp. 167-176.

**Gaspard S. et al.** (2008), "Activated Carbon in Waste Recycling, Air and Water Treatment, and Energy Storage" in: *Environmental Management, Sustainable Development and Human Health*, CRC Press, New York, pp. 441-459.

**Godskesen B. et al.** (2012), "Life cycle assessment of central softening of very hard drinking water", *Journal of Environmental Management* 105, pp. 83-89.

**Gonzalez-Garcia C.M. et al.** (2001), "Analysis of the Adsorption Isotherms of a Non-ionic Surfactant from Aqueous Solution onto Activated Carbons", *Carbon* 39, pp. 849-855.

**Gonzalez-Garcia C.M. et al.** (2004a), "Nonionic surfactants adsorption onto activated carbon. Influence of the polar chain length", *Powder Technology* 148, pp. 32-37.

**Gonzalez-Garcia C.M. et al.** (2004b), "Ionic Surfactant Adsorption onto Activated Carbons", *Journal of Colloid and Interface Science* 278, pp. 257-264.

**Góral M. et al.** (2011), "IUPAC-NIST Solubility Data Series. 91. Phenols with Water. Part 2. C<sub>8</sub> to C<sub>15</sub> Alkane Phenols with Water", *Journal of Physical and Chemical Reference Data* 40(3), 033103-1-033103-60.

**Higgins C.P. and Luthy R.G.** (2006), "Sorption of Perfluorinated Surfactants on Sediments", *Environmental Science and Technology* 40, pp. 7251-7256.

**Hu J. et al.** (2007), "Comparative study of various magnetic nanoparticles for Cr(VI) removal", *Separation and Purification Technology* 56, pp. 249-256.

**Ifelebuegu A.O.** (2011), "The fate and behavior of selected endocrine disrupting chemicals in full scale wastewater and sludge treatment unit processes", *International Journal of Environmental Science and Technology* 8(2), pp. 245-254.

**Ihara I. et al.** (2004), "High gradient magnetic separation combined with electrocoagulation and electrochemical oxidation for the treatment of landfill leachate", *IEEE Transactions on Applied Superconductivity* 14(2), pp. 1558-1560.

**Ihara I. et al.** (2009), "Magnetic separation of antibiotics by electrochemical magnetic seeding", *Journal of Physics Conference Series* 156.

**Ishiwata T. et al.** (2010), "Removal and recovery of phosphorus in wastewater by superconducting high gradient magnetic separation with ferromagnetic adsorbent", *Physica C* 470, pp. 1818-1821.

**Ji Y.Q. et al.** (2007), "Hydrophobic Coagulation and Aggregation of Hematite Particles with Sodium Dodecylsulfate", *Colloids and Surfaces A: Physicochemical and Engineering Aspects* 298, pp. 235-244.

**Jia Z. et al.** (2011), "Preparation and Application of Novel Magnetically Separable  $\gamma$ -Fe<sub>2</sub>O<sub>3</sub>/Activated Carbon Sphere Adsorbent", *Material Science and Engineering B* 176, pp. 861-865.

**Jonsson B.** (2006), *Risk assessment on butylphenol, octylphenol and nonylphenol, and estimated human exposure of alkylphenols from Swedish fish*, Graduate Project, Uppsala University, Uppsala, Sweden.

**Kawamura S.** (2000), *Integrated Design and Operations of Water Treatment Facilities*. Second Edition, John Wiley and Sons Ltd New York, pp. 523-529.

**Katsou E. et al.** (2011), "Regeneration of natural zeolite polluted by lead and zinc in wastewater treatment systems", *Journal of Hazardous Materials* 189, pp. 773-786.

**Kogelbauer A.** and Prins R.(2001), "C2.12 Zeolites" in *Encyclopedia of Chemical Physics and Physical Chemistry, Volume III: Applications*, Moore and Spencer Eds., IOP Publishing, Bristol and Philadelphia.

**Landau L.D.** and Lifshitz E.M. (2011), *Fluid mechanics*, Elsevier, pp. 73-75.

**Li A.** and Ahmadi G. (1992), "Dispersion and deposition of spherical particles from point sources in a turbulent channel flow", *Aerosol Science and Technology* 16, pp. 209-226.

**Li L.Y. et al.** (2007), "Remediation of acid rock drainage by regenerable natural clinoptilolite", *Water, Air, and Soil Pollution* 180(1-4), pp. 11-27.

**Lim J.** and Okada M. (2005), "Regeneration of Granular Activated Carbon using Ultrasound", *Ultrasonics Sonochemistry* 12, pp. 277-282.

**Lu Q.** and Sorial G.A. (2007), "The effect of functional groups on oligomerization of phenolics on activated carbon", *Journal of Hazardous Materials* 148, pp. 436-445.

**Lu M. et al.** (2013), "Surface modification of porous suspended ceramsite used for water treatment by activated carbon/Fe<sub>3</sub>O<sub>4</sub> magnetic composites", *Environmental Technology* 34, pp.2301-2307.

**Madsen T.** (2004), "Biodegradability and Toxicity of Surfactants" in: *Handbook of Detergents: Environmental Impact, part B*, U. Zoller Ed. CRC Press, New York, pp. 211-248.

**Malik M.** (1996), *In-sewer treatment of domestic wastewater*, Ph.D. diss., University of Newcastle upon Tyne, NE 17 RU United Kingdom.

**Margeta K. et al.** (2013), "Natural Zeolites in Water Treatment – How Effective is Their Use" in: *Water Treatment*, Walid Elshorbagy and Rezaul Kabir Chowdhury Eds., InTech, chapter 5.

**Mariani G., Fabbri M., Negrini F. and Ribani P.L.** (2009), "High-gradient magnetic separation of micro-pollutant from wastewaters", *La Houille Blanche* 6, pp. 109-117.

**Mariani G., Fabbri M., Negrini F. and Ribani P.L.** (2010), "High-gradient magnetic separation of pollutant from wastewaters using permanent magnets", *Separation and Purification Technology* 72, pp. 147-155.

**Meng H.** and Van der Geld C.W.M. (1991), "Particles trajectory computations in steady non uniform liquid flows" in *Liquid Solid Flows: First ASME/JSME Fluids Engineering Conference*, Portland, Oregon, pp. 183-193.

**Metcalf & Eddy** (2003), *Wastewater Engineering: Treatment and Reuse, Fourth Edition*, The McGraw Hill Companies.

**Mishima F., Akiyama Y. and Nishijima S.** (2010), "Research and development of magnetic purification system for used wash water of drum", *IEEE Transactions on Applied Superconductivity* 20, pp. 937-940.

**Mitsuhashi K.** (2003), "Purification of endocrine disrupter-polluted water using high temperature superconducting HGMS", *Physical Separation in Science and Engineering* 12(4), pp. 205-213.

**Mohan D. et al.** (2011), "Development of magnetic activated carbon from almond shells for trinitrophenol removal from water", *Chemical Engineering Journal* 172, pp. 1111-1125.

**Morandi A.**, Fabbri M. and Ribani P.L. (2010), "A modified formulation of the volume integral equations method for 3D magnetostatics", *IEEE Transactions on Magnetics* 46, pp. 3848-3859.

**Nah I.W. et al.** (2008), "Removal of ammonium ion from aqueous solution using magnetically modified zeolite", *Environmental Technology* 29(6), pp. 633-639.

**Nakahira A. et al.** (2006), "Synthesis of magnetic activated carbons for removal of environmental endocrine disrupter using magnetic vector", *Journal of the Ceramic Society of Japan* 114(1), pp. 135-137.

**Nassar N.N.** (2010), "Rapid removal and recovery of Pb(II) from wastewater by magnetic nanoadsorbents", *Journal of Hazardous Materials* 184, pp. 538-546.

**Naylor C.G.** (2004), "The environmental safety of alkylphenol ethoxylates demonstrated by risk assessment and guidelines for their safe use" in *Handbook of detergents: Part B: environmental impact*, U. Zoller Ed., CRC Press, New York, pp. 429-445.

**Nethaji S. et al.** (2013), "Preparation and characterization of corn cob activated carbon coated with nano-sized magnetite particles for the removal of Cr(VI)", *Bioresource Technology* 134, pp. 94-100.

**Newns A.** and Pascoe R.D. (2002), "Influence of path length and slurry velocity on the removal of iron from kaolin using a high gradient magnetic separator", *Minerals Engineering* 15, pp. 465-467.

**Ning B. et al.** (2007), "Degradation of Octylphenol and Nonylphenol by Ozone – Part I: Direct Reaction", *Chemosphere* 68, pp. 1163-1172.

**Nishijima S.** and Takeda S. (2006), "Superconducting high gradient magnetic separation for purification of wastewater from paper factory", *IEEE Transactions on Applied Superconductivity* 16, pp. 1142-1145.

**Oberteuffer J.A.** (1973), "High gradient magnetic separation", *IEEE Transactions on Magnetics* 9(3), pp. 303-306.

**Oberteuffer J.A.** (1976), "Engineering development of high gradient magnetic separators", *IEEE Transactions on Magnetics* 12, pp. 444-449.

**Odenbach S.** and Stork H. (1998), "Shear dependence of field-induced contributions to the viscosity of magnetic fluids at low shear rates", *Journal of Magnetism and Magnetic Materials* 183, pp. 188-194.

**Okada H. et al.** (2002), "High Gradient Magnetic Separation for Weakly Magnetized Fine Particles", *IEEE Transactions on Applied Superconductivity* 12(1), pp. 967-970.

**Oliveira L.C.A. et al.** (2004), "Magnetic zeolites: a new adsorbent for removal of metallic contaminants from water", *Water Research* 38, pp. 3699-3704.

**Ostrumov S.A.** (2006), *Biological Effects of Surfactants*, CRC Press, New York, pp. 1-25.

**Payra P.** and Dutta P.K. (2003), "Zeolites: a Primer" in: *Handbook of Zeolite Science and Technology*, Auerbach, Carrado, Dutta Eds., CRC Press, New York.

**Reymond J.P.** and Kolenda F. (1999), "Estimation of the Point of Zero Charge of Simple and Mixed Oxides by Mass Titration", *Powder Technology* 103, pp. 30-36.

**Rossier M. et al.** (2012), "Scaling up magnetic filtration and extraction to the ton per hour scale using carbon coated metal nanoparticles", *Separation and Purification Technology* 96, pp. 68-74.

**Sannino F. et al.** (2012), "Cyclic process of simazine removal from waters by adsorption on zeolite H-Y and its regeneration by thermal treatment", *Journal of Hazardous Materials* 229-230, pp.354-360.

**Shariati S. et al.** (2011), "Fe<sub>3</sub>O<sub>4</sub> Magnetic Nanoparticles Modified with Sodium Dodecyl Sulfate for Removal of Safranin O Dye from Aqueous Solutions", *Desalination* 270, pp. 160-165.

**Shen Y.F. et al.** (2009a), "Preparation and application of magnetic Fe<sub>3</sub>O<sub>4</sub> nanoparticles for wastewater purification", *Separation and Purification Technology* 68, pp. 312-319.

**Shen, Y.F. et al.** (2009b), "Tailoring size and structural distortion of Fe<sub>3</sub>O<sub>4</sub> nanoparticles for the purification of contaminated water", *Bioresource Technology* 100, pp. 4139-4146.

**Showell M.S.** (2005), *Handbook of Detergents: Formulation, part D*, Chapter 1, CRC Press, New York.

**Soares A. et al.** (2008), "Nonylphenol in the environment: A critical review on occurrence, fate, toxicity and treatment in wastewaters", *Environment International* 34, pp. 1033-1049.

**Soria-Sanchez M. et al.** (2010), "Adsorption of non-ionic surfactants on hydrophobic and hydrophilic carbon surfaces", *Journal of Colloid and Interface Science* 343, pp. 194-199.

**Svoboda J.** (1987), *Magnetic methods for the treatment of minerals*, Elsevier, Amsterdam.

**Svoboda J.** (2004), *Magnetic Techniques for the Treatment of Materials*, Kluwer Academic Publishers, London.

**Taffarel S.R. and Rubio J.** (2009), "On the removal of Mn<sup>2+</sup> ions by adsorption onto natural and activated Chilean zeolites", *Minerals Engineering* 22, pp. 336-343.

**Wang L.K. and Yapijakis C.** (2004), "Treatment of Soap and Detergent Industry Wastes" in: Wang, L.K. *Handbook of industrial and Hazardous Wastes Treatment*, CRC Press, New York, pp. 307-362.

**Wang S. and Peng Y.** (2010), "Natural zeolites as effective adsorbents in water and wastewater treatment", *Chemical Engineering Journal* 156, pp. 11-24.

**Wang X. et al.** (2007), "The Study on Magnetite Particles Coated with Bilayer Surfactants", *Applied Surface Science* 253, pp. 7516-7521.

**WHO** (2006), *Guidelines for drinking-water quality: incorporating first addendum. Vol. 1, Recommendations. 3rd edn*, WHO, Geneva, Switzerland, ISBN 92 4 154696 4.

**WRC** (1974), *Determination of investment cost functions of water treatment plants*, WRC Research report n. 87, Department of Business Administration University of Illinois, Urbana, Illinois.

**Yavuz C.T. et al.** (2006), "Low-field magnetic separator of monodisperse Fe<sub>3</sub>O<sub>4</sub> nanocrystals", *Science* 314, pp. 964-967.

**Yavuz C.T. et al.** (2009), "Magnetic separations: from steel plants to biotechnology", *Chemical Engineering Science* 64, pp. 2510-2521.

**Ying F. et al.** (2012), "Comparative evaluation of nonylphenol isomers on steroidogenesis of rat Leydig Cells", *Toxicology in Vitro* 26(7), pp. 1114-1121.

**Ying G.G.** (2004), "Distribution, Behavior, Fate and Effects of Surfactants and the Degradation Products in the Environment" in: *Handbook of Detergents: Environmental Impact, part B*, U. Zoller Ed., CRC Press, New York, pp. 78-109.

**Zappone M. et al.** (2008), "Applications of Detergents in Laundering", in: *Handbook of detergents: Part E: Applications*, Chapter 4, U. Zoller Ed., CRC Press, New York, pp. 75-76.



## Acronyms list

**ACs** Activated Carbons  
**AEs** Alkylethoxylates  
**AESs** Alkylethoxy Sulfates  
**APs** Alhylphenols  
**APEs** Alkylphenol Ethoxylates  
**ASs** Alkyl Sulfates  
**BOD** Biochemical Oxygen Demand  
**COD** Chemical Oxygen Demand  
**CMC** Critical Micelle Concentration  
**CPU** Central Processing Unit  
**DD** Dishwashing Detergent  
**DDAB** Didecyldimethylammonium bromide  
**DWQS** Drinking Water Quality Standard  
**EC<sub>50</sub>** Half Maximal Effective Concentration  
**EDS** Energy Dispersive X-ray Spectrometry  
**EDTA** Ethylenediaminetetraacetic acid  
**EO** Ethylene Oxide  
**EPA** Environmental Protection Agency  
**FCC** Face Centred Cubic  
**FD** Floor Degreaser  
**FTU** Formazin Turbidity Unit  
**HGMS** High Gradient Magnetic Separation  
**LASs** Linear Alkylbenzene Sulfonates  
**LC<sub>50</sub>** Median Lethal Concentration  
**MACs** Magnetic Activated Carbons  
**MCL** Maximum Contaminants Level  
**NP** Nonylphenols  
**NPEs** Nonylphenols Ethoxylated  
**OP** Octylphenols  
**OPEs** Octylphenols Ethoxylated  
**PBU** Primary Building Units  
**PMs** Permanent Magnets  
**QACs** Quaternary Ammonium-based Compounds  
**SBU** Secondary Building Units  
**SC** Surface Cleaner  
**SDS** Sodium Dodecyl Sulphate  
**SEM** Scanning Electron Microscopy  
**TEM** Transmission Electron Microscopy  
**WHO** World Health Organization  
**WS** Washing machine Softener  
**WWTP** Wastewater Treatment Plant